博士論文

# A New Metal-Hydride-Based Catalysis toward C-C Bond Forming Reaction and $H_2$ Energy System

（メタルヒドリド活性種を基盤とした新規触媒系の開発と
炭素-炭素結合形成反応並びに水素貯蔵放出エネルギーシステムへの応用）

Graduate School of Pharmaceutical Sciences,

The University of Tokyo

東京大学大学院薬学系研究科 分子薬学専攻　有機合成化学研究室

Yutaka Saga

嵯峨　裕

# Contents

# Abbreviations

| | |
|---|---|
| Ac | acetyl |
| acac | acetylacetonate |
| aq. | aqueous solution |
| Ar | aryl |
| atm | atomosphere |
| Bn | benzyl |
| Boc | *tert*-butoxy carbonyl |
| bpy | bipyridyl |
| Bu | butyl |
| $^{t}$Bu | *tert*-butyl |
| Bz | benzoyl |
| cod | 1,5-cyclooctadiene |
| Cp | cyclopentadienyl |
| $Cp^{*}$ | pentamethylcyclopentadienyl |
| CSA | camphorsulfonic acid |
| Cy | cyclohexyl |
| DCE | dichloroethane |
| DCM | dichloromethane |
| DFT | density functional theory |
| DG | directing group |
| DIBAL | diisobutylaluminium hydride |
| DMA | *N*, *N*-dimethylacetamide |
| DMF | dimethylformamide |
| DMSO | dimethylsulfoxide |
| DNB | dinitrobenzene |
| DOE | (United States) Department of Energy |
| dppp | 1,3-bis(diphenylphosphino)propane |
| dtbpy | di-*tert*-butyl pyridine |
| e | electron |
| E | electrophile |

| | |
|---|---|
| EBTHI | ethylene bis(tetrahydroindenyl) |
| ee | enantiomeric excess |
| Et | ethyl |
| EWG | electron-withdrawing group |
| GB | glove box |
| GC | gas chromatography |
| Gly | glysine |
| h | hour(s) |
| HMPA | hexamethylphosphoramide |
| HOMO | highest occupied molecular orbital |
| IMes | 1,3-(2,6-trimethylphenyl)imidazole-2-ylidene |
| IPA | 2-propanol |
| IPr | 1,3-(2,6-diisopropylphenyl)imidazole-2-ylidene |
| L | ligand |
| LA | Lewis acid |
| LED | light emitting diode |
| LiDMAE | $Me_2N(CH_2)_2OLi$ |
| Ln | lanthanoids |
| LOHC | liquid organic hydride carrier (s) |
| LUMO | lowest unoccupied molecular orbital |
| M | metal |
| MAD | $(2,6\text{-}^tBu_2\text{-}4\text{-}MeC_6H_2O)_2AlMe$ |
| Me | methyl |
| Mes | mesityl |
| min | minute |
| Mt | metal |
| MTBE | methyl *tert*-butyl ether |
| NHC | *N*-heterocyclic carbine |
| NMP | *N*-methyl-2-pyrrolidinone |
| NMR | nuclear magnetic resonance |
| PCET | proton-coupled electron transfer |
| PEM | proton exchange membrane |

| | |
|---|---|
| Ph | phenyl |
| phen. | phenthroline |
| photo-cat. | photoredox catalyst |
| Piv | pivaloyl |
| PMP | 4-methoxyphenyl |
| $^{i}$Pr | 2-propyl |
| RCRC | rivoflavin tetraacetate |
| RFTA | radical-conjudated redox catalysis |
| r.t. | room temperature |
| S | substrate |
| TCD | thermal conductivity detector |
| TEMPO | 2, 2, 6, 6-tetramethyl-1-piperidinyloxy radical |
| Tf | trifluoromethanesulfonyl |
| TFA | trifluoroacetic acid |
| TFE | 2, 2, 2-trifluoroethanol |
| THF | tetrahydrofuran |
| TMPMgCl | tetramethylpiperidinomagnesium chrolide |
| TMS | trimethylsilyl |
| TPT | triphenyl pyririum tetrafluoroborate |
| Ts | *p*-toluenesulfonyl |
| Val | valine |
| Wh | watt hour |

# 1. Cobalt-Catalyzed C-4 Selective Direct Alkylation of Pyridines

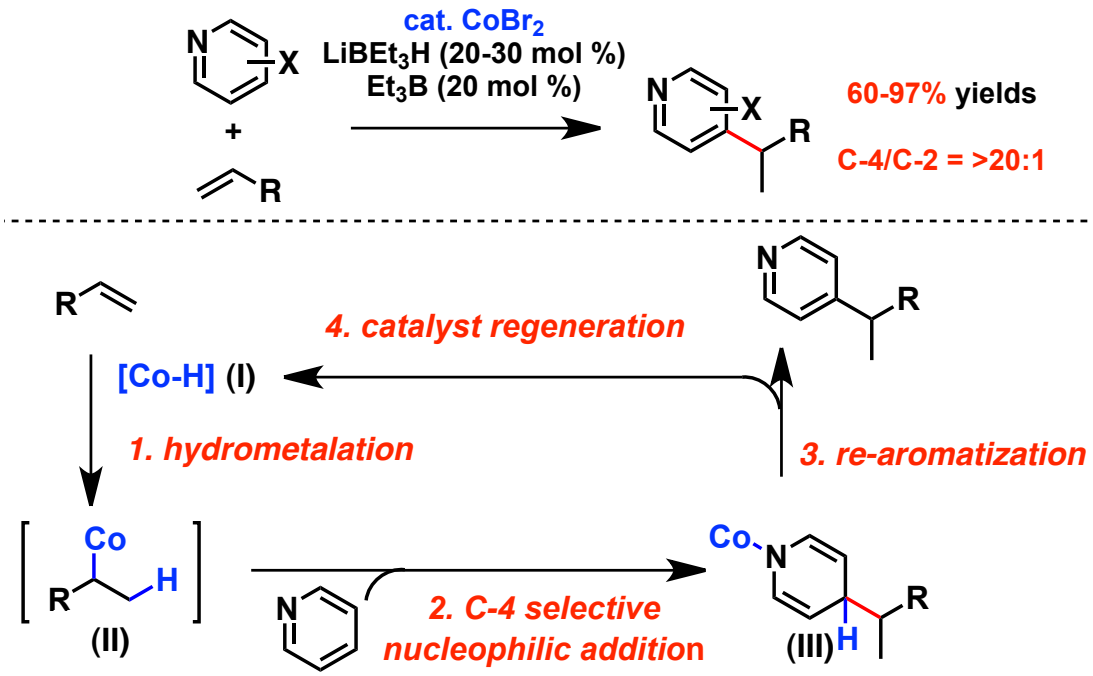


Andou, T.†; Saga, Y.†; Komai, H.; Matsunaga, S.; Kanai, M. *Angew. Chem. Int. Ed.* 2013, *52*, 3213.
(† Contributed equally)

## 1-1. Research Background

### 1-1-1. Pyridines as ubiquitous motifs

Pyridine derivatives are essential motifs exiting in numerous biologically active compounds, drugs, and useful materials (Figure 1-1).

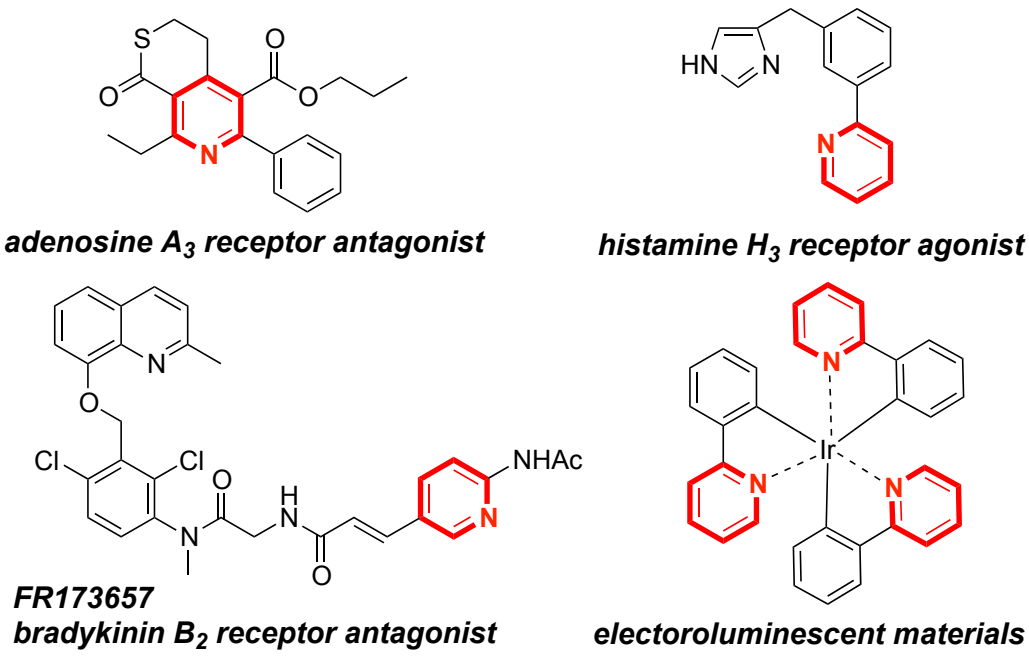


**Figure 1-1.** Pyridines as essential motifs

Due to these multiple utilities, sophisticated methods to provide pyridine derivatives regioselectively[1] are in high demand. The previous investigations mainly focused on C-2 functionalizaion, such as C-2 selective nucleophilic addition of organometallic reagents and nucleophilic attack to various electrophiles by C-2 selective deprotonation using lithium bases[2] (Scheme 1-1).

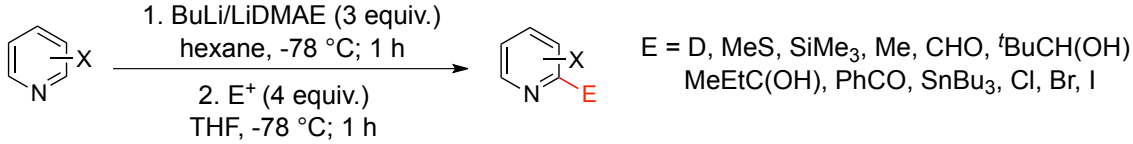


**Scheme 1-1.** Lithiation of chloropyridines with BuLi/LiDMAE

## 1-1-2. C-2 selective direct functionalization of pyridines

Recently, transition metal-catalyzed regioselective direct C-H bond functionalization of pyridines[3] has attracted considerable attentions because the methodologies provide easy access to functionalized pyridines in atom-economical[4] and step-economical[5] fashion. Many researchers have achieved C-2 selective direct C-H bond functionalization utilizing a Lewis basic $sp^2$ nitrogen atom as the directing group. Especially for C-2 selective catalytic direct alkylation of pyridines without prior activation, there are several intriguing reports (Scheme 1-2). In 1989, Jordan *et al*. disclosed C-2 selective alkylation of 2-picoline with propene under 1 atm of hydrogen atmosphere using a cationic alkyl zirconium complex[6a]. They also succeeded the enantioselective version with a chiral ethylene bis(tetrahydroindenyl)-Zr complex[6b], although the activity was about 10 times lower than the activity of the achiral complex under comparable conditions. In 2007, Ellman and Bergman group developed a Rh(I) catalyst for the C-2 selective direct alkylation of pyridines and quinolines with various functionalized aliphatic olefins[6c]. Their system exhibited good to excellent linear selectivity. In 2010, Daugulis group reported a method for iron-catalyzed deprotonative alkylation of various types of arenes, such as pyridines, furans and thiophenes by alkyl iodides and bromides[6d]. In 2011, Hou group demonstrated that half-sandwich rare-earth dialkyl complexes $(C_5Me_5)Ln(CH_2C_6H_4NMe_2\text{-}o)_2$ (Ln = Sc, Y) with $B(C_6F_5)_3$ were effective for the direct C-2 selective alkylation of pyridine derivatives[6e]. Their catalytic conditions showed excellent C-2 selectivity, functional group tolerance, and broad substrate scope generality.

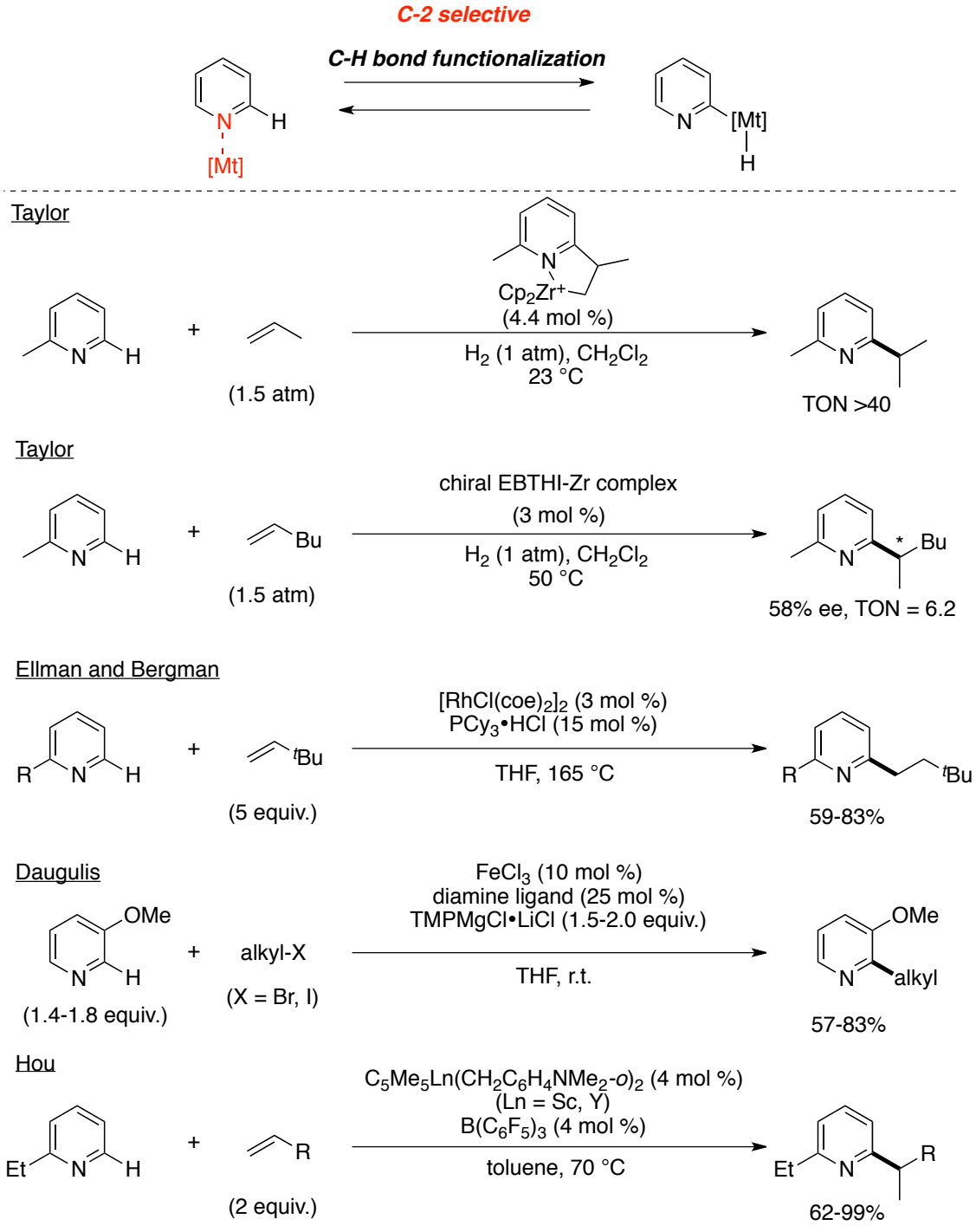


**Scheme 1-2.** C-2 selective catalytic direct alkylation of pyridines

## 1-1-3. C-3 selective direct functionalization of pyridines

In contrast to many achievements for C-2 selective C-H bond functionalizations, there are only limited examples on C-3 and C-4 selective C-C bond forming reactions without using an additional coordinating directing group[7] (Scheme 1-3). Yu and co-workers reported the first C-3 selective alkenylation of pyridines under Pd(II)/1,10-phenanthroline system[8a]. Their strategy involved the use of a bidentate pyridyl ligand to enhance the ligand exchange due to a strong *trans*-effect. They expected that a small change of the equilibrium from form **I** to form **II** might trigger the desired C-3 selective reaction (Scheme 1-3). In 2011, Shi *et al* developed a Ir catalyst with hydrosilane for C-3 selective nucleophilic addition reaction of pyridines to aromatic aldehydes[8b]. Although the detailed mechanistic scenario remained unclear, they insisted that a silyl iridium complex might be the key active catalytic intermediate.

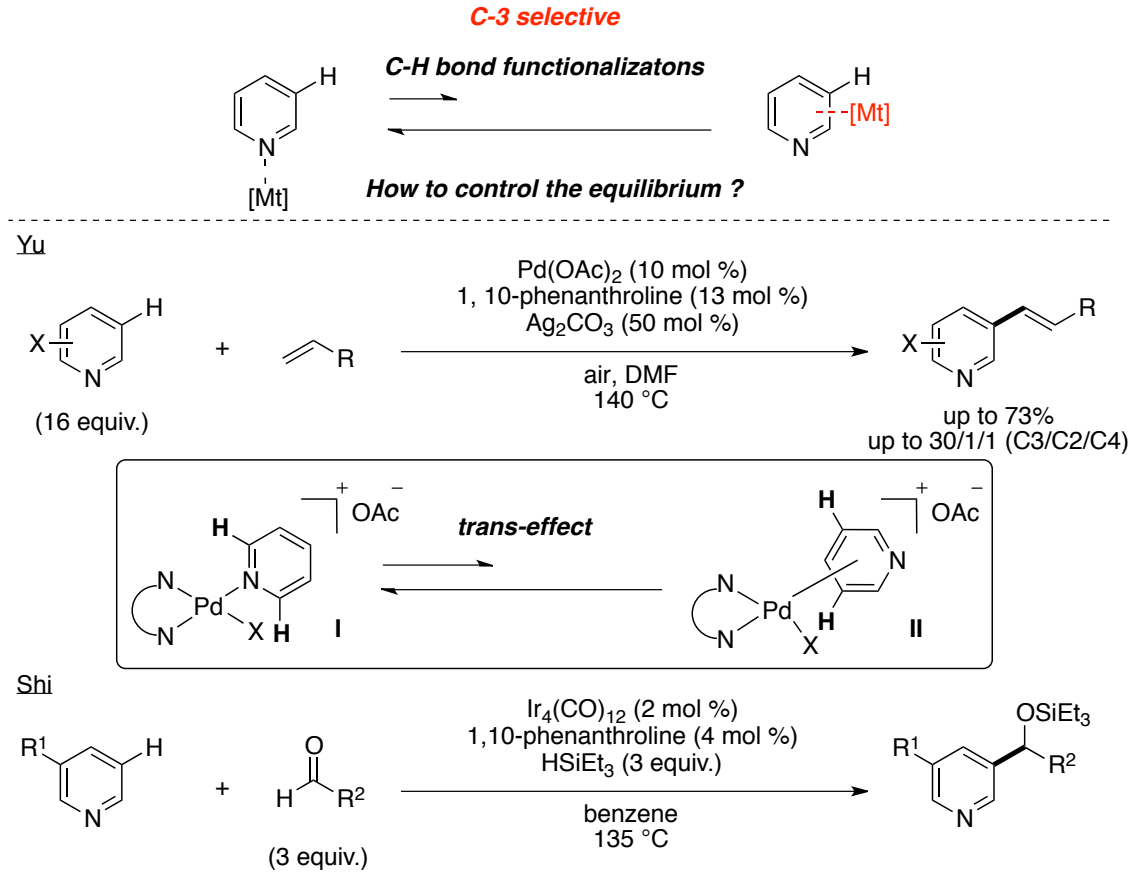


**Scheme 1-3.** C-3 selective catalytic direct C-H functionalization of pyridines

## 1-1-4. C-4 selective direct functionalization of pyridines

Concerning direct C-4 selective functionalization of pyridines, examples were also limited to the reaction with a coordinating directing group at C-3 position[9]. In 2010, however, Nakao/Hiyama *et al*[10a]. and Ong *et al*[10b]. independently disclosed the first C-4 selective functionalization of pyridines in the absence of any guiding directing groups using $Ni^0$/Al catalysis through oxidative addition/insertion/reductive elimination sequence (Scheme 1-4). Their key to success was considered to be the appropriate combination between sterically demanded NHC carbene ligands and bulky Lewis acidic aluminums. They proposed that the steric repulsion between $Ni^0$ complexes and Lewis acids directed the reductive elimination step exclusively at desired C-4 position. From several mechanistic studies, they insisted that the last reductive elimination step was irreversible and the regioselectivity-determining step, while the oxidative addition step and insertion step were reversible. However, there remained rooms for improvements especially in terms of mild reaction conditions and the involvement of new strategy.

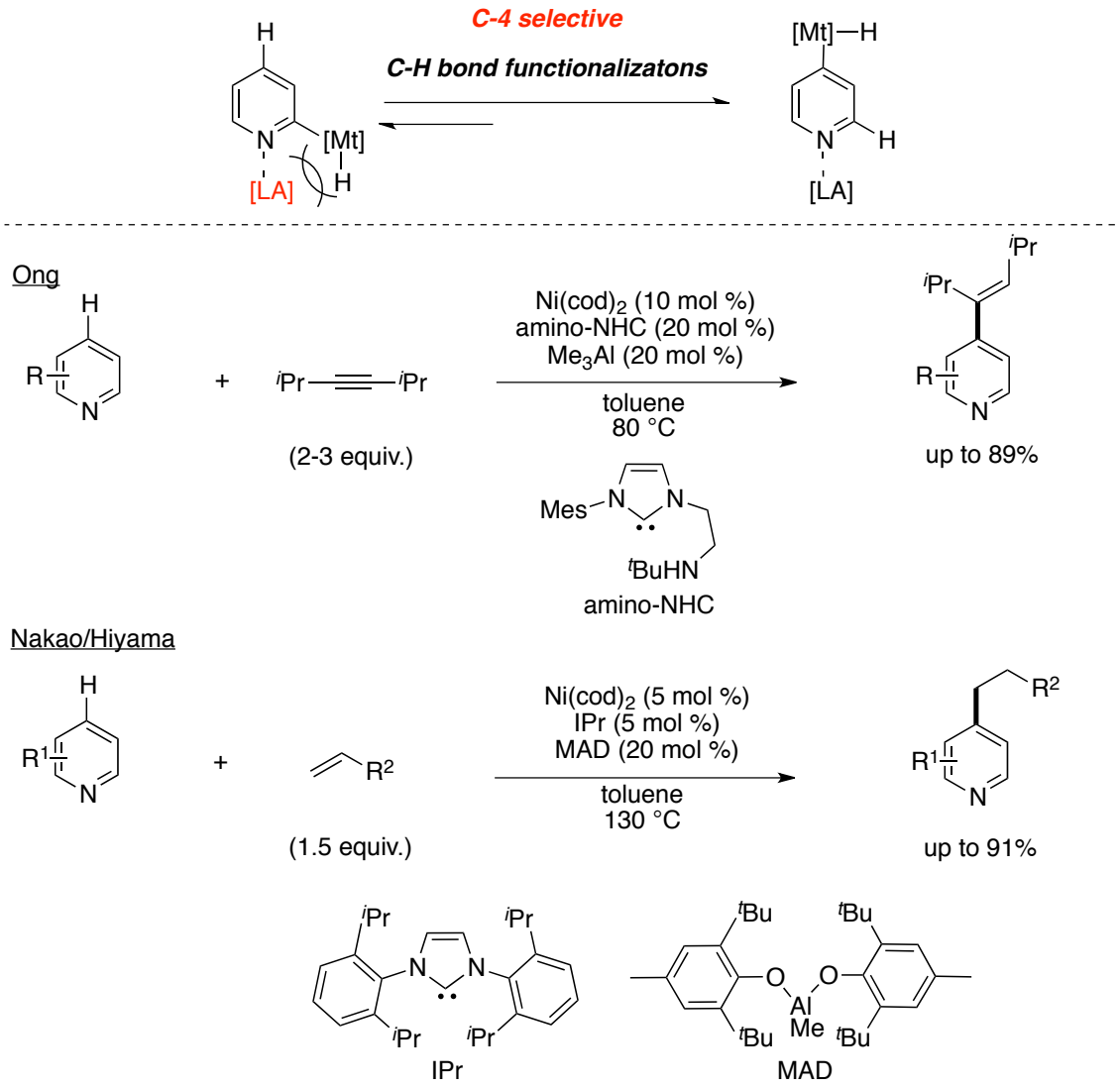


**Scheme 1-4.** C-4 selective catalytic direct C-H functionalization of pyridines

## 1-2. Reaction Design

According to the previous reports for regioselective direct C-C bond forming reactions of pyridines, the strategy in almost all cases relied on the oxidative addition of C-H bond by metal catalysis/insertion/reductive elimination sequence. The current situation motivated me to pursue the development of C-4 selective direct alkylation of pyridines *via* a conceptually different reaction mechanism.

I focused on the alkyl metal species as potentially active nucleophiles generated from hydrometallation of olefins by metal hydride species. In 1989, Mukaiyama and Isayama developed Co-catalyzed hydration reaction of olefin derivatives[11a]. After the prominent work, Carreira group intensively documented the catalytic functionalization of unactivated olefins through hydrometallation chemistry (Scheme. 1-5). In 2004, they reported an olefin hydrohydrazination reaction to afford alkyl hydrazides using a Co-Schiff base complex and $PhSiH_3$ catalysis[11b]. They successfully applied their Co-hydride catalyst system to other variants, such as hydroazidation[11c, d], hydrocyanation[11e], and hydrochlorination[11f].

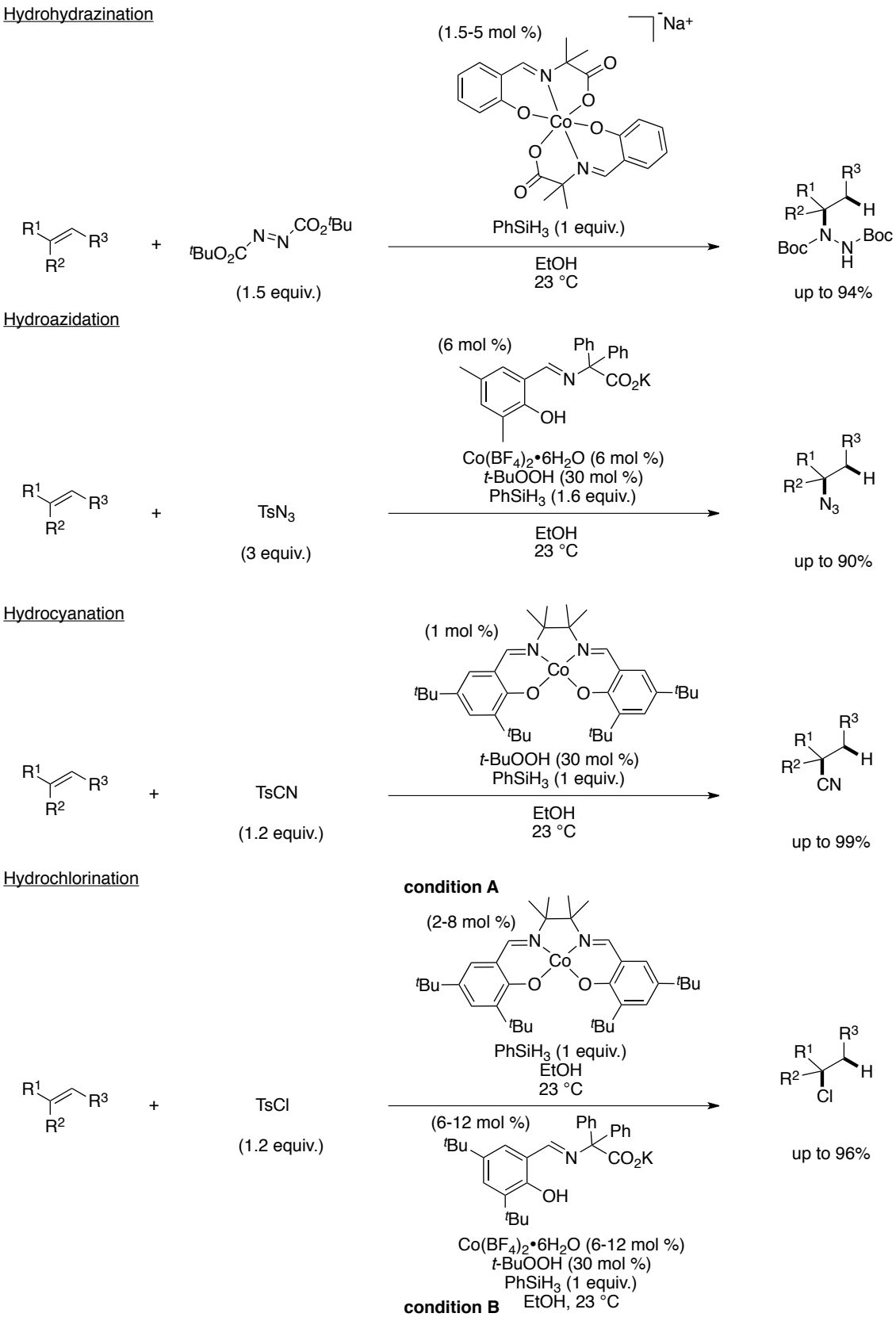


**Scheme 1-5.** Catalytic functionalizations of unactivated olefins developed by Carreira group

Based on the variable reactivity of alkyl metal species to a variety of electrophiles, I envisaged that an adequate alkyl metal species might also be a good nucleophile to pyridine derivatives. I expected that such nucleophilic addition strategy may realize C-4 selective direct alkylation of pyridines *via* completely different mechanism; *1. hydrometallation/2. catalytic nucleophilic addition to pyridines/ 3. re-aromatization* sequence.

My working hypothesis is described in Scheme 1-6. Hydrometallation of alkenes with a metal hydride species would initiate catalytic cycle to give an alkyl metal species. If the alkyl metal species has sufficient nucleophilicity to pyridines, the addition reaction might occur to afford a dihydropyridine intermediate. Hydride elimination from the dihydropyridine intermediate is expected to be critical to realize an atom-economical process without any oxidants. Rearomatization of pyridine and regeneration of metal hydride species would complete the catalytic cycle.

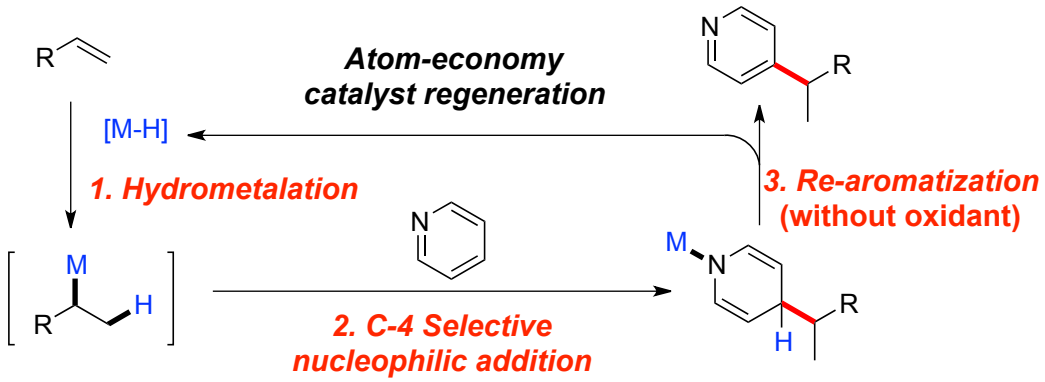


**Scheme 1-6.** Working hypothesis

About the C-C bond forming reactions to pyridines through nucleophilic addition fashion, there are several precedent works (Scheme 1-7). In 2009, Tobisu and Chatani *et al*. demonstrated a Ni-catalyzed nucleophilic addition reaction of aryl zinc reagents to electron-deficient heteroarenes at C-2 position[12a]. They mentioned that the aryl zinc reagent functions as both an aryl donor and an oxidant. In 2010, Baran and co-workers developed a direct arylation of electron-deficient heteroarenes with aryl boronic acids using a silver catalyst and co-oxidant[12c]. The reaction was postulated to proceed *via* Minisci-type aryl radical addition pathway. The similar type of radical addition protocol was reported by Molander group[12d]. They have achieved the first direct alkylation of various heterocycles with potassium alkyl- and alkoxymethyltrifluoroborates. Although their systems allowed easy access to broadly functionalized heteroarenes including pyridine derivatives, there remained problems to be solved in that they required the stoichiometric oxidants and the regioselectivity was only limited to C-2 position[13] using pyridines except for 2,6-disubstituted pyridines[12a]. I envisioned that I could solve the problems if my working hypothesis works well.

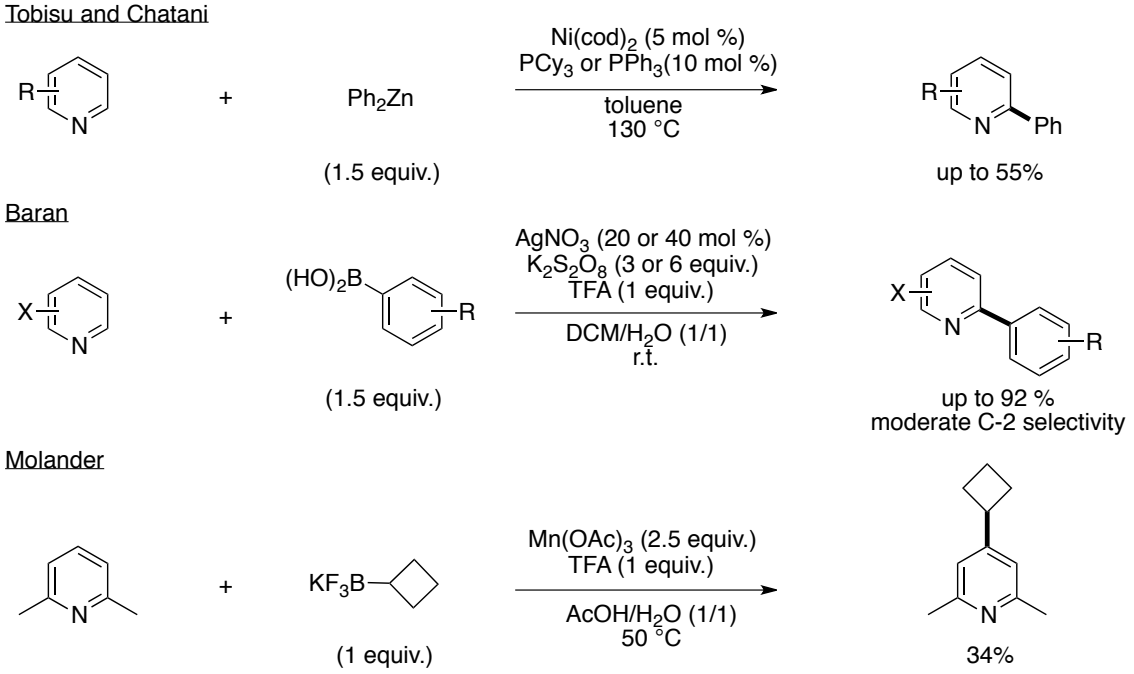


**Scheme 1-7.** Direct C-C bond forming reactions of pyridines *via* nucleophilic addition pathway

## 1-3. Reaction Development

Based on the reaction design, I started the initial investigations of metal hydride species that fulfilled the requirements described in Scheme 1-6 using a pyridine as a substrate and a styrene as an olefin. The preliminary studies gave me several important information. 1) $LiBEt_3H$ as a hydride source showed good reactivity to give the desired products in moderate yield. 2) Non-polar solvents (hexane, benzene, toluene, *o*-xylene) were effective while polar solvents (THF, NMP, DMSO, DCM) showed almost no reactivity. 3) The addition of several different types of ligands (1, 10- phenanthroline, dppp, $PCy_3$, $PPh_3$, IMes) never improved the reactivity and the regioselectivity.

First I investigated the metal salts in the presence of $LiBEt_3H$ in toluene at 70 °C (Table 1-1). In the absence of any metal salts, the reaction rarely proceeded (entry 1). Among a variety of metal salts, $CoBr_2$ revealed to be the best metal source in terms of the reactivity though C-4 selectivity was not satisfactory (entries 2-5 *vs* entry 6).

**Table 1-1.** Metal effects

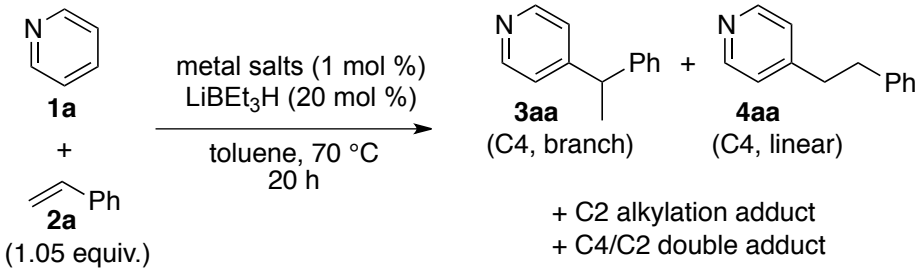


| entry | metal salts | yield (%) | C4/C2/double product ratio |
|---|---|---|---|
| 1 | none | 4 | >20:1:0 |
| 2 | $FeBr_2$ | 10 | >20:1:0 |
| 3 | $NiBr_2$ | 24 | >20:1:0 |
| 4 | $MnBr_2$ | 22 | >20:1:0 |
| 5 | CuBr | 3 | >20:1:0 |
| 6 | **$CoBr_2$** | **77** | 1.8/1/0.2 |

In order to enhance C-4 selectivity, I also performed the investigations on each component (Table 1-2). I screened other hydride sources, but I observed drastic decrease of reactivities

(entries 1-4). The results suggested the importance of Li cation in the catalytic reaction. Control experiment using $CoBr_2$ alone never afforded the product at all indicating that the combination of $CoBr_2$ and $LiBEt_3H$ was essential (entry 5). Addition of ligands such as phosphines, phenanthrolines, NHC carbenes sometimes displayed slight improvements on C-4 selectivity (entries 6-8). On the other hand, $BEt_3$ proved to be the effective additive to enhance C-4 selectivity to give the product in 95 % yield with branch/linear = >20/1 and C-4/C-2 = 7.0/1 selectivities[14] (entry 9). I also tested other cobalt salts, but only found a little deterioration in yields (entries 10-11). At this stage, I anticipated that successive addition of the second additives, which could make good effects on Li species, might influence the regioselectivity. As expected, the addition of 12-crown-4-ether slightly enhanced C-4 selectivity while the reactivity got worse (entry 12). Finally I found out that 30 mol % of hexamethylphosphoramide (HMPA) in combination with $BEt_3$ further improved C-4/C-2 selectivity to > 20/1[15] (entry 13). I speculated that the addition of HMPA additive may accelerate nucleophilic addition by forming more naked anion species or deaggregating the lithium oligomers because HMPA is known to strongly coordinate to Li cations.

**Table 1-2.** Optimization studies on each component

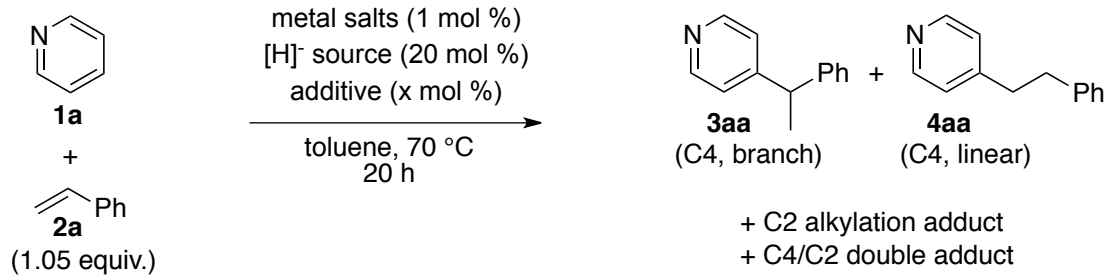


| entry | metal | $[H]^-$ | additive (x mol %) | yield (%) | C4/C2/double product ratio |
|---|---|---|---|---|---|
| 1 | $CoBr_2$ | $LiBEt_3H$ | none | 77 | 1.8/1/0.2 |
| 2 | $CoBr_2$ | $NaBEt_3H$ | none | 10 | 1.3/1/0 |
| 3 | $CoBr_2$ | $KBEt_3H$ | none | 2 | > 20/1/0 |
| 4 | $CoBr_2$ | DIBAL-H | none | 2 | 0/1.3/1 |
| 5 | $CoBr_2$ | none | none | 0 | - |
| 6 | $CoBr_2$ | $LiBEt_3H$ | $PCy_3$ (3) | 77 | 1.3/1/0 |
| 7 | $CoBr_2$ | $LiBEt_3H$ | 1,10-phen. (3) | 77 | 3.5/1/0.3 |
| 8 | $CoBr_2$ | $LiBEt_3H$ | IMes (3) | 34 | 2.5/0/1 |
| 9 | $CoBr_2$ | $LiBEt_3H$ | $BEt_3$ (20) | 95[a] | 7.0/1/0.52 |
| 10 | $CoCl_2$ | $LiBEt_3H$ | $BEt_3$ (20) | 82 | 6.7/1/0.25 |
| 11 | $Co(acac)_2$ | $LiBEt_3H$ | $BEt_3$ (20) | 88 | 7.4/1/0.26 |
| 12 | $CoBr_2$ | $LiBEt_3H$ | $BEt_3$ (20) + crown ether (20) | 42 | 9.5/1/0 |
| 13 | $CoBr_2$ | $LiBEt_3H$ | **$BEt_3$ (20) + HMPA (30)** | 91[a] | **> 20/1/0.38** |

[a]Combined yield of alkylated products after purification by silica gel column chromatography.

## 1-4. Substrate Generality

### 1-4-1. Substrate generality with aromatic olefins

I examined the substrate scope with aromatic olefins (Table 1-3). The reaction with pyridine derivatives **1** and styrene derivatives **2** proceeded smoothly using 1 mol % of $CoBr_2$, 20-30 mol % of $LiBEt_3H$, and 20 mol % of $BEt_3$[16]. I achieved good to excellent branched selectivity (>20/1-7.4-1) and excellent C-4 selectivity (>20/1) in all cases.

**Table 1-3.** Substrate scope with aromatic olefins

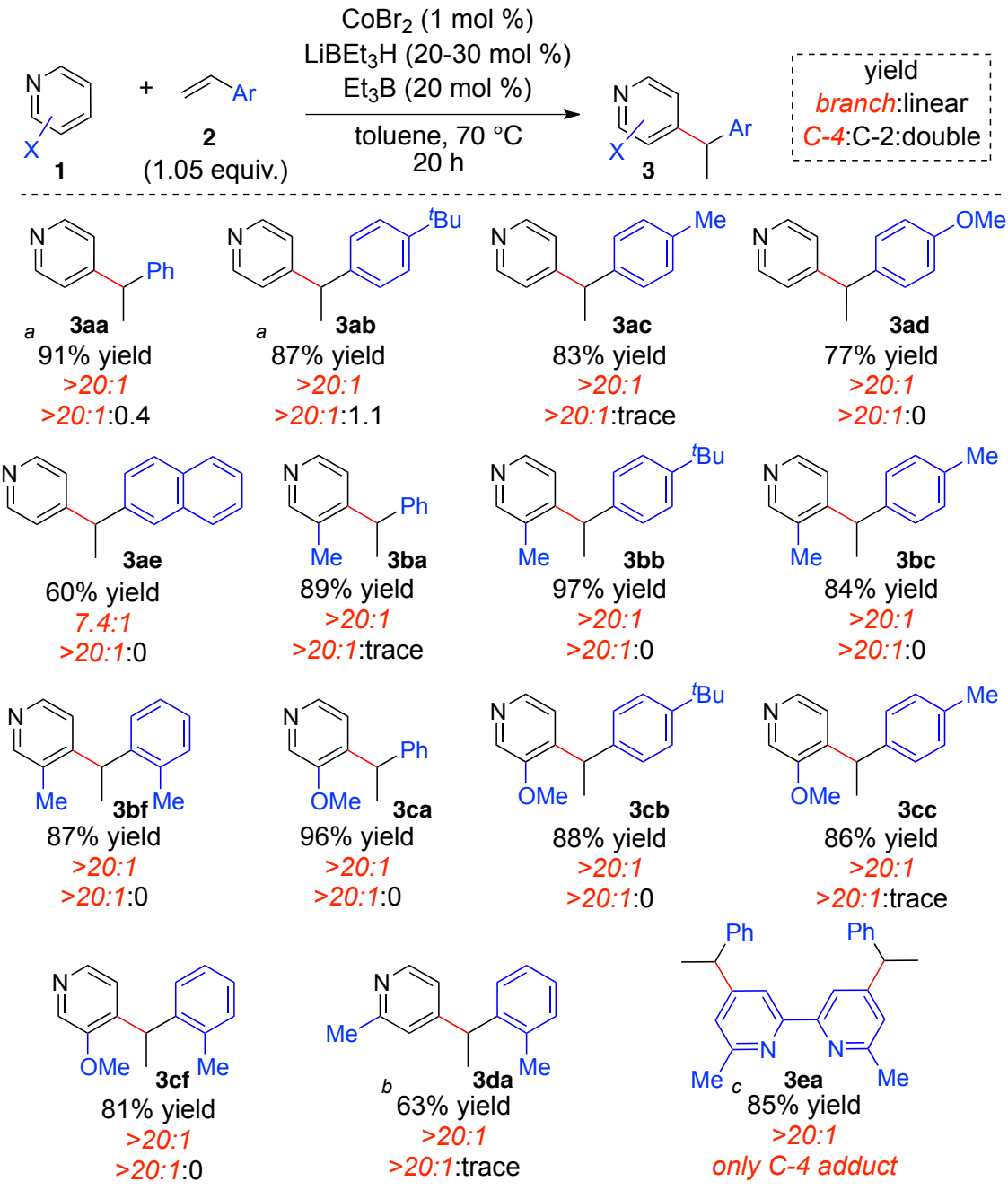


[a]30 mol % of HMPA was used. [b]Reaction was run in the absence of $BEt_3$. [c]5 equiv. of styrene were used.

## 1-4-2. Substrate generality with aliphatic olefins

I, then, turned my attention to aliphatic olefins as the substrates. Aliphatic olefins, however, exhibited much lower reactivities than aromatic olefins under optimized conditions. After further attempts to realize the sufficient reactivities, I found out that increase of the catalyst amounts facilitated the reaction. In the presence of 6 mol % of $CoBr_2$, 200-300 mol % of $LiBEt_3H$, 20 mol % of $BEt_3$ and excess alkenes, desired products **4** were obtained in moderate to good yield (58-86 %) with excellent C-4 selectivity (C-4/C-2 = >20/1) (Table 1-4). For aliphatic alkenes, it was of note to exclusively obtain the linear adducts (branched/linear = 1/>20), whereas branched adducts were produced for aromatic alkenes (branched/linear = >20/1).

The observed linear/branched selectivity difference between the aromatic alkenes and aliphatic alkenes would be ascribed to the relative stability differences in the alkyl cobalt intermediates (Scheme 1-8). Because I observed H/D scrambling at both the α- and β- positions of styrene when I carried out the H/D scrambling experiment with [$D_5$]pyridine and styrene, I believe the hydrometallation step should be reversible at least for aromatic alkenes. For aromatic alkenes, the thermodynamically stable π-conjugated benzylic-cobalt intermediate would be the active nucleophilic species to pyridines, while the reaction with aliphatic alkenes would proceed from the kinetically favored linear alkyl cobalt intermediate[17].

**Table 1-4.** Substrate scope with aliphatic olefins

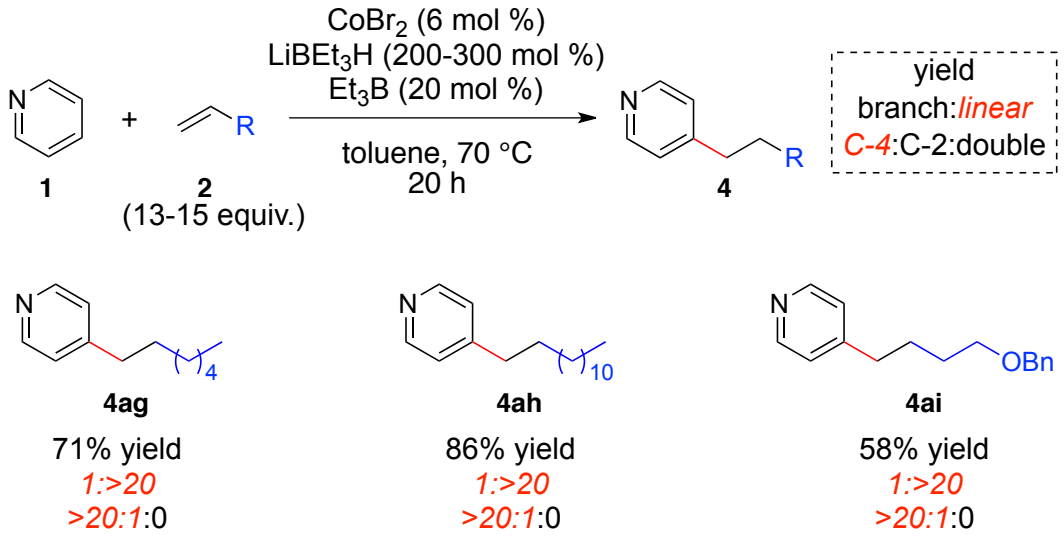

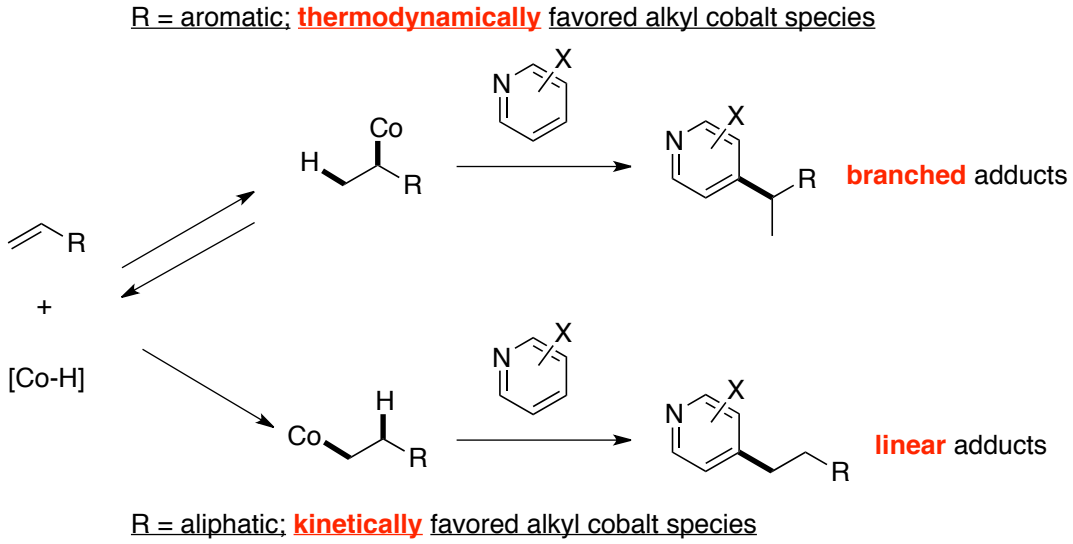


**Scheme 1-8.** Explanation for branched/linear selectivity difference

## 1-4-3. Limitations

Despite the good reactivity, excellent regioselectivity, and excellent linear/branch selectivity in the catalytic system, I had difficulties to achieve functional group tolerance. As described in Table 1-5, the reactions with pyridine derivatives bearing polar substituents, such as halogen, $CF_3$, ester, amide, and nitrile, were unsatisfactory. It was also the case for various types of heteroarenes, such as pyrimidines, furans, indoles, and phenanthrolines and so on.

**Table 1-5.** Limitations in my catalytic system

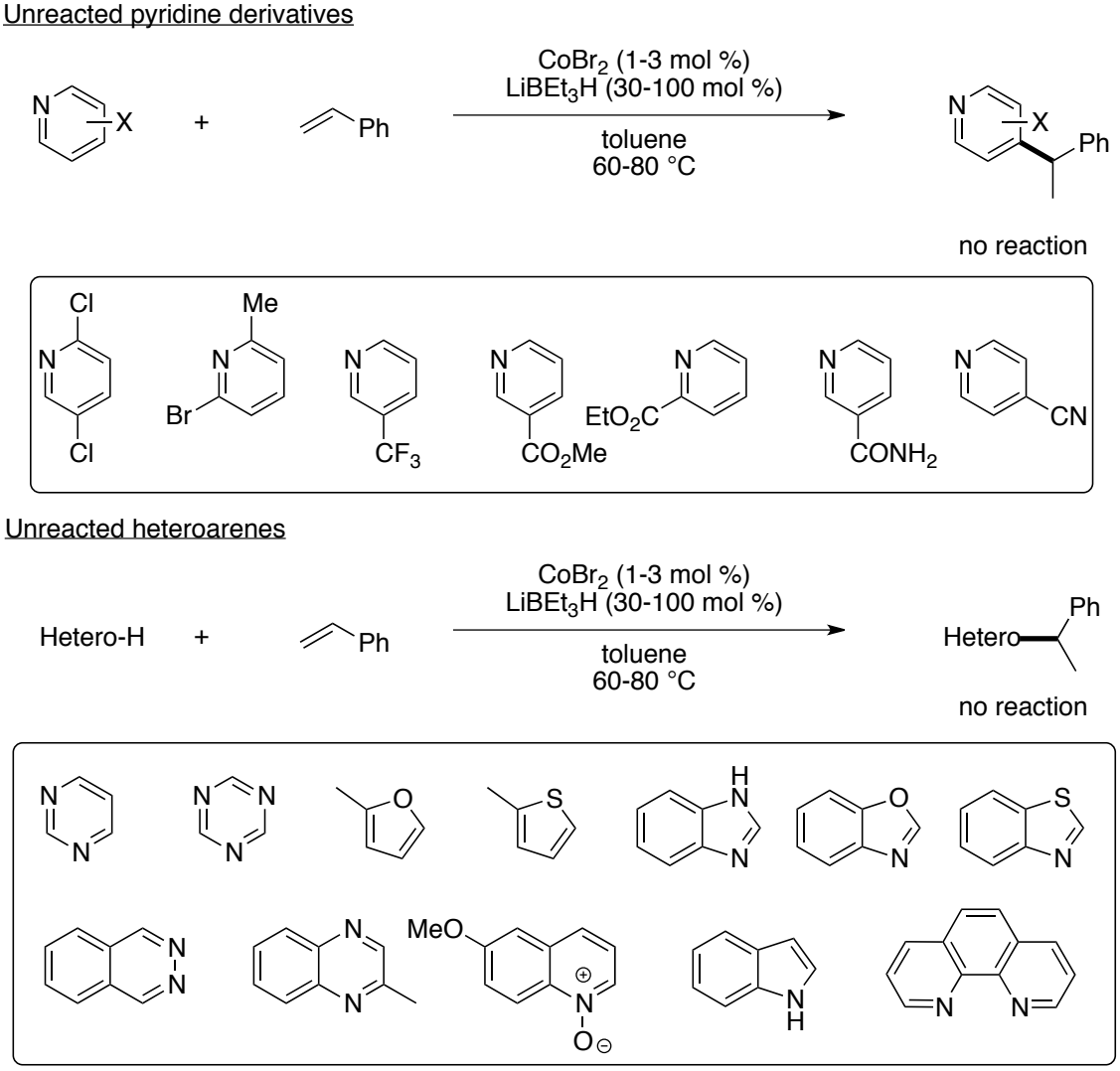

I speculated that polar-functional groups might destroy or have adverse effects on the active cobalt hydride catalyst. Indeed, addition of the catalytic amount of 8-chloro quinoline **A** completely inhibited the reaction under optimized conditions, while the reaction proceeded smoothly in the absence of **A** (Scheme 1-9). The result indicated that pyridines with polar-functionalities might be the ligand to the active cobalt hydride species to somehow decelerate the activity.

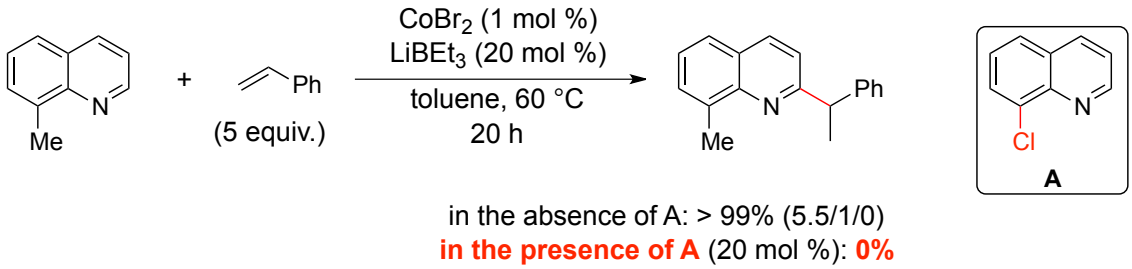


in the absence of A: > 99% (5.5/1/0)
**in the presence of A** (20 mol %): **0%**

**Scheme 1-9.** Complete inhibition in the presence of 8-chloro quinoline.

Exploration of more reactive catalyst to broader substrates with various functional groups is underway.

## 1-5. Mechanism Study

On the above working hypothesis, I deemed that there are three key concerns to be elucidated; *1. Which sequence is more plausible, nucleophilic addition sequence or oxidative addition sequence? 2. What is the role of $BEt_3$ as an additive? 3. Is cobalt-hydride species actually regenerated in situ?* (Scheme 1-10). In order to gain preliminary insight into these three questions, I performed several mechanistic investigations.

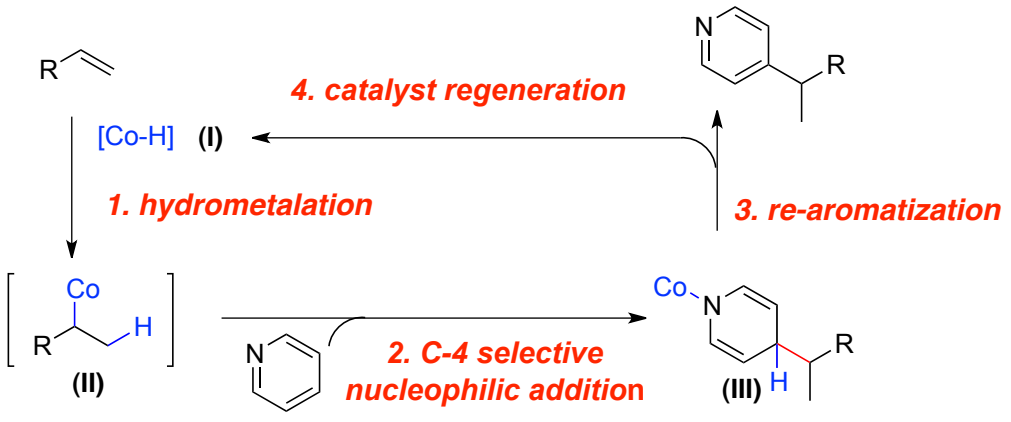


1. Which sequence is more plausible, nucleophilic addition or oxidative addition?
2. What is the role of $BEt_3$ as an additive?
3. Is cobalt-hydride species actually regenerated in situ?

**Scheme 1-10.** Three key mechanistic points to be elucidated.

## 1-5-1. Which sequence is more plausible, nucleophilic addition sequence or oxidative addition sequence?

There is no direct evidence to exclude a reaction mechanism involving oxidative addition/ insertion/ reductive elimination sequence catalyzed by low-valent cobalt species[18] formed by cobalt salts and $LiBEt_3H$ *in situ* (Scheme 1-11).

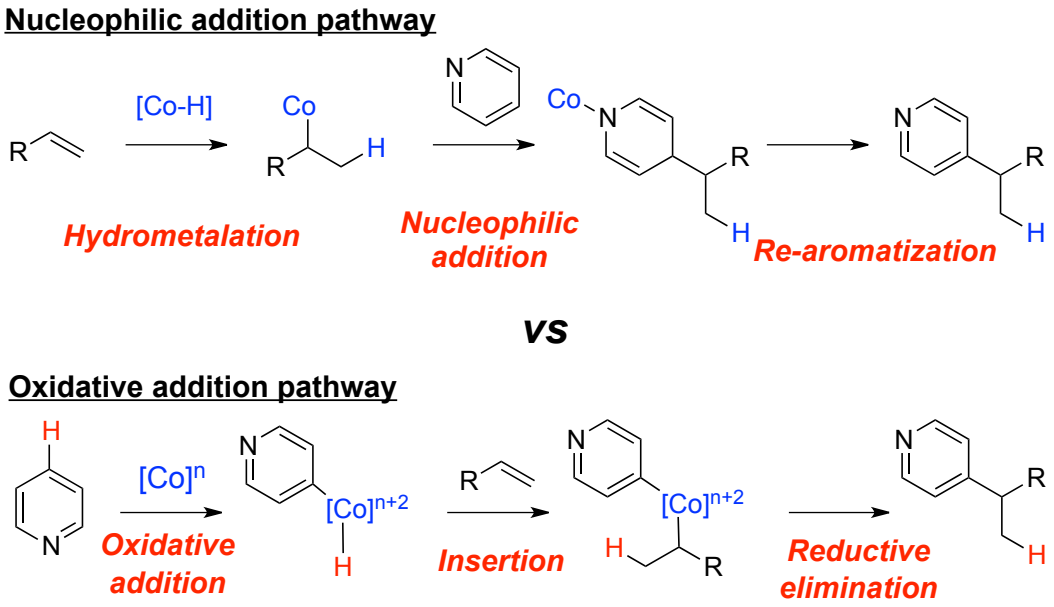


**Scheme 1-11.** Nucleophilic addition pathway *vs* oxidative addition pathway

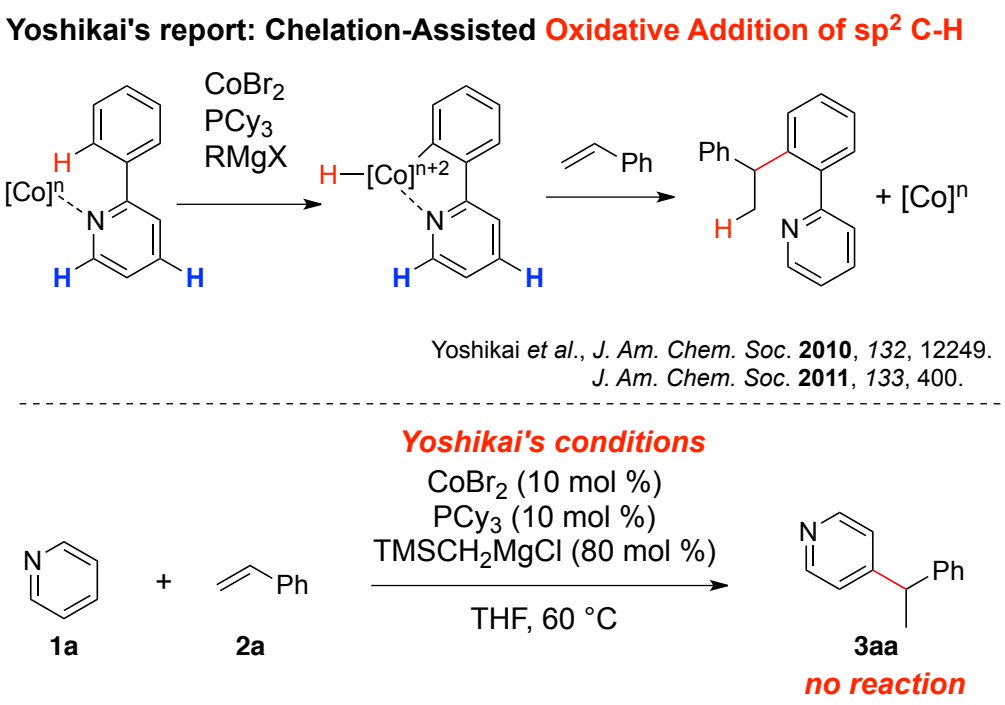


**Scheme 1-12.** Yoshikai's system was not effective for my reaction.

To exclude the possibility, I planed to put my substrates on the system, which was reported to promote oxidative addition/insertion/reductive elimination sequence by using low-valent cobalt species[19]. Yoshikai group disclosed low-valent cobalt-catalyzed chelation-assisted hydroaryration reactions with styrenes[19a]. Because they proposed that low-valent cobalt species generated *in situ* could catalyze oxidative addition of $sp_2$ C-H bond /insertion/reductive elimination sequence in their system, I carried out the reaction with a pyridine and a styrene as substrates under their optimum conditions. I found out that their system was not effective for the present pyridine alkylation reactions (Scheme 1-12). The results would suggest that there might be an alternative sequence in my reaction other than oxidative addition sequence.

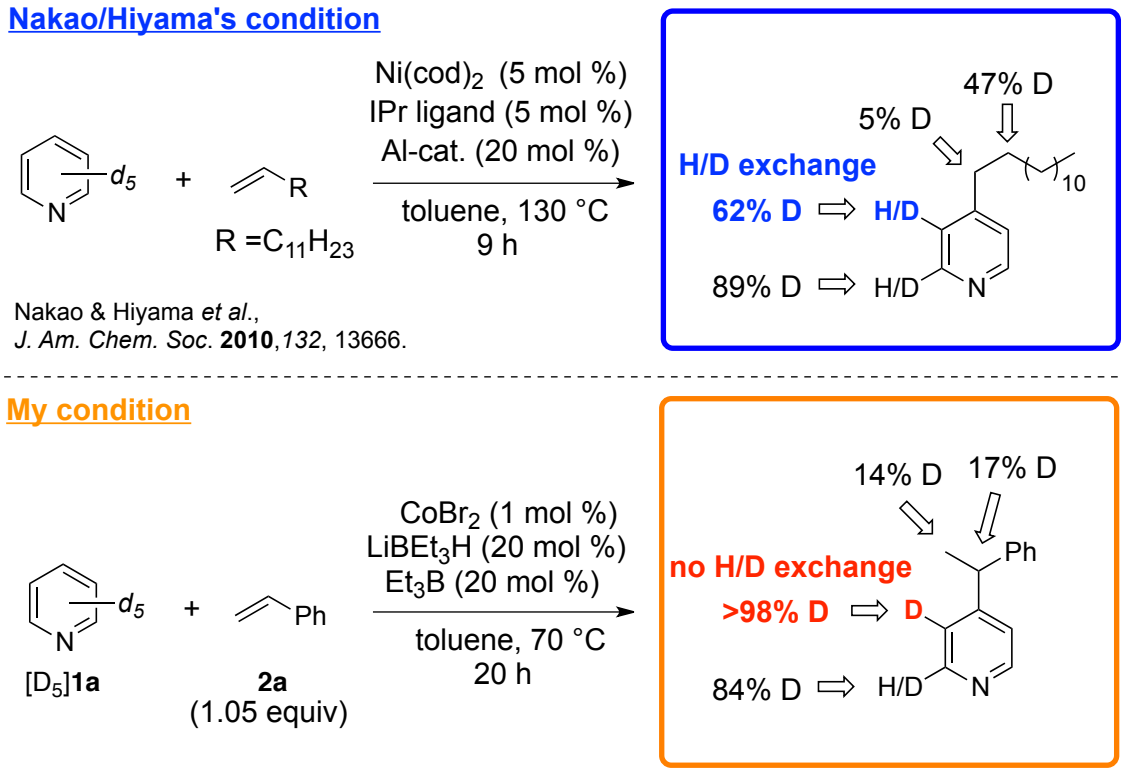


**Scheme 1-13.** Different profiles of H/D scrambling

In order to obtain more precise mechanistic insight into the oxidative addition sequence, I implemented H/D scrambling experiment with [$D_5$] pyridine as a substrate (Scheme 1-13). Compared with the $Ni^0$/Al catalysis developed by Nakao/Hiyama[10a] and Ong[10b], profiles of H/D scrambling were drastically different. My conditions provoked selective H/D scrambling at the electrophilic C-2 and C-4 position, possibly through the reversible addition and elimination of cobalt-hydride species (Scheme 1-14). On the contrary, under $Ni^0$/Al system, because oxidative addition of C-H bond by $Ni^0$ catalysis occurred at all positions on pyridines, H/D scrambling at both C-3 and C-2 positions were observed. Altogether, these contrasting observations indicate that the present C-4 selective direct alkylation reaction might proceed through *hydrometallation/ nucleophilic addition to pyridines/ re-aromatization* sequence not through *oxidative addition/ insertion/ reductive elimination sequence*.

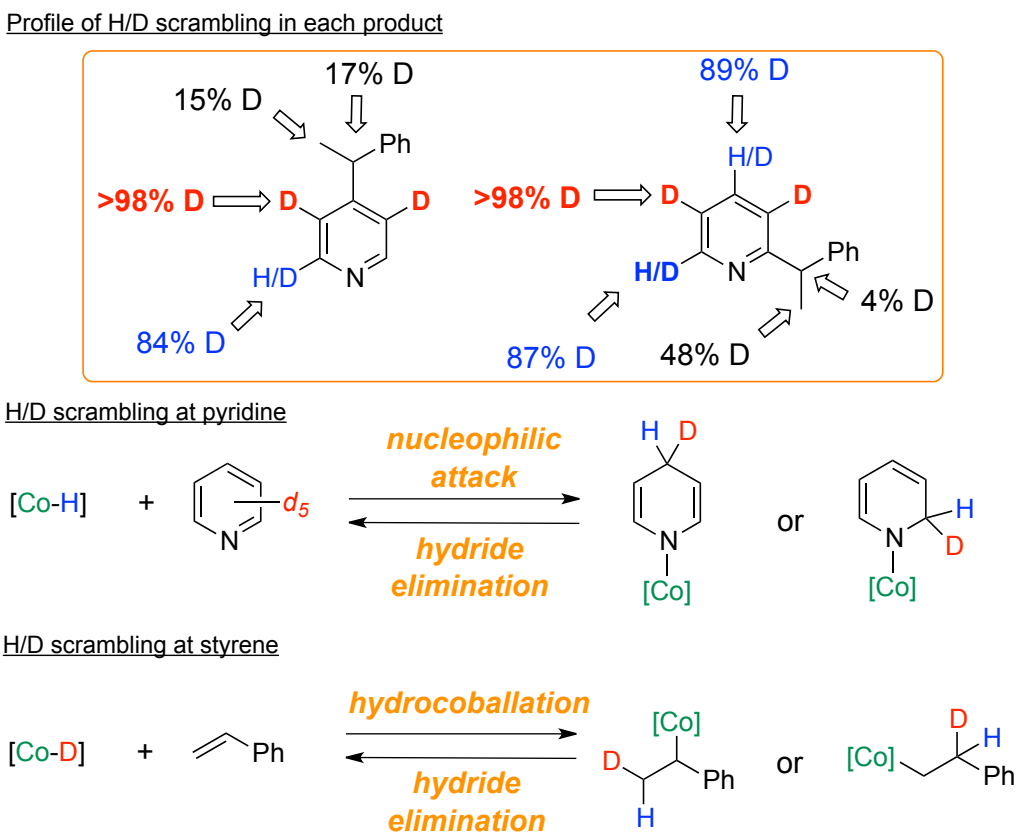


**Scheme 1-14.** H/D Scrambling in my catalytic system

## 1-5-2. What is the role of $BEt_3$ as an additive ?

During the course of study for achieving high C-4 selectivity, I discovered that addition of catalytic amount of $BEt_3$ markedly enhanced C-4 selectivity (Table 1-2. entry1 *vs* entry 9). To assess the possible role of $BEt_3$[20], I conducted the reaction using 4-methyl-substituted pyridine with styrene in the absence of or in the presence of 20 mol % of $BEt_3$ (Scheme 1-15). Whereas in the presence of $BEt_3$, C-2 alkylated product was produced in 68% yield, in the absence of $BEt_3$, the reactivity was higher to afford the same product in 92% yield. The result suggests that $BEt_3$ is not likely to function as a Lewis acid to simply increase the electrophilicity of pyridines, but might function to decelerate undesired C-2 alkylation pathway by avoiding access of alkyl cobalt species. At this stage, $BEt_3$ might competitively refrain alkyl cobalt species from coordination by pyridines, which would lead to undesired C-2 alkylation pathway. This steric effect may result in a relative enhancement in the C-4 selectivity for C-4-unsubstituted pyridine derivatives (Scheme 1-16).

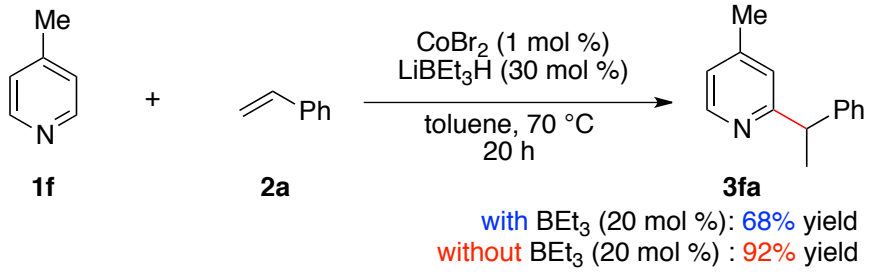


**Scheme 1-15.** Reactions of C-4-substituted pyridines in the presence and absence of $BEt_3$

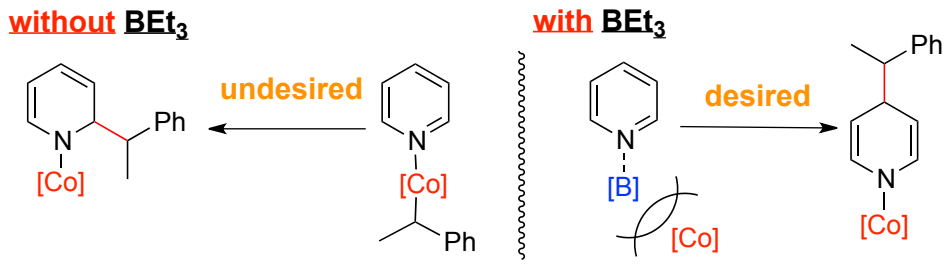


**Scheme 1-16.** Speculation for C-4 selectivity in the presence of $BEt_3$

Although further detailed studies were required to identify the actual role of $BEt_3$, I postulated that $BEt_3$ might alternatively form an organocobalt(0)ate species[21] as active catalytic species, which favored desired C-4 alkylation pathway because an organocobalt(0)ate species was considered to be a soft nucleophilic species. Though I have no direct or indicative experimental information about generation of an organocobalt(0)ate species in my system, the fact that the selection of Lewis acidic additives dramatically influenced both the reactivity and the regioselectivity[14] may suggest that $BEt_3$ possesses the other specific effects than simple Lewis acidic effect or simple steric effect.

## 1-5-3. Is cobalt hydride species actually regenerated *in situ* ?

I assumed that the present catalytic reaction might proceed through hydrocoballation by cobalt-hydride species/ nucleophilic addition to pyridines/ re-aromatization for regeneration of cobalt-hydride species. To confirm catalyst regeneration process, I performed the reaction starting from a postulated cobalt amide **A**, prepared by the method described in Scheme 1-17.

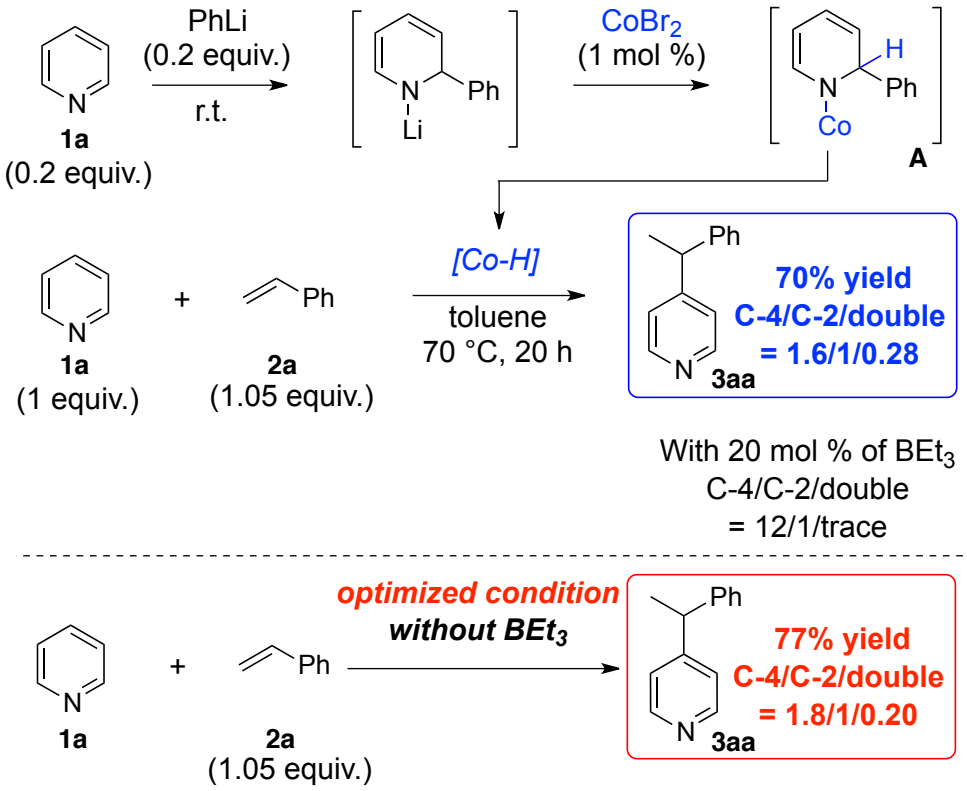


**Scheme 1-17.** In situ generation of active [Co-H] species in the absence of $LiBEt_3H$ and $BEt_3$

First, I mixed 0.2 equiv. of pyridine and 0.2 equiv. of PhLi to afford lithium amide. Then 1 mol % of $CoBr_2$ was added to the reaction mixture to form cobalt amide **A**. I expected that an active [Co-H] species would be generated from the intermediate **A** through β-hydride elimination. Using the presumed [Co-H] species in the absence of $BEt_3$ and $LiBEt_3H$, I obtained alkylated product in similar yield with similar selectivity to the condition without $BEt_3$ shown in entry 1 of Table 1-2. This observation clearly implied the intermediacy and regeneration of [Co-H] species in the actual catalytic cycle.

## 1-6. Conclusion

I have developed a new cobalt catalyst system for the atom-aconomical C-4 selective direct alkylation of pyridines. In the presence of catalytic amount of $CoBr_2$ and catalytic amount of $LiBEt_3H$, the reaction proceeded smoothly to give branched adducts from aromatic alkenes and linear adducts from aliphatic alkenes. All substrates exhibited good to excellent yield with 7.4-> 20/1 branched selectivity, and > 20/1 C-4 selectivity. $BEt_3$ was vital additive to achieve drastic improvement for C-4 selectivity. Though there are no direct evidence, several investigations for mechanistic insight suggest that the reaction might involve hydrometallation/ nucleophilic addition to pyridines[22]/ re-aromatization sequence. Several challenges, however, have remained yet; 1) to expand the substrate scope to other heteroarenes and pyridines with polar functional groups, 2) to clarify the exact reaction mechanism in detail. Further studies for these challenges are ongoing.

## 1-7. References


1. Reviews: a) Joule, J. A. ; Mills, K. *Heterocyclic Chemistry*. 4th ed., Blackwell Publishing, Oxford. 2000, pp. 63-120. b) Henry, G. D. *Tetrahedron* **2004**, *60*, 6043. c) Schlosser, M.; Mongin, F. *Chem. Soc. Rev.* **2007**, *36*, 1161. d) Hill, M. D. *Chem. Eur. J.* **2010**, *16*, 12052. e) Bull, J. A.; Mousseau, J. J.; Pelletier, G.; Charette, A. B. *Chem. Rev.* **2012**, 2642.
2. Review: Gros, P. C.; Fort, Y. *Eur. J. Org. Chem.* **2009**, 4199.
3. For a review on the C-H functionalization of pyridines, see: Nakao, Y. *Synthesis* **2011**, 3209.
4. Trost, B. M. *Science* **1991**, *254*, 1471.
5. Wender, P. A.; Miller, B. L. *Nature* **2009**, *460*, 197.
6. a) Jordan, D. F.; Taylor, D. F. *J. Am. Chem. Soc.* **1989**, *111*, 778. b) Rodewald, S.; Jordan, R. F. *J. Am. Chem. Soc.* **1994**, *116*, 4491. c) Lewis, J. C.; Bergman, R. G.; Ellman, J. A. *J. Am. Chem. Soc.* **2007**, *129*, 5332. d) Tran, L. D.; Daugulis, O. *Org. Lett.* **2010**, *12*, 4277. e) Guan, B.-T.; Hou, Z. *J. Am. Chem. Soc.* **2011**, *133*, 18086.
7. For the directing-group-assisted C3- or C4- selective catalytic functionalization of pyridine derivatives, see: a) Wasa, M.; Worrell, B. T.; Yu, L.-Q. *Angew. Chem. Int. Ed.* **2010**, *49*, 1275. b) Gurbuz, N.; Ozdemir, I.; Cetinkaya, B. *Tetrahedron Lett.* **2005**, *46*, 2273. d) Grigg, R.; Savic, V. *Tetrahedron Lett.* **1997**, *38*, 5737.
8. a) Ye, M.; Gao, G.-L.; Yu, J.-Q. *J. Am. Chem. Soc.* **2011**, *133*, 6964. b) Li, B. J.; Shi, Z.-J. *Chem. Sci.* **2011**, *2*, 488. for a review on Ir-catalyzed regioselective borylation, see: c) Hartwig, J. F. *Chem. Soc. Rev.* **2011**, *40*, 1992.
9. For the functionalization of 2,3,5,6, $F_4$-pyridine, see: a) Wei, Y.; Su, W. *J. Am. Chem. Soc.* **2010**, *132*, 16377. b) He, C.-Y.; Fan, S.; Zhang, X. *J. Am. Chem. Soc.* **2010**, *132*, 12850. c) Wei, Y.; Kan, M.; Wang, W.; Su, M.; Hong, M. *Org. Lett.* **2009**, *11*, 3346. d) Do, H.-Q.; Daugulius, O. *J. Am. Chem. Soc.* **2008**, *130*, 1128. e) Lafrance, M.; Rowley, C. N.; Woo, T. K. Fagnou, K. *J. Am. Chem. Soc.* **2006**, *128*, 8754. for the C-4 selective catalytic silaboration/rearomatization of pyridines, see: f) Oshima, K.; Ohmura, T.; Suginome, M. *J. Am. Chem. Soc.* **2011**, *133*, 7324.
10. a) Nakao, Y.; Yamada, Y.; Kashihara, N.; Hiyama, T. *J. Am. Chem. Soc.* **2010**, *123*, 13666. b) Tsai, C.-C.; Shih, W.-C.; Fang, C.-H.; Li, C.-Y.; Ong, T.-G.; Yap, G. P. A. *J. Am. Chem. Soc.* **2010**, *132*, 11887.
11. a) Isayama, S. : Mukaiyama, T. *Chem. Lett.* **1989**, 1071. b) Waser, J.; Carreira, E. M. *J.*

*Am. Chem. Soc.* **2004**, *126*, 5676. c) Waser, J.; Nambu, H.; Carreura, E. M. *J. Am. Chem. Soc.* **2005**, *127*, 8294. d) Waser, J.; Gaspar, B.; Nambu, H.; Carreira, E. M. *J. Am. Chem. Soc.* **2006**, *128*, 11693. e) Gaspar, B.; Carreira, E. M. *Angew. Chem. Int. Ed.* **2007**, *46*, 4519. f) Gaspar, B.; Carreira, E. M. *Angew. Chem. Int. Ed.* **2008**, *47*, 5758.

12. a) Tobisu, M.; Hyodo, I.; Chatani, N. *J. Am. Chem. Soc.* **2009**, *131*, 12070. for a related work on acridine arylation and alkylation, see: Hyodo, I.; Tobisu, M.; Chatani, N. *Chem. Commun.* **2012**, *48*, 308. c) Seiple, I. B.; Su, S.; Rodriguez, R. A.; Gianatassio, R.; Fujiwara, Y.; Sobel, A. L.; Baran, P. S. *J. Am. Chem. Soc.* **2010**, *132*, 13194. d) Molander, G. A.; Colombel, V. A.; Braz, V. A. *Org. Lett.* **2011**, *13*, 1852. e) for a review, see: Duncton, M. A. *Med. Chem. Commun.* **2011**, *2*, 1135.

13. For other selected examples of non-selective pyridine functionalization by a radical addition/ rearomatiztion, see: a) Yanagisawa, S.; Ueda, K.; Taniguchi, T. Itami, K. *Org. Lett.* **2008**, *10*, 4673. b) Kobayashi, O.; Uraguchi, D.; Yamakawa, T. *Org. Lett.* **2009**, *11*, 2679. c) Li, M.; Hua, R. *Tetrahedron Lett.* **2009**, *50*, 1478.

14. For the preliminary study using 8-methylquinoline as a substrate, trials to enhance regioselectivity by adding the catalytic amounts of Lewis acidic additives were carried out. In the absence of any additives, undesired C-2 adduct was preferentially obtained (entry 1). Addition of Zn, Mg, Al, B additives deteriorated the reactivity and never improved regioselectivity (entries 2-5). On the contrary, I found out that C-2 selectivity was dramatically enhanced in the presence of 20 mol % of $BEt_3$ although C-2 adducts were not desired products (entry 6).

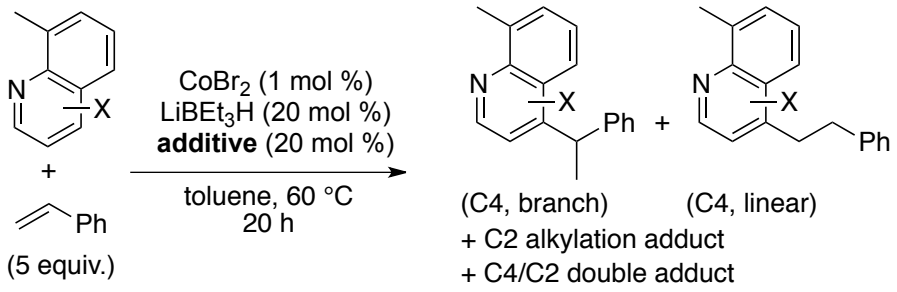


| entry | additive | yield (%) | C2/C4/double product ratio |
|---|---|---|---|
| 1 | none | > 99 | ~4/1/0 |
| 2 | $Zn(OTf)_2$ | 28 | 1.5/1/0 |
| 3 | $MgCl_2$ | 49 | 5.1/1/0 |
| 4 | $Al(OTf)_3$ | 0 | - |
| 5 | $B(C_6F_5)_3$ | 0 | - |
| 6 | **$BEt_3$** | 85 | **18.9/1/0** |

For our work on C-4 selective alkylation of quinolines, see: Yamamoto, S.; Saga, Y.; Andou, T.; Matsunaga, S.; Kanai, M. *Adv. Synth. Cat.* **2014**, *356*, 401.

15. HMPA without $BEt_3$ was not effective, giving alkylated products with modest selectivity (87 % yield, C-4/C-2/double = 3.2/1/0.1)
16. In Table1-4, HMPA (30 mol %) was added only when there remained room for improvement in the C-4 selectivity.
17. For a similar discussion, see: Nakao, Y.; Kashihara, N.; Kanyva, K.S.; Hiyama, T. *Angew. Chem. Int. Ed.* **2010**, *49*, 4451.
18. For a review on Co-catalyzed C-H activation, see: a) Yoshikai, N. *Synlett* **2011**, 1047.; for a general review on Co-catalyzed cross coupling reactions, see: b) Cahiez, G.; Moyeux. *Chem Rev.* **2010**, *110*, 1435.
19. a) Gao, K.; Yoshikai, N. *J. Am. Chem. Soc.* **2011**, *133*, 400. b) Gao, K.; Lee, P.-S.; Fujita, T.; Yoshikai, N. *J. Am. Chem. Soc.* **2010**, *132*, 12249. Fo selected resent examples of other Co-catalyzed C-H functionalization reactions, see: c) Chen, Q.; Ilies, L.; Nakamura, E. *J. Am. Chem. Soc.* **2011**, *133*, 428. d) Li, B.; Wu, Z.-H.; Gu, Y.-F.; Sun, C.-L.; Wang, B.-Q.; Shi, Z.-J. *Angew. Chem. Int. Ed.* **2011**, *50*, 1109. e) Song, W.; Ackermann, L. *Angew. Chem. Int. Ed.* **2012**, *51*, 8251.
20. To avoid oxygen contamination of the reaction vial, all experiments were performed in a glove box ($O_2$: < 0.5 ppm). Thus, the possibility that $BEt_3$ acts as a radical initiator is less probable.
21. For representative catalytic reactions through organocobalates, see: a) Wakabayashi, K.; Yorimitsu, H.; Ohshima, K. *J. Am. Chem. Soc.* **2001**, *123*, 5374. b) Czaplik, W. M.; Mayer, M.; Jacobi von Wangelin, A. *Synlett* **2009**, 2931. Ding, Z.-H.; Yoshikai, N. *Org. Lett.* **2010**, *12*, 4180
22. The actual nucleophilic species has not identified yet. Two possible candidates were considered. One is the alkyl cobalt species, which would provoke the nucleophilic addition in anionic fashion. The other is the radical species formed by homolytic cleavage from the alkyl metal species, which would provoke the nucleophilic addition in radicalic fashion. In order to clarify the actual nucleophilic species, the reactions with 3-methyl pyridines as substrates in the presence of and in the absence of TEMPO radicals were conducted. The reaction in the presence of 20 mol % of TEMPO was markedly suppressed, while the reaction in the absence of TEMPO proceeded smoothly to afford the product in 89% yield. Although it is possible that the addition of TEMPO might inhibit the radicalic pathway,

the addition of TEMPO could inhibit also the anionic pathway because the reaction with the substrate bearing polar functional groups was poor. From the study, no conclusions for the actual nucleophilic species were drawn.

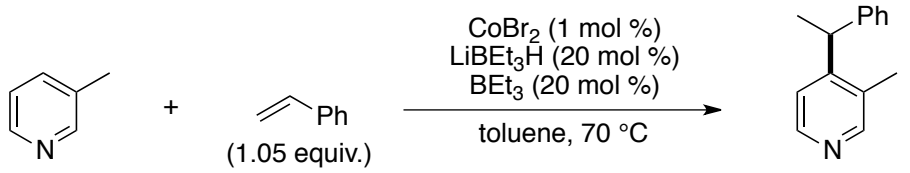


in the absence of TEMPO (20 mol %): 89% (>20/1/0)

in the presence of TEMPO (20 mol %): 7% (>20/1/0)

# 2. Radical-Conjugated Redox Catalysis (RCRC) for the Dehydrogenation of *N*-Heterocycles

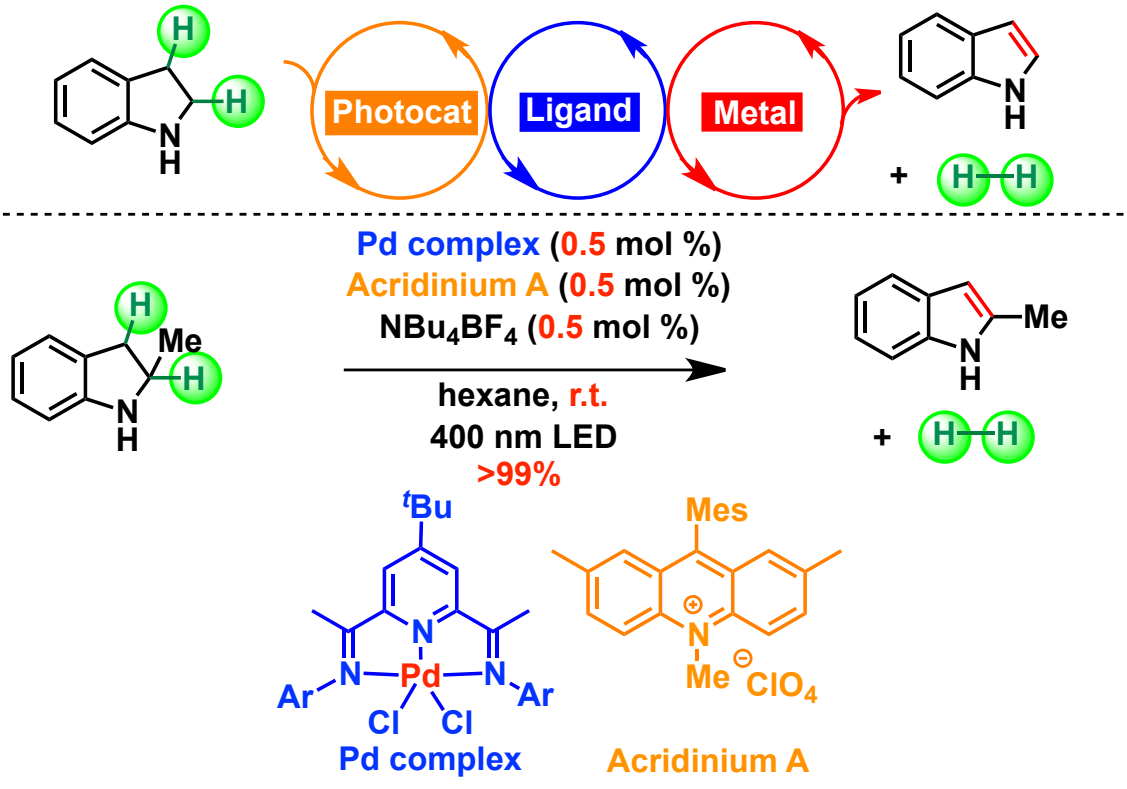

## 2-1. Research Background

### 2-1-1. Toward $H_2$-based energy society

The current energy generation system is vastly based on the carbon-based carriers, like fossil fuels, oils, and natural gases[1]. Considering long-term sustainable energy supply, these energy carriers are not suitable because of two basic factors; 1) such carbon-based carriers are finite resources, 2) the carbon dioxide gas released during the combustion of carbon-based carriers is reported to cause severe damages to the environment by bringing about drastic climate changes[2].

According to the current urgent situation, it is announced that *hydrogen gas* would be one of the ideal and alternative energy carriers because hydrogen gas is sustainable energy fuels that can be generated from water and liberates only water after work. In order to shift from the current carbon-based energy carriers towards ideal 'hydrogen economy'[3], we have to overcome the technological and social obstacles for three key stages (Figure 2-1); 1) the production of hydrogen gas, 2) the storage and transportation of hydrogen gas, 3) the conversion of chemical energy to electronic energy.

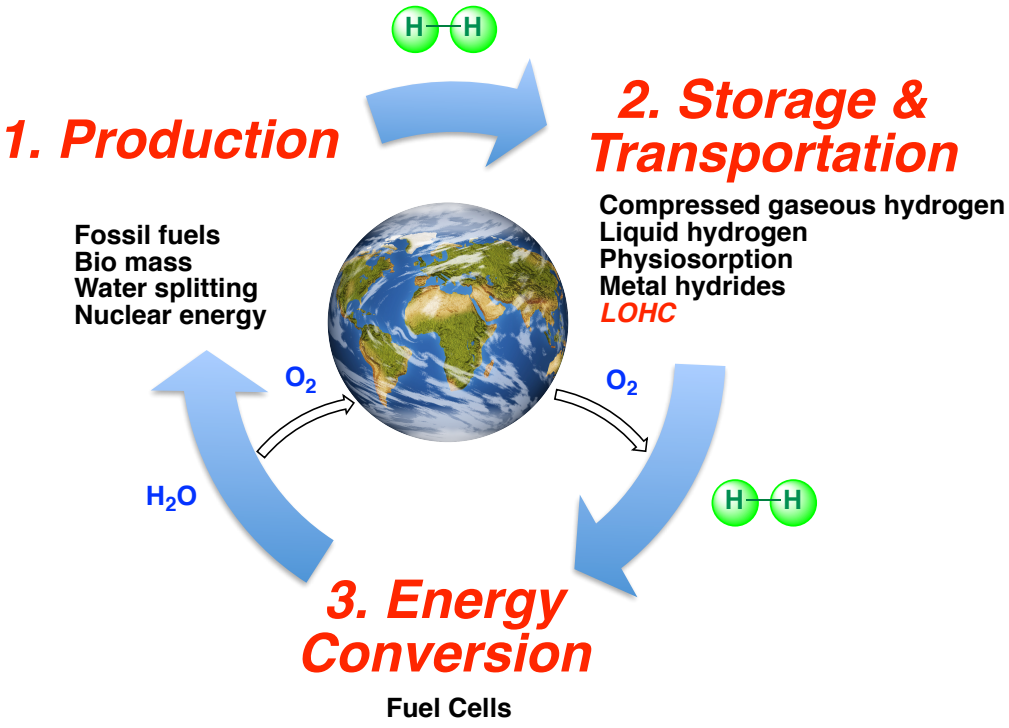


**Figure 2-1**. Three key stages for ideal hydrogen society

## 2-1-2. Production of $H_2$

**Hydrocarbons**

At present, a vast majority of hydrogen gas is produced by steam reforming on hydrocarbons[4]. Although this method is not appropriate because such fossil fuels, of course, generate undesirable carbon dioxide gas, the new technologies for capture and sequestration of carbon dioxide gas[4c] is under development, especially using coals and methane. However, coals are non-renewable. More sustainable and reliable methods are strongly required.

**Biomass**

The second candidate is the use of biomass[5]. Biomass is constituted of numerous materials, such as agricultural residues, wood processing and photosynthetic microbes. Hydrogen gas can be produced by gastification and pyrolysis using biomass materials.

**Water splitting**

Water splitting technique through electrolysis, photo-electrolysis and high temperature decomposition is one of the attractive and clean methodologies for the production of hydrogen gas[6]. While photo-electrolysis by solar energy is recognized as advantageous way among them, innovative improvements on low-cost and efficient hydrogen production using sun light is necessary for practical applications.

**Nuclear energy**

Nuclear energy is also utilized for the production of hydrogen gas by using thermochemical electrolysis of water. It is considered, however, to be hardly clean method because it causes the dangerous and hazardous radioactive compounds.

## 2-1-3. Conversion to electrical energy

A Fuel cell is an efficient and ultimately clean device, which produces electricity by combining hydrogen with oxygen without processing combustion[7]. The most general hydrogen fuel cell is a proton exchange membrane (PEM) fuel cell (Figure 2-2)[8a]. In the PEM fuel cell, hydrogen gas is split into two electrons and two protons at the anode side. Protons are transferred to the cathode side through a polymer membrane, while electrons are delivered to the cathode side via an external circuit. During the transition, the electrical energy can be produced. On the other hand, transferred protons, electrons and oxygen are combined at the cathode to generate water as a green waste.

PEM fuel cells can convert 30-45% of chemical energy in hydrogen into electrical energy, and 35-40% of that into heat energy. The maximum efficiency is considered to reach up to 85%. It is noteworthy that fuel cells exhibit high scalability, which enables a broad application from cell-phones to automobiles.

In future, several technological obstacles in terms of cost reduction and higher performance of each component have to be solved[8b,c].

Proton exchange membrane (PEM) hydrogen fuel cells

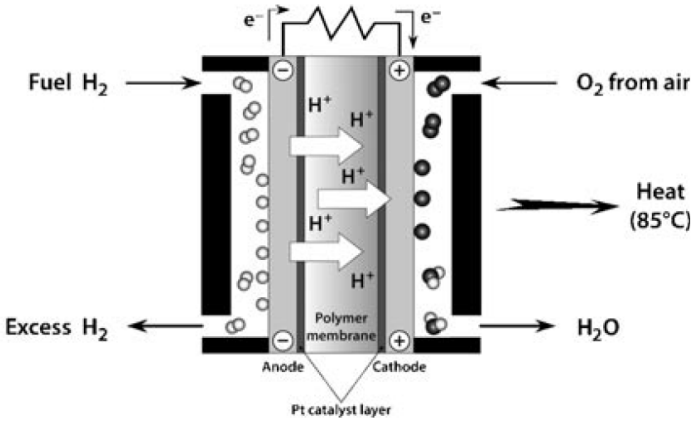


Balzani, V. *et al. ChemSusChem* **2011**, *4*, 21

Anode side

$$H_2 \longleftrightarrow 2H \longleftrightarrow 2H^+ + 2\,e$$

Cathode side

$$1/2\,O_2 + 2H^+ + 2\,e \longleftrightarrow 2H_2O$$

$$2\,H_2 + O_2 \longrightarrow 2H_2O$$

**Figure 2-2**. PEM fuel cells

## 2-1-4. Storage and transportation of $H_2$

Storage and transportation of hydrogen gas is also a critical technology to realize hydrogen-based energy system[9a]. It is claimed that there are four key requirements to be considered for an ideal storage transportation carrier[9b]: 1) Safe, feasible and environmentally benign handling 2) Production of sufficient energy with low cost 3) Compact and light for mobility. Whereas the volume and high weight are not major concerns in stationary use like domestic or industrial scales, in transportation use like automobiles, these two factors should be considerably restricted. 4) Availability of the exiting energy infrastructure such as tank ships, storage tanks and fueling stations. Based on these important criteria, several storage-transportation systems in physical and chemical manner have been intensively studied.

**Compressed hydrogen**

Hydrogen gas itself possesses a high energy density by weight (33.3 Wh $kg^{-1}$) but a poor energy density by volume (2.5 Wh $L^{-1}$). In order to improve the energy per volume ratio, it is necessary to compress hydrogen gas into adequate volume for applicable space. Indeed, newly developed tanks can keep hydrogen gas under 350 or 700 atm[3d]. However, there are many problems to be solved in this method. First, the special tanks made from new composite materials are very expensive. In addition, compression of hydrogen gas requires about 10-15% of the energy content of hydrogen.

**Liquid hydrogen**

Liquid hydrogen is another alternative. However, it is stated that hydrogen gas is the most difficult gas to liquefy and about 30-40% of the energy content of the hydrogen gas is consumed for its liquefaction[3d]. Besides, hydrogen leaks from tanks is expected to provoke the serious accidents.

**Physisorption**

In physisorption method, hydrogen gas is absorbed onto porous organic solids like activated carbon, carbon nanotubes, fullerenes and graphene. It is required that materials contain specific surface areas as large as possible for sufficient hydrogen absorption[10a]. Recently many researchers have paid considerable attention to microporous metal organic framework (MOF) materials as attractive candidates for hydrogen storage because chemists are able to modify the

pore structure in chemical manner[10b].

**Metal Hydrides**

Hydrogen gas can be absorbed into many metals and metallic alloys as metal hydrides such as NaH, $LiBH_4$ and $NaBH_4$. Metal hydrides are advantageous regarding their compact character compared with other carriers and applicability for the exiting cars[11]. On the other hand, their gravimetric energy capacities are quite poor and the maximum material $NaAlH_4$ can contain energy capacity of only 5.5 wt% hydrogen, which is still lower than the original United States Department of Energy (DOE) target for 2010 of 6 wt %[3d]. Difficult reversible uptake of hydrogen gas is another critical concern.

## 2-1-5. Liquid Organic Hydrogen Carriers (LOHC)

Among above several candidates, it is deduced that Liquid Organic Hydrogen Carriers (LOHC) are the best carriers for realization of hydrogen-based energy society[12]. LOHC is pronounced to meet all four key tasks required for hydrogen-transportation material (Section 2-1-4): 1) LOHC can be safe, non-toxic, non-explosive and chemically stable liquid fuels compared with compressed gaseous hydrogen and liquid liquefied hydrogen. 2) Storage energy density of LOHC is much higher than other carriers taking into account power generation losses[12] (Fig 2-3 a). 3) Regarding mobility, energy density of LOHC both by weight and volume is much greater than other systems[12] (Fig 2-3 b). 4) We can receive many benefits by step-wise transition from the current fossil fuels to LOHC because LOHC compounds are similar to gasoline and diesel and are applicable for the exiting infrastructure.

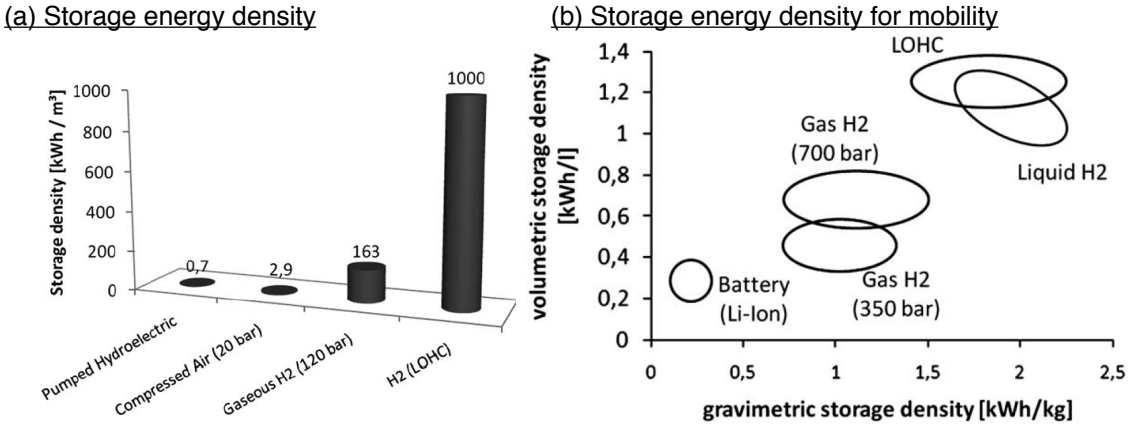


Teichmann, D. *et al. Energy Environ. Sci.*, **2011**, *4*, 2767

**Figure 2-3**. Storage energy density for various storage systems

The conceptual flow in LOHC storage system is depicted in Fig 2-4[12]. Electrolysis device first produces hydrogen gas. Resulting hydrogen is used for uptake in LOHC by a catalytic hydrogenation reaction. LOHC can be transported to desired places and stored in storage tanks until the need of energy. At a desired time, hydrogen gas is released by a catalytic dehydrogenation reaction. Liberated hydrogen gas can be utilized for the conversion to electric energy by fuel cell devices.

Hydrogenation reactions of aromatic LOHC in large scale are established methods in industry. On the contrary, dehydrogenation process especially for the usage in vehicles is not standard

process because the dehydrogenation reactions are in general performed using noble metals at 200-230 °C.

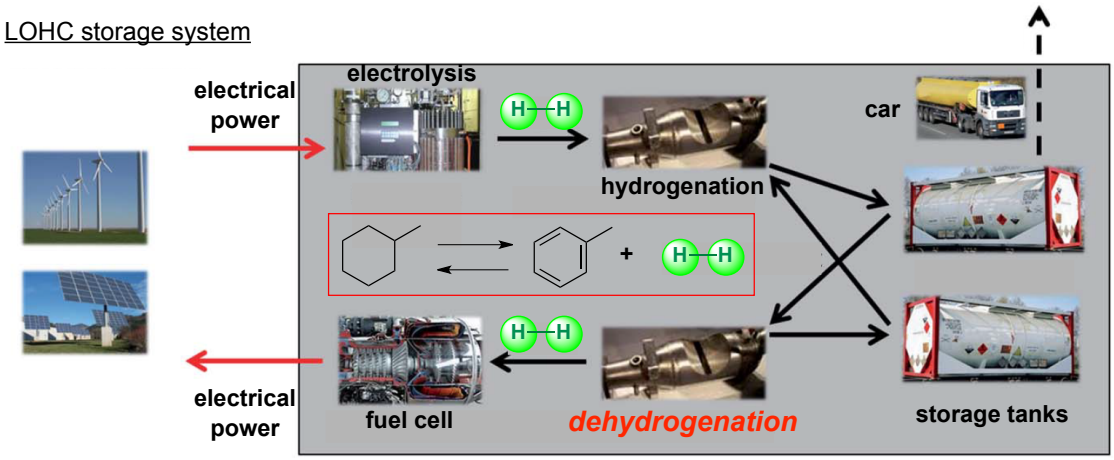


Teichmann, D. *et al. Energy Environ. Sci.*, **2011**, *4*, 2767

**Figure 2-4**. Concept of an ideal electricity cycle by intervention of storage devices using LOHC

## 2-1-6. *N*-Heterocycles as ideal carriers

Whereas LOHC is the most attractive hydrogen storage-transportation carrier, the dehydrogenation reactions of LOHC is reported to be unfavorable both in kinetic and thermodynamic aspects. In contrast, Pez and co-workers proposed in the patent[13] that the incorporation of nitrogen atom into LOHC accelerates the dehydrogenation reactions by computational and experimental analysis.

Crabtree/Eisenstein and co-workers investigated the thermodynamic data per hydrogen gas released ($\Delta H_d$, $\Delta G_d$, $\Delta S_d$; B3PW91/aug-cc-pVDZ calculations) for the conversions from saturated LOHC to unsaturated LOHC[14]. In order to indicate the effects on thermodynamic data after incorporation of nitrogen atom, they used a temperature $T_d$ value, which refers the temperature at which the calculated $\Delta G$ gets zero. Although experimental hydrogen release temperature is expected to differ from the calculated $T_d$ value, they insisted that the thermodynamic trends in various LOHC could be discussed using $T_d$ value.

The thermodynamic data for selected model LOHC compounds are summarized in Figure 2-5[14]. The results obviously show that incorporation of nitrogen atom into LOHC compounds preferred the dehydrogenation by decreasing $T_d$ value. The effects are simply attributed to the facts that an N-H bond is weaker than a C-H bond and C-H bonds adjacent to a nitrogen atom are also weakened. They also insisted that a five-membered ring is more favored for the dehydrogenation because a five-membered system requires four C-H cleavage for aromatic stabilization while a six-membered one needs five C-H cleavage. In extreme case, $T_d$ value can get lower than 50 K in a five membered nitrogen containing LOHC (Figure 2-5).

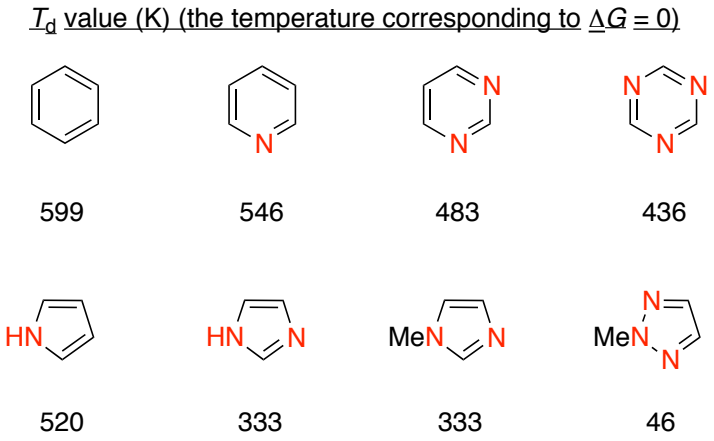


**Figure 2-5**. Thermodynamic hydrogen release temperatures by DFT calculations

## 2-1-7. Precedent reports for the dehydrogenation of *N*-heterocycles

Despite the favored property of *N*-heterocyclic compounds, the examples for the homogeneous dehydrogenation of *N*-heterocycles without using any acceptors are quite limited. Although several examples for heterogeneous systems[15] and oxidative systems with oxidants like oxygen or peroxide without releasing hydrogen gas[16] are developed, it was only recently that the first report for homogeneous dehydrogenation of *N*-heterocycles emerged. In 2009, Fujita and Yamaguchi group disclosed the first catalytic homogeneous system for the dehydrogenation reaction of *N*-heterocycles using an Ir catalyst[17a] (Scheme 2-1). They also illustrated that the same catalyst was effective for reversible hydrogenation and dehydrogenation of *N*-heterocycles. They suggested that the catalyst was converted to a hydride-bridged Ir dinuclear complex under hydrogen atmosphere. By DFT calculation studies, other groups postulated that the ligand promoted hydrogen abstraction from substrates without changing the oxidation state of Ir metal[18].

In 2014, the same group succeeded the first homogeneous perdehydrogenation reaction of fused bicyclic *N*-heterocycles[17b]. They proposed that the use of a new Ir complex bearing a rigid functional 1,10-phenanthroline-2,9-dione ligand was key to success. The same catalyst was also applicable for reversible perhydrogenation reaction though the hydrogen pressure was quite high (70 atm).

First example for the dehydrogenation of *N*-heterocycles

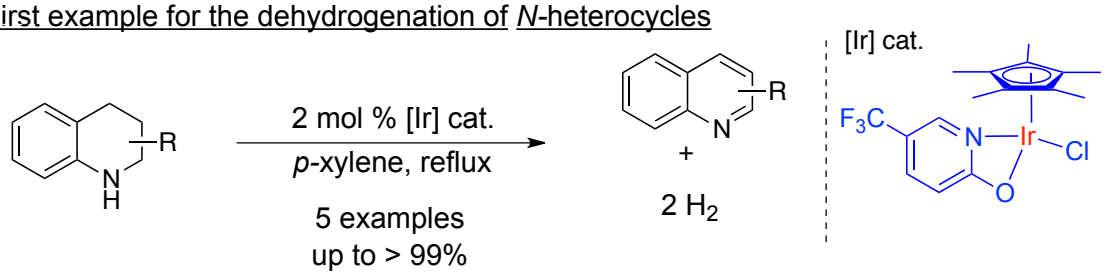


Fujita, K.; Yamaguchi, R. *et al. J. Am. Chem. Soc.* **2009**, *131*, 8410.

Reversible hydrogenation and dehydrogenation

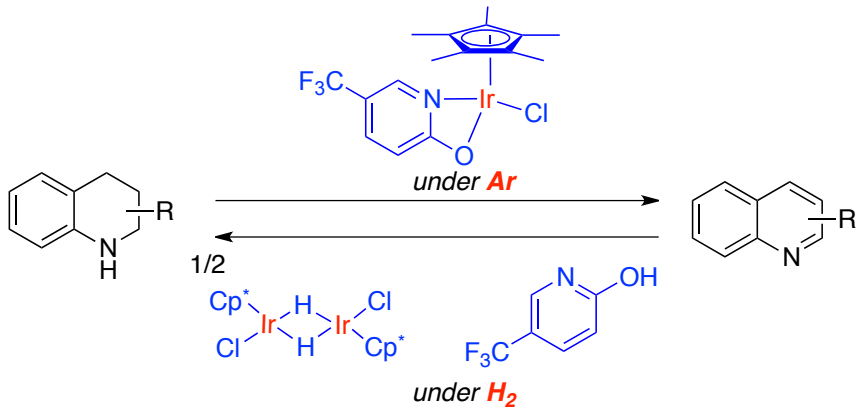


First example for the perdehydrogenation of bicyclic *N*-heterocycles

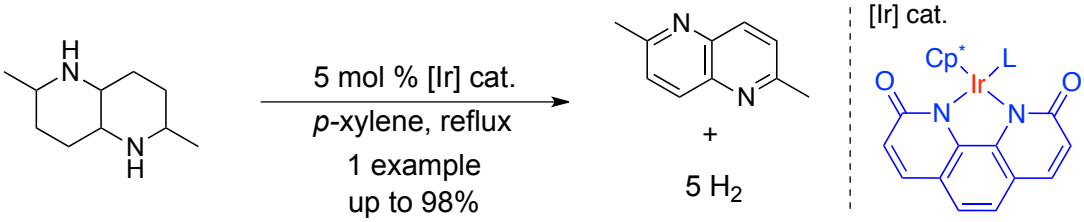


Fujita, K.; Yamaguchi, R. *et al. J. Am. Chem. Soc.* **2014**, *136*, 4829.

**Scheme 2-1**. Pioneering works by Fujita and Yamaguchi group

Pioneered by Fujita and Yamaguchi works, well-defined Ir catalysts for acceptorless dehydrogenation were developed[19, 20] (Scheme 2-2). In 2009, Jensen and co-workers reported the dehydrogenation of *N*-ethyl perhydrocarbazole compound using a POCOP pincer iridium complex[19a]. Though dehydrogenation to the fully unsaturated *N*-ethyl carbazole was not observed in most cases, *N*-ethyl octahydrocarbazole and *N*-ethyl tetrahydrocarbazole were obtained. They also applied the similar catalyst for perdehydrogenations of several compounds such as perhydrodibenzofuran and perhydroindole, but generally resulted in unsatisfactory reactivities[19b].

Inspired by the Fujita/Yamaguchi Ir catalyst, Xiao *et al*. developed a new cyclometalated Ir catalyst for the acceptorless dehydrogenation of *N*-heterocyclic compounds[20]. It was remarkable that their catalyst was effective for various types of *N*-heterocycles such as indolines, quinolines and isoquinolines with a low catalyst loading. They pronounced that TFE solvent was essential for both dissociation of halides from catalysts and protonation of metal hydride species to accelerate the release of hydrogen gas.

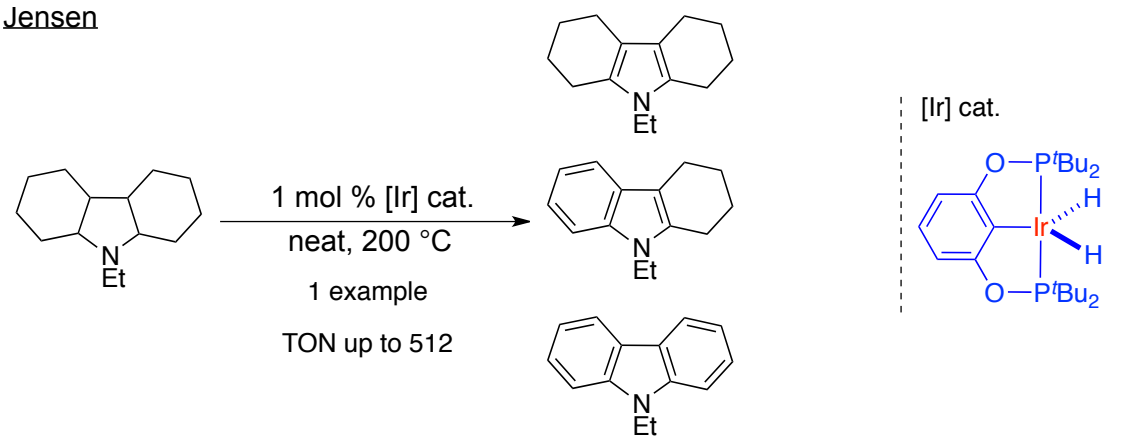


Jensen, *et al. J. Organomet. Chem.* **2009**, *694*, 2854., *Faraday Discuss.* **2011**, *151*, 297.

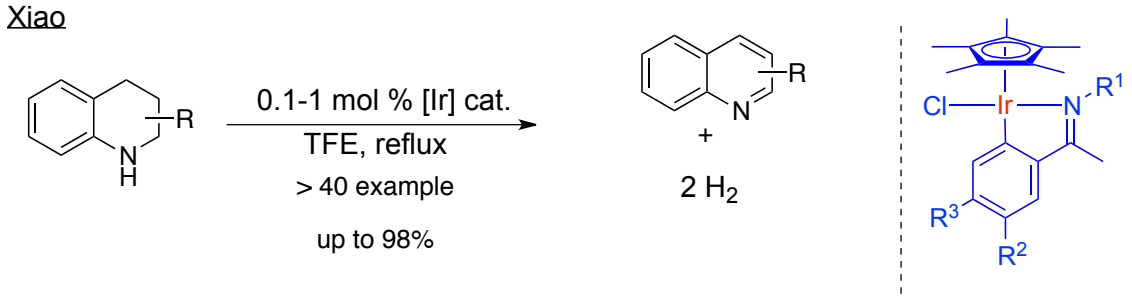


Xiao, J. *et al. Angew. Chem. Int. Ed.* **2013**, *52*, 6983.

**Scheme 2-2**. Precedents for the dehydrogenation of *N*-heterocycles with Ir complex

The use of inexpensive earth-abundant base metal catalysts is highly desirable. Only recently, two groups achieved the base-metal catalyzed acceptorless dehydrogenation of *N*-heterocyclic compounds[21] (Scheme 2-3). Crabtree group reported the electrocatalytic dehydrogenation of tetrahydroquinaldine with a Ni complex bearing a quinone-NHC carbene conjugated ligand[21a]. They insisted that the Ni complex was an effective molecular catalyst to realize the electrode-driven ($H^+ + e^-$) release of hydrogen gas at room temperature. However, the use of expensive Pt electrode is not approved. In 2014, Jones *et al*. demonstrated the acceptorless Fe-catalyzed dehydrogenation of *N*-heterocyclic compounds[21b]. A molecular Fe-based catalyst with a PNP pincer ligand, which is also used for several chemical conversions, proved to be vital for the reaction. They also succeeded in the reversible hydrogenation of saturated compounds under 5-10 atm of hydrogen atmosphere.

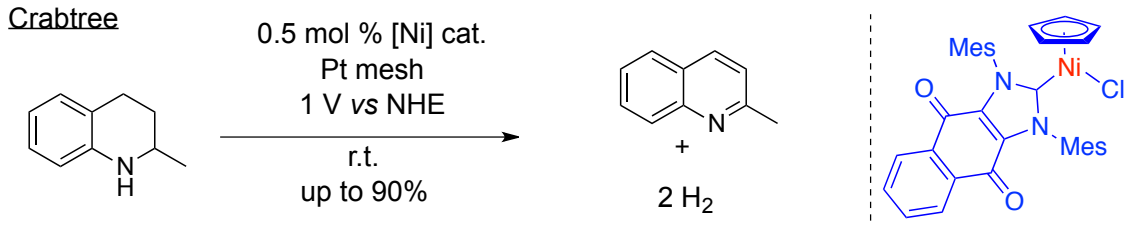


Crabtree, R. H. *et al. New. J. Chem.* **2013**, *37*, 3402.

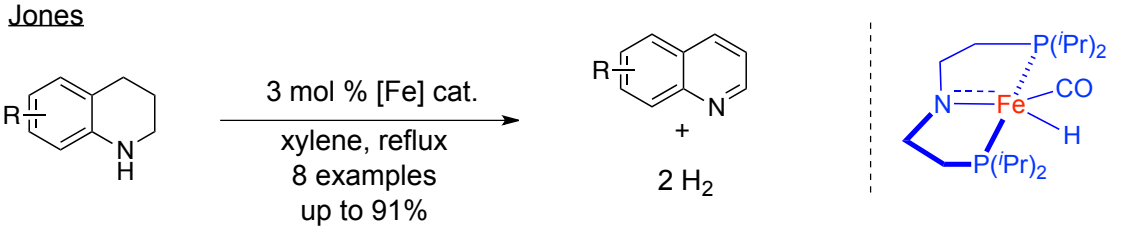


Jones, W. D. *et al. J. Am. Chem. Soc.* **2014**, *136*, 8564.

**Scheme 2-3**. Precedents for the dehydrogenation of *N*-heterocycles with base-metal catalysts

## 2-2. Reaction Design

Although several fine-tuned catalysts for the dehydrogenation of *N*-heterocycles have been developed, they all required quite harsh reaction conditions (in almost all cases at >100 ℃). There remain rooms for improvements especially in terms of reaction temperature.

I envisioned that *Radical-Conjugated Redox Catalysis (RCRC) concept*, which involves one-electron mediation, might be an alternative and potentially attractive solution to the current problem. Inspired by two key catalysis concepts as discussed in more detail below, I determined to establish new cooperative RCRC system and achieve the dehydrogenation of *N*-heterocycles under mild conditions.

## 2-2-1. Dual catalysis merging a photo-catalyst with another catalyst

First concept is the *dual catalyst system merging a photo-catalyst with another catalyst*. Nature can fruitfully convert solar energy to chemical energy in photosynthesis. Chemists have also developed several organic and inorganic photo-catalysts which can mimic the Nature's ability. Photo-catalysts, upon irradiation with visible light, excite an electron from HOMO to LUMO, and generates a relatively long-lived triplet exited state[22]. This reactive intermediate has an ability to be both a stronger one-electron reductant and oxidant than the ground state[23]. Based on the powerful activation mode of photo-catalysts to mediate one-electron redox process, dual catalyst concept[24] merging the photo-catalyst with another catalyst[25] has recently emerged for the one-electron mediated chemical reactions involving radical species or single-electron intermediates.

*Photo-catalyst with enamine catalyst*

A landmark work was reported by MacMillan group in 2008 using a dual catalyst system merging photo-catalyst and enamine catalyst[26] (Scheme 2-4). In the presence of 0.5 mol % of $[Ru(bpy)_3]Cl_2$ as a photo-catalyst and 20 mol % of MacMillan's catalyst, the first catalytic intermolecular enantioselective α–alkylation proceeded to afford the products with high enantioselectivity. In a postulated mechanism, the condensation of an imidazolidinone catalyst and an aldehyde to form an enamine intermediate initiates the catalytic cycle. Reduction of an alkyl halide by the photo-catalyst generates an electrophilic alkyl radical, which couples with chiral enamine intermediate. One-electron oxidation of the resulting α-amino stabilized radical intermediate by the oxidized photo-catalyst, followed by hydrolysis produces the enantio-enriched product. They intensively expanded the concept of merging photo-catalyst and enamine catalyst to α-perfluoroalkylation[27a], α-benzylation[27b] and β-functionalization of aldehydes[27c] and ketones[27d].

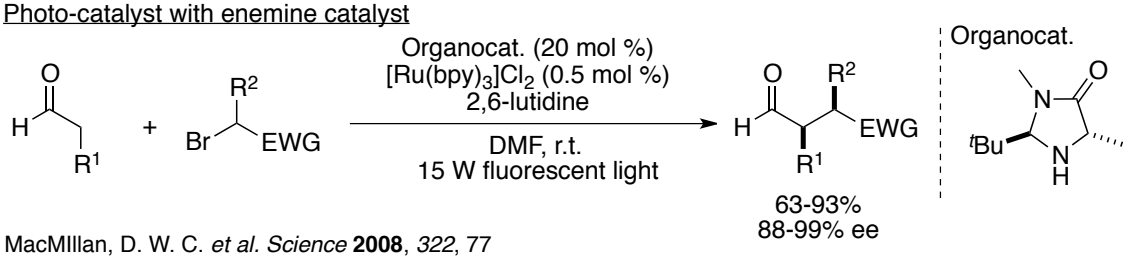


**Scheme 2-4**. Merging photo-catalyst with enamine catalyst

*Photo-catalyst with NHC carbene catalyst*

In 2012, Rovis *et al*. achieved catalytic asymmetric α-acylation of tertiary amines using a dual catalysis merging a photo-catalyst with an NHC carbene catalyst[28] (Scheme 2-5). Their strategy consists of two distinct activation modes; one is generation of highly nucleophilic Breslow intermediates from aldehydes and an NHC carbene, the other is formation of electrophilic iminium ions through photoinduced oxidation of tetrahydroisoquinolines. The presence of 1,3-dinitrobenzene (*m*-DNB) was proposed to be essential for high reactivity as an oxidative quencher of photo-catalysts.

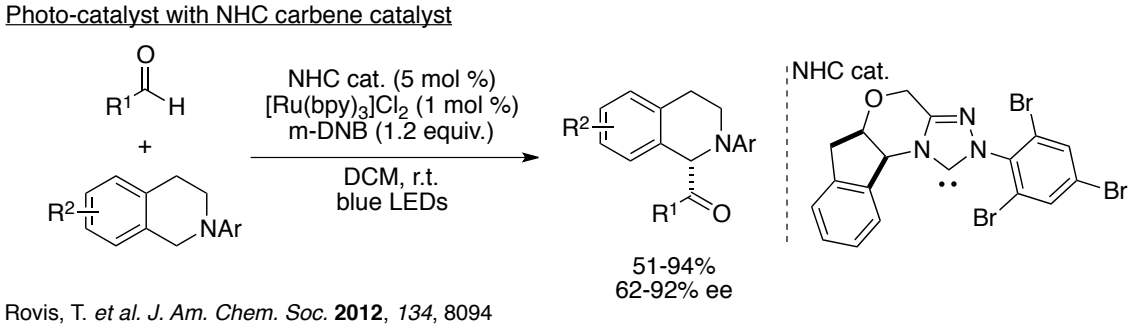


**Scheme 2-5**. Merging photo-catalyst with NHC-carbene catalyst

*Photo-catalyst with hydrogen-bonding catalyst*

In 2014, Jacobsen and Stephenson *et al*. established a dual catalysis merging photo-catalyst and anion-binding organocatalyst for the enentioselective synthesis of β-amino esters[29] (Scheme 2-6). Photo-catalysts were used for generation of iminium cations by photoredox-mediated oxidation. On the other hand, a chiral thiourea can function as an activator of the resulting iminium cation through binding of a chloride anion. A tight ion pair between iminium cations and a chloride anion activated by well-tuned chiral thiourea was key to realize the high enantioinduction.

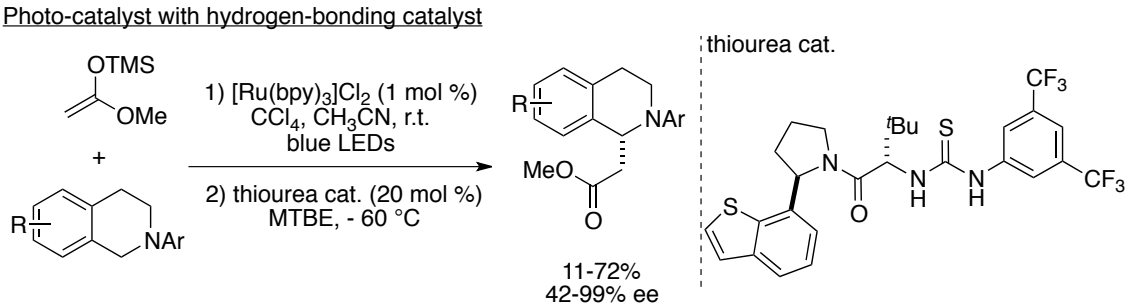


Jacobsen, E. N.; Stephenson, C. R. *et al. Chem. Sci.* **2014**, *5*, 112

**Scheme 2-6.** Merging photo-catalyst with hydrogen-bonding catalyst

*Photo-catalyst with acid catalyst*

Acid catalysis can be successfully merged with photo-catalyst for several useful chemical reactions. Knowles group addressed a dual catalyst concept merging photo-catalyst and Brønsted acid catalyst and succeeded in catalytic asymmetric aza-pinacol cyclization reaction[30a,b] (Scheme 2-7). They proposed that PCET process, which involves simultaneous one-electron reduction by photo-catalyst and protonation by chiral phosphoric acid catalyst, was critical for radical generation. Subsequent intramolecular radical addition to alkene followed by hydrogen abstraction provided the desired enantio-enriched products. Similarly, Lewis acid catalysts were revealed to be applicable for a related dual system with photo-catalyst. Only recently, Oisaki and Kanai *et al*. developed chemoselective aerobic photo-oxidation of fluorene derivatives using the combination of photo-catalyst and copper-salt[30c]. Although there is no direct experimental evidence, they anticipated that a copper salt might work as a Lewis acid to activate generated radical peroxygen species.

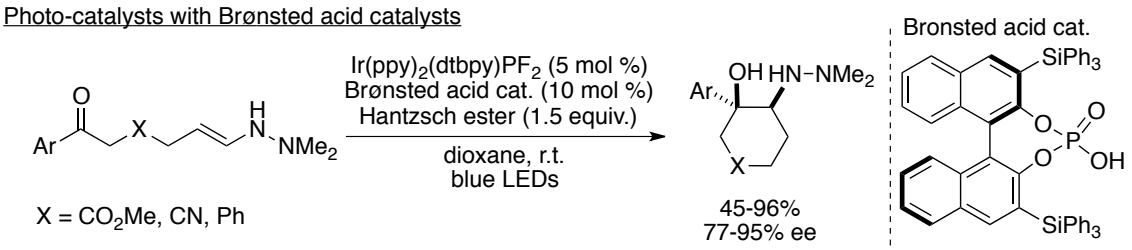


Knowles, R. R. *et al. J. Am. Chem. Soc.* **2013**, 135, 10022., *J. Am. Chem. Soc.* **2013**, 135, 17735

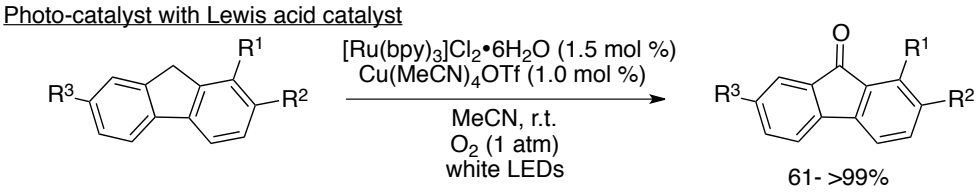


Oisaki, K.; Kanai, M. *et al. Tetrahedron Lett.* **2014**, *in press*

**Scheme 2-7.** Merging photo-catalysts with acid catalysts

*Photo-catalyst with transition metal catalyst*

A dual catalyst concept combining photo-catalyst with transition metal catalyst has been advanced in a recent few years (Scheme 2-8). In 2011, Sanford group described the chelation-directed $sp^2$ C-H arylation reaction catalyzed by a dual catalysis merging photo-catalyst with Pd catalyst[31a]. It was of note that the reaction could be conducted at room temperature. Requirement of high reaction temperature in their previous report prompted them to pursue the alternative and mild catalyst system. Photo-catalyst was proposed to function both as a one-electron reductant to generate aryl radical species from diazonium salt and as a one-electron oxidant of Pd catalyst. The dual activation mode allowed to form key reactive Pd(IV) species under ambient conditions.

Sanford group also succeeded in the application of similar dual activation system with photocatalyst/Cu combination for trifluoromethylation of aryl boronic acid derivatives[31c]. Their strategy included simultaneous generation of trifluoromethyl radical species and Cu(III) intermediates.

In 2013, Glorius and co-workers developed a dual catalyst with photo-catalyst with gold complex for intramolecular oxy- and aminoarylation of alkenes[31d]. No requirements of stoichiometric amounts of strong oxidants were noteworthy.

Photo-catalyst with Pd catalyst

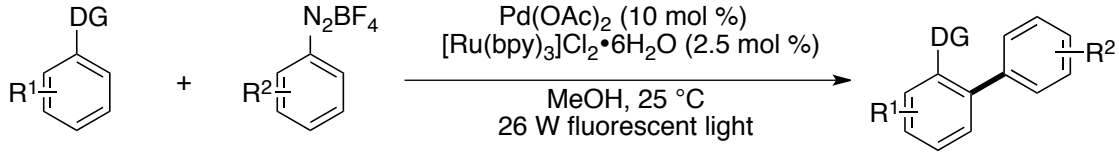


DG = Directing Group

44-87%

Sanford, M. *et al. J. Am. Chem. Soc.* **2011**, *133*, 18566

Photo-catalyst with Cu catalyst

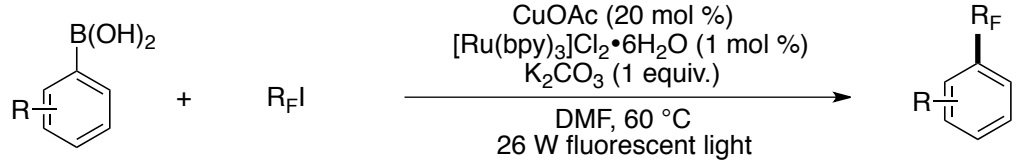


$R_F$ = $CF_3$, $C_4F_9$, $C_{10}F_{21}$

39-97%

Sanford, M. *et al. J. Am. Chem. Soc.* **2012** *134*, 9034

Photo-catalyst with Au catalyst

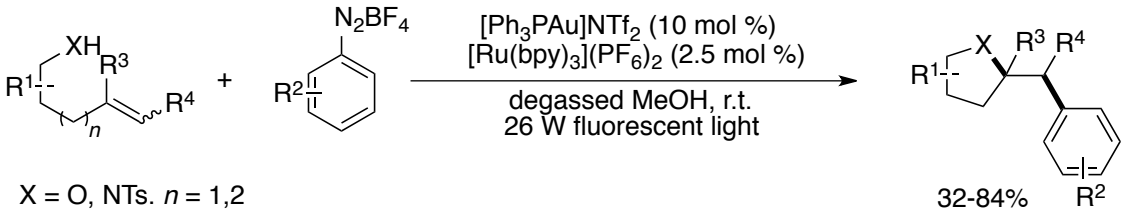


X = O, NTs. *n* = 1,2

32-84%

Glorius, F. *et al. J. Am. Chem. Soc.* **2013**, *135*, 5505

**Scheme 2-8.** Merging photo-catalyst with transition metal catalyst

## 2-2-2. Redox non-innocent ligand

Second concept is the *redox non-innocent ligand* concept[32]. Ligands have played critical roles in transition metal complexes. In general, vital roles of ligands are the steric and electronic modifications in metal complexes, while the fundamental chemical conversions and redox process occur at metal centers. In contrast, the recent new strategy involves the use of special ligands, which are able to play a critical role in chemical bond-forming reactions and redox mediations. Various types of such *redox non-innocent ligands* are reported and synthesized based on Nature's enzyme active sites like the copper (II) radical site of galactose oxidase enzyme[33] (Figure 2-6).

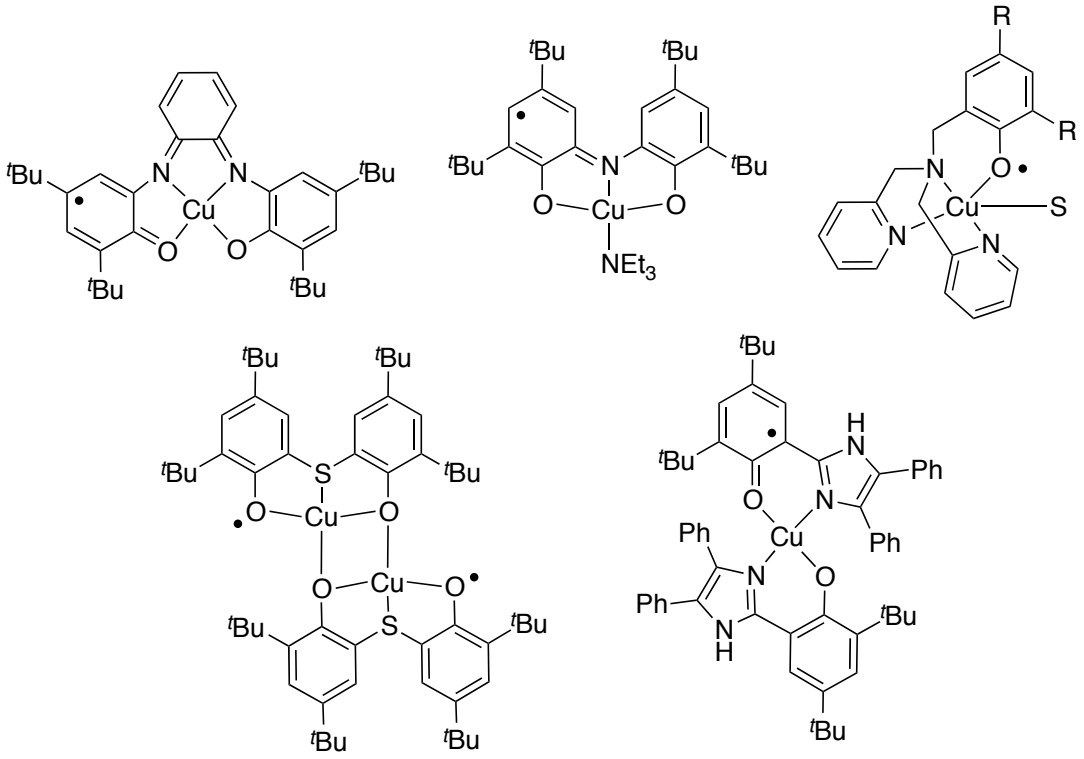


Thomas, F. *et al. Eur. J. Inorg. Chem.* **2007**, 2379

**Figure 2-6.** Biomimetic redox non-innocent complexes

Recently, several useful chemical conversions using redox non-innocent ligand have been actively developed. Strategies making use of redox non-innocent ligand can be divided into four main modes[32c] (Figure 2-7). Strategy I aims at tuning of the Lewis acidity of the metal through one-electron oxidation/reduction in a ligand. In strategy II, a ligand bearing radicalic character aggressively participates in the making and breaking of chemical bonds. Cooperative function of a ligand with a metal might realize a new chemical catalytic bond formation. Strategy III involves the activation and tuning of a substrate in radicalic fashion.

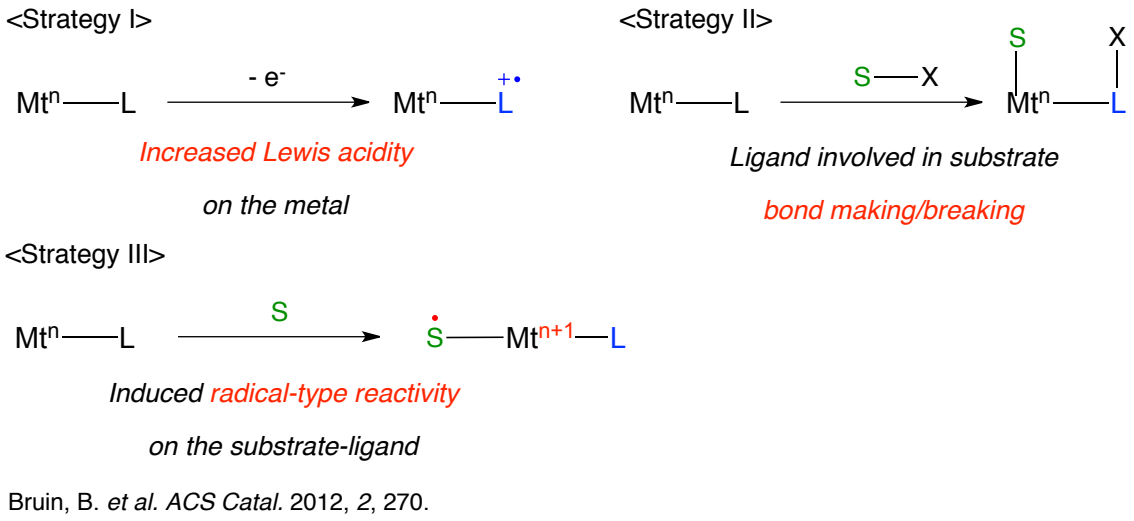


**Figure 2-7.** Strategies when using redox non-innocent ligand

Among them, I especially focused on strategy IV[32c] (Scheme 2-8). Strategy IV targets a virtual electron sink in ligands. For conventional metal salts, one-electron communication with substrates forces the metals to go through unstable metal oxidation states, such as Pd(III) or Fe(IV). On the contrary, the use of redox non-innocent ligand, which can function both as an electron reservoir and an electron mediator, retain stable oxidation state in metals.

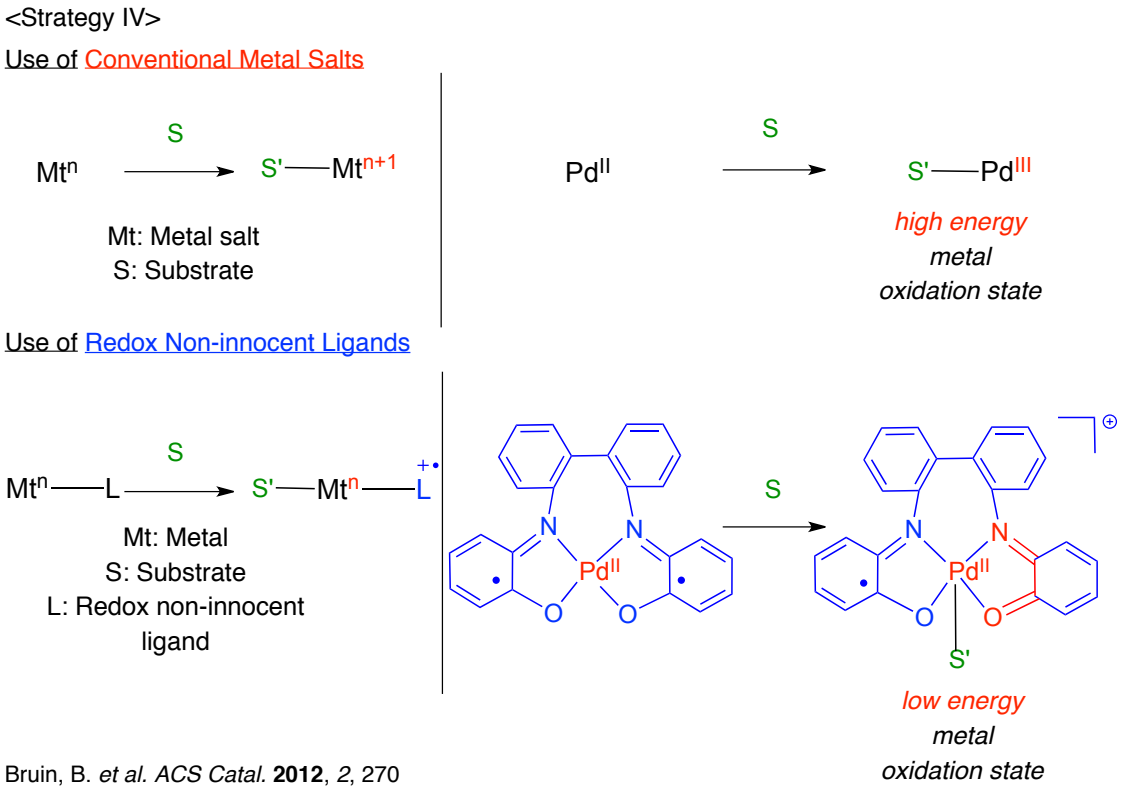


**Figure 2-8** Strategies when using redox non-innocent ligand

Chirik group has intensively studied the redox non-innocent complex for strategy IV[34]. In 2006, they reported a Fe-catalyzed cycloaddition reaction of α, ω-dienes using redox non-innocent 2,6-diiminopyridine ligand[34a,b] (Figure 2-9). Though the reaction is formally a two electron oxidative addition process, they insisted that the two electrons come from ligand not from metals. Thus, the use of redox non-innocent ligand enables Fe metal to keep the energetically stable $Fe^{II}$ and avoids much more unstable $Fe^{IV}$ state throughout the catalytic cycle. They also expanded their system to hydrogen-mediated reductive cyclization of enynes and diynes[34c], intermolecular [2π + 2π] cycloaddition reaction[34d].

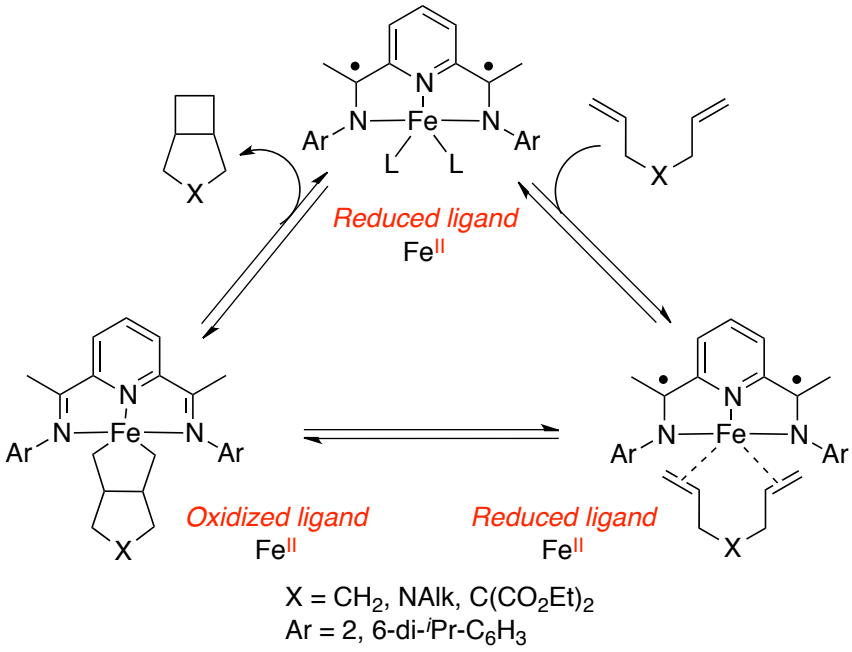


Chrik, P. J. *et al. J. Am. Chem. Soc.* **2006**, *128*, 13340., *Science* **2010**, *327*, 794

**Figure 2-9**. Fe-catalyzed [2+2] cycloaddition using redox non-innocent ligand

Heyduk *et al*. reported the first example of a $d^0$ Zr (IV) metal catalyst which achieved the multielectron ttransformations, such as oxidative addition[35a] (Figure 2-10). They used the ortho-diamido Zr (IV) complex for the disproportionation reaction of diphenyl hydrazine to aniline and azobenzene. Although the oxidative addition by a $d^0$ Zr (IV) metal is theoretically impossible because a Zr (IV) metal cannot possess any available *d*-electrons, the redox non-innocent ligand instead donates two electrons to realize the seemingly impossible oxidative addition step. The redox non-innocent ligand not only maintain the stable Zr(IV) oxidation state throughout the reaction, but also achieve the impossible chemical conversion if Zr (IV) alone

was used. They successfully applied a related Zr (IV) redox non-innocent complex for nitrene transfer reactions[35b].

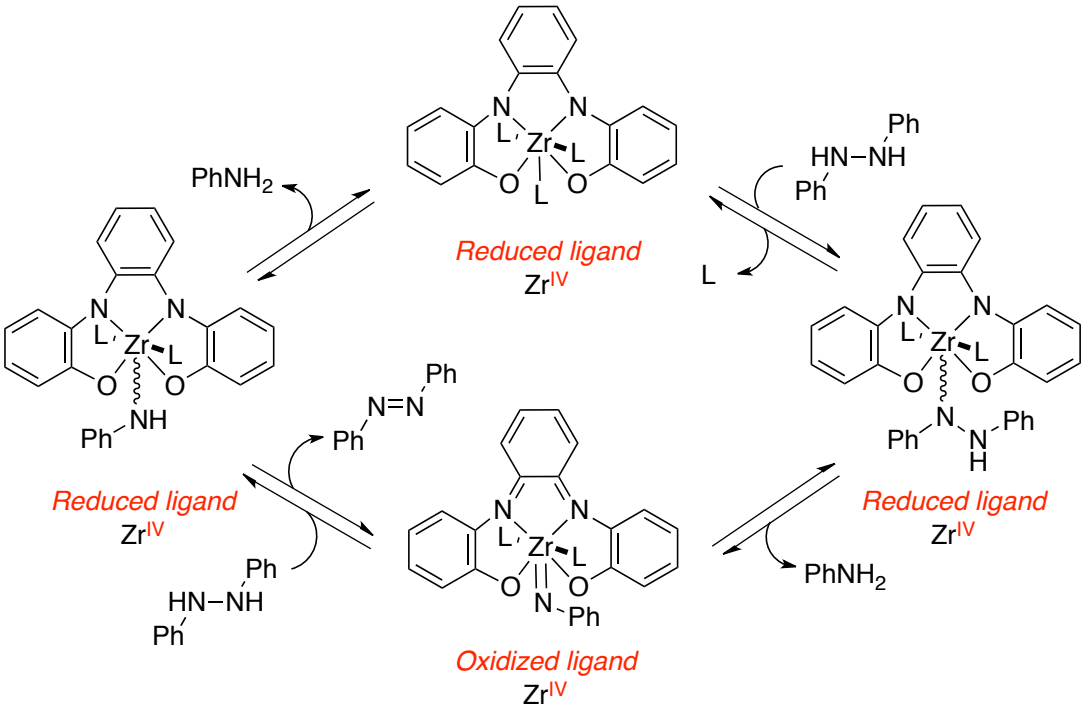


Heyduk, A. F. *et al. J. Am. Chem. Soc.* **2008**, *130*, 2728.

**Figure 2-10**. Zr-catalyzed disproportionation of diphenylhydrazine using redox non-innocent ligand

## 2-2-3. My strategy

One of the problems to be solved in dehydrogenation reaction of *N*-heterocycles is requirement of harsh reaction conditions. According to the first concept, I envisaged that the capacity of photoredox catalyst both to generate radical intermediates and mediate one electron redox conversions under remarkably mild conditions might overcome the current obstacles. From second concept, I hypothesized a redox non-innocent complex may be a powerful partner with a photo-catalyst to function more cooperatively than a conventional metal salt through the efficient one electron communication between the catalyst and a substrate. In addition, I expected that by using redox non-innocent ligand the strategic use of base-metals might be possible for the multielectron process. General two electron process like dehydrogenation reactions are typically catalyzed by precious metal catalysts which undergo two electron redox reactions ($Ir^{I}$ and $Ir^{III}$), not by base-metal catalysts which undergo one electron redox reactions ($Cu^{I}$ and $Cu^{II}$). I surmised that combining one electron process in ligand and one electron process in base-metal might realize two electron overall redox conversions in entire metal complex.

Based on the considerations, I illustrate my strategy in Figure 2-11. My strategy involves *Radical-Conjugated Redox Catalysis (RCRC) merging photo-catalysts, metals, and redox non-innocent ligands*. In the hypothetical concept, both the one electron oxidation of a substrate and the one electron reduction of a redox non-innocent ligand are mediated by a photo-catalyst. I envisioned that radical coupling event between the resulting radical cation and radical anion might achieve the alternative and more cooperative interaction between them.

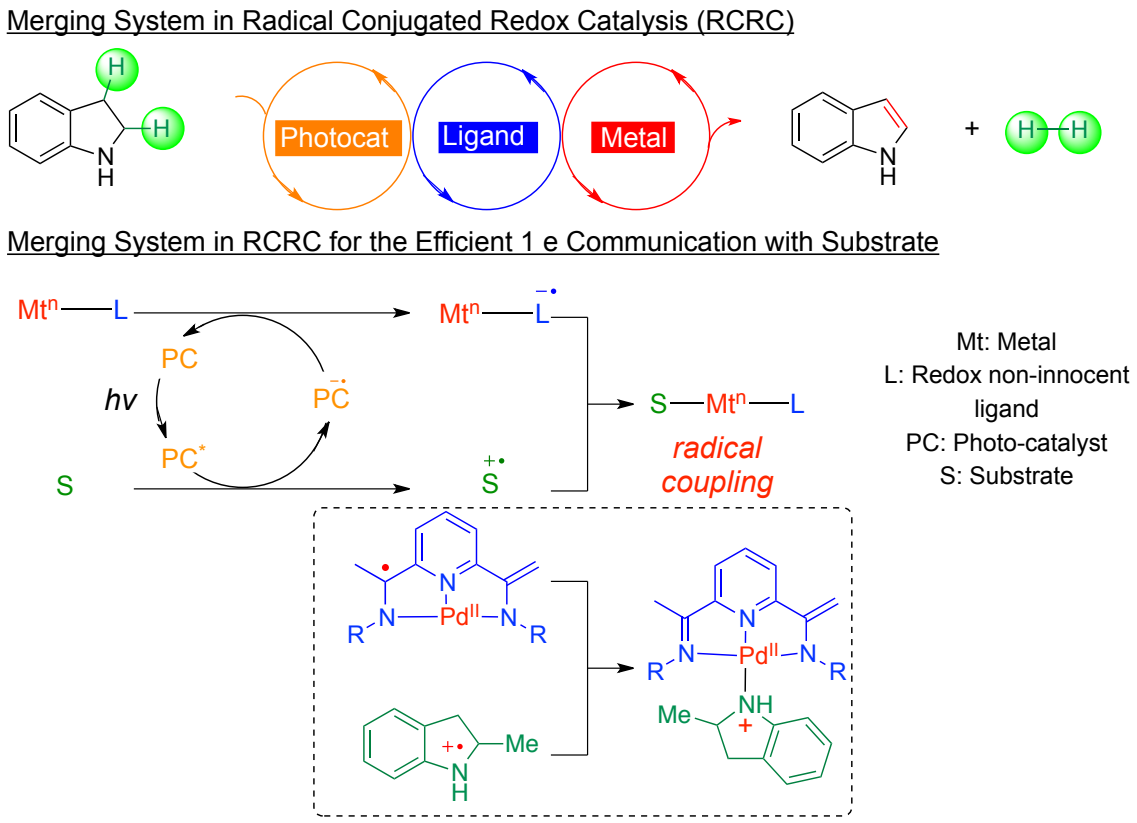


**Figure 2-11**. Merging RCRC concept

Hypothetical catalytic cycle for the dehydrogenation of *N*-heterocycles based on my strategy is depicted in Figure 2-12. First, the one electron oxidation of a *N*-heterocyclic compound by a photo-catalyst, which is exited by an adequate light source, would initiate the catalytic cycle giving an amine radical cation intermediate (Figure 2-12, I). If the reduced photo-catalyst has sufficient reduction power, the reduction of redox non-innocent metal complex may occur to give reduced metal complex (Figure 2-12, II). Radical coupling between amine radical cation and metal complex might afford the key metal amide intermediate without using any basic additives under mild conditions (Figure 2-12, III). I believe that the use of redox non-innocent ligand would accelerate both step II and step III, which undergo one electron mediated processes. Additionally, I expected that the base-free mild conditions would facilitate the last $H_2$ release step because strong bases are difficult to donate protons to metal hydrides. If the β-hydride elimination proceeded from the resulting key metal amide, the metal hydride species would be formed along with the liberation of the desired product (Figure 2-12, IV). Last critical hydrogen gas release step would complete the catalyst cycle regenerating the metal complex (Figure 2-12, V).

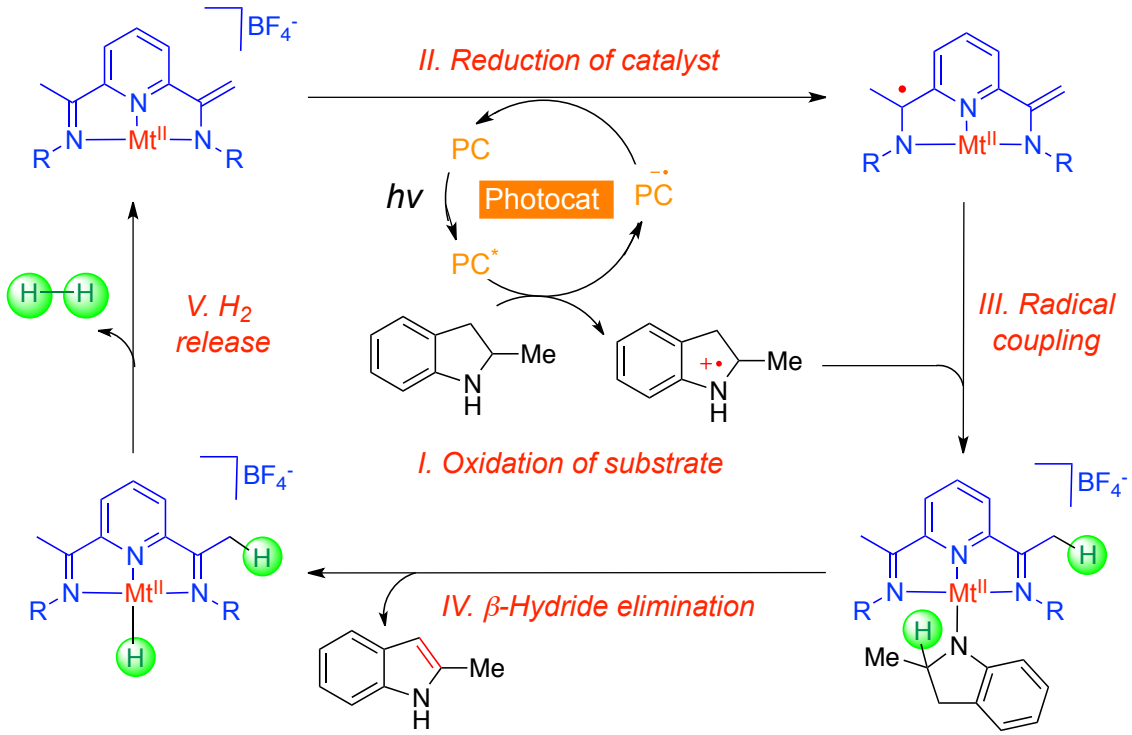


**Figure 2-12**. Hypothetical catalytic cycle for the dehydrogenation of *N*-heterocycles

## 2-3. Reaction Development

### 2-3-1. Base-metal catalysts for dehydrogenation of an indoline

Based on the hypothetical catalytic cycle, I started investigation of each reaction component using an indoline as a substrate and several redox non-innocent complexes bearing base metals under white LED irradiation. At the initial stage of investigations, I found three key observations. 1) The results using a tetrahydroquinoline as a substrate and a base-metal complex as a catalyst were quite poor to afford the product in less than 10% yield. 2) The Cu-SMe complex[36] shown in Figure 2-12 exhibited a little superior reactivity than other base-metal complexes using an indoline as a substrate. 3) The oxidation by air during the quenching step was sometimes troublesome. To avoid the aerobic oxidation of the substrate, I determined to perform all operations (preparation of reactions, performing reactions and quenching reactions) in glove box.

The screening of photo-catalysts is described in Table 2-1. I examined several organic-dye-based photo-catalysts and metal-based photo-catalysts in the presence of 20 mol % of the Cu-SMe complex[36] as a redox non-innocent complex. Among them, 2 mol % of Erythrosine B showed a little better reactivity than other photo-catalysts giving the desired product in 38 % yield.

**Table 2-1.** Investigation of photocatalysts

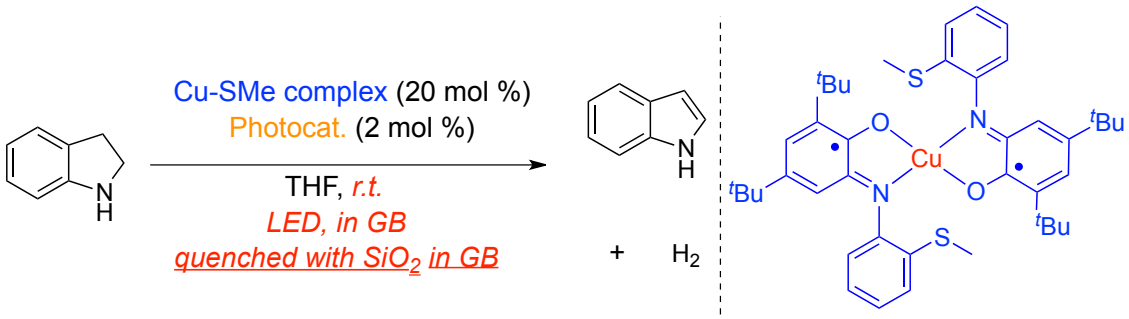


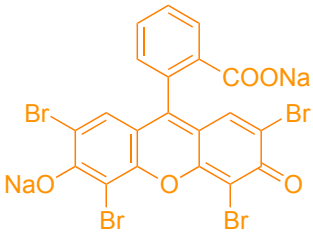


Eosin Y

31%

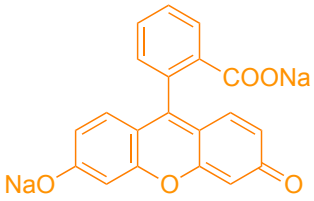


Fluoroscein

27%

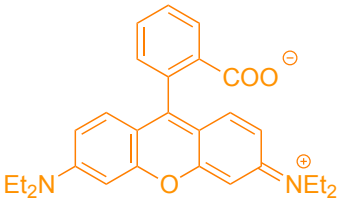


Rhodamine

21%

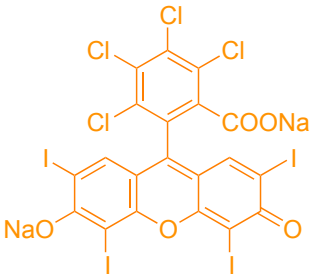


Rose bengal

37%

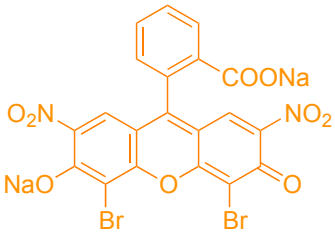


Eosin B

23%

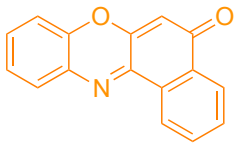


Nile red

27%

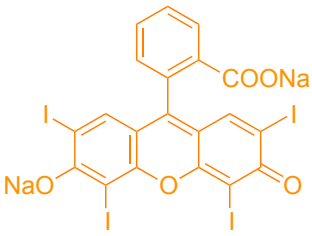


Erythrosin B

38%

$Ir(ppy)_2(dtbpy)PF_6$

33%

none

25%

I, then, turned my attention to screening of the redox non-innocent complexes. As shown in Table 2-2, I tested a variety of redox non-innocent ligands with base-metals. First, in the absence of metal complexes, no reaction occurred. Co and Ni complexes with the same SMe ligand never improved the results compared with the Cu-SMe complex. Other different types of redox non-innocent complexes also proved to be inferior to the Cu-SMe complex. Although solvent screening and additive screening like a triethylamine as a sacrificing reductant were investigated, I found no positive effects on the reactivity.

**Table 2-2.** Investigation of redox non-innocent complexes

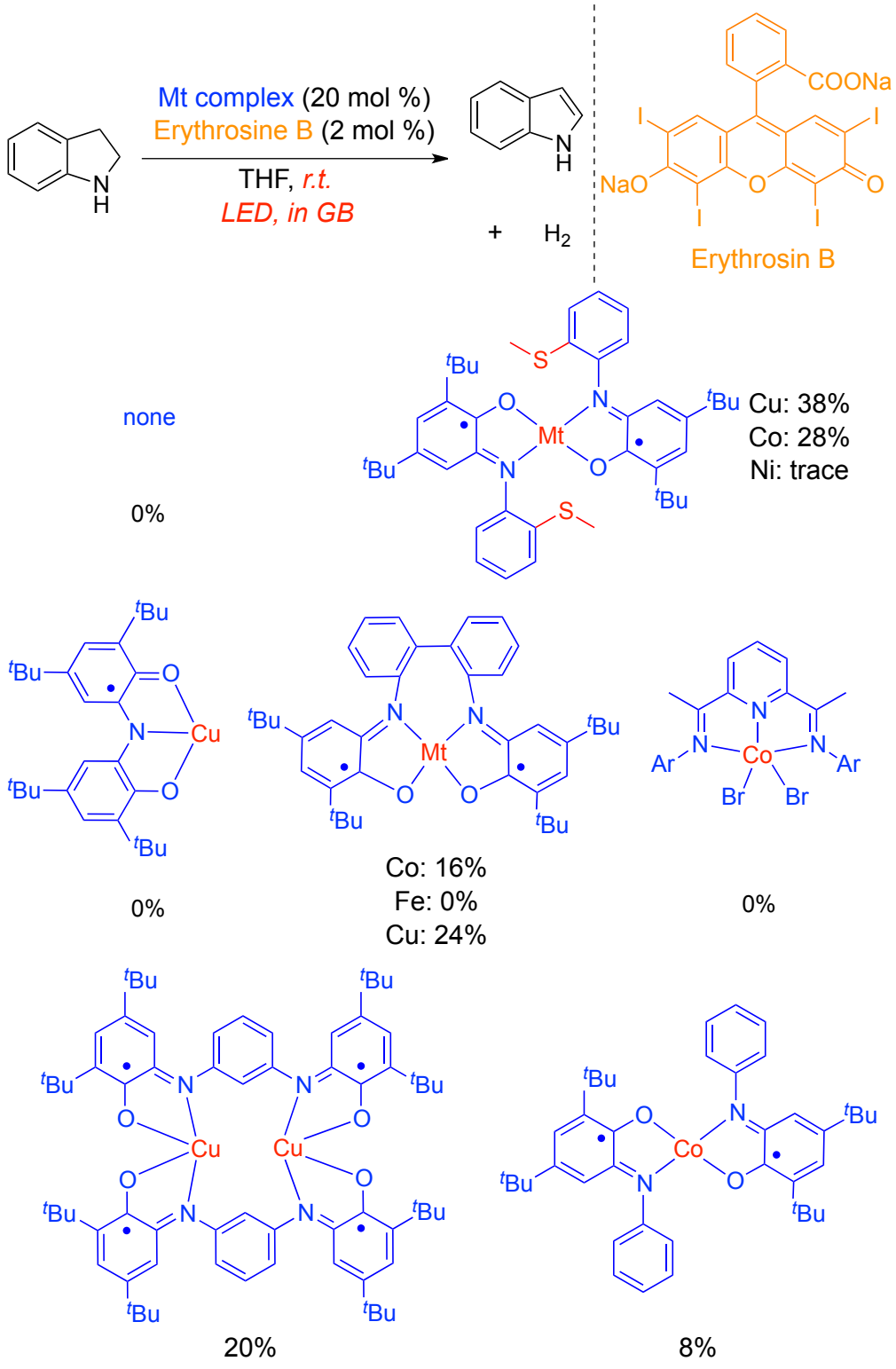

Though the reactivity was still moderate, I tried to confirm the hydrogen evolution at this stage (Scheme 2-9). In order to gain the clear evidence that hydrogen gas was released in my Cu catalyst system, I performed the dual reaction involving the dehydrogenation of an indoline and the hydrogenation of cyclohexene. In one test tube, I carried out the dehydrogenation reaction under my optimum conditions. On the other hand, hydrogenation under the Wilkinson catalyst conditions was tested in another test tube. The two test tubes were connected *via* a rubber tube to allow gases to transfer freely. However, cyclohexane was not observed at all in the hydrogenation reaction vessel, while the dehydrogenation of the indoline proceeded to produce the indole in 34% yield. The result indicats that my catalyst system never evolved hydrogen gas from the indoline substrate. I speculated that contamination of a trace amount of oxygen gas might cause the oxidation of the indoline instead of the desired dehydrogenation.

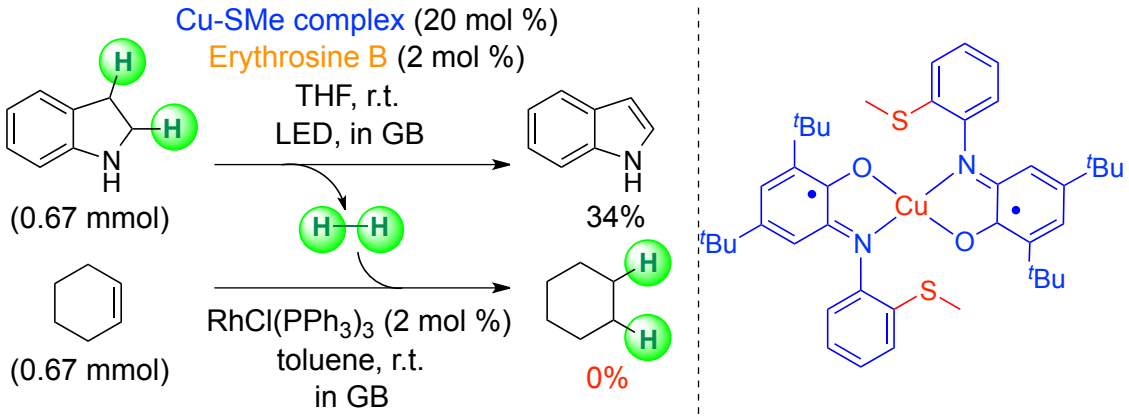


**Scheme 2-9.** Dual reaction using the Cu catalyst system

## 2-3-2. Pd catalysts for dehydrogenation of an indoline

Due to the failure of the dehydrogenation reaction using base-metal complexes, I tried to study Pd-based redox non-innocent complexes because I envisioned that a Pd-based complex might accelerate the β-hydride elimination step to achieve hydrogen evolution compared with base-metal complexes (Figure 2-12).

A study of various photo-catalysts with a tetradentate-type Pd redox non-innocent complex[37] was summarized in Table 2-3. In general, the reactivity with a Pd complex was higher than the reactivity with a base-metal complex (10 mol % of a Pd complex in Table 2-3 *vs* 20 mol % of a Cu complex in Table 2-1). The highest reactivity was observed in the presence of 2 mol % of Rhodamine B with 10 mol % of a Pd complex to give the product in 42% yield.

**Table 2-3.** Investigations of photo-catalysts with a Pd complex

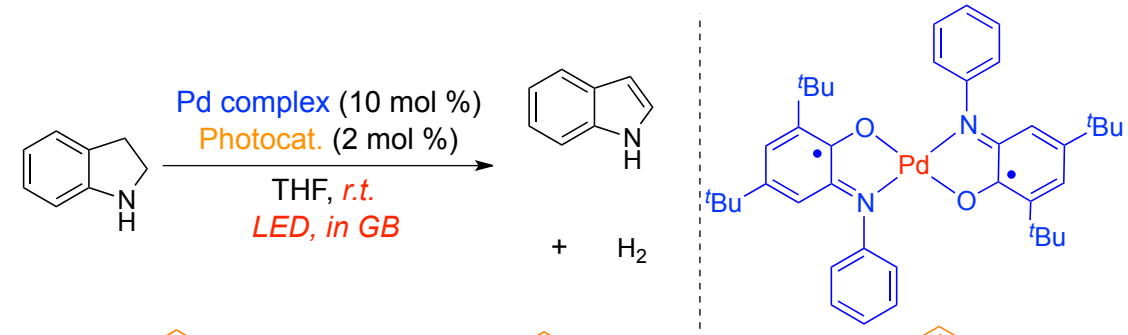


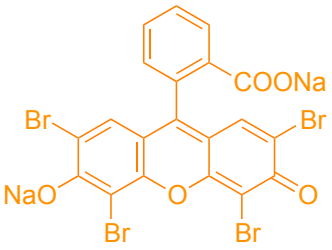

Eosin Y

22%

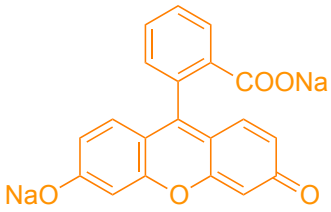

Fluoroscein

20%

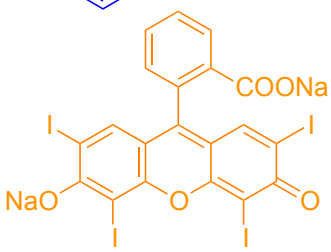

Erythrosin B

18%

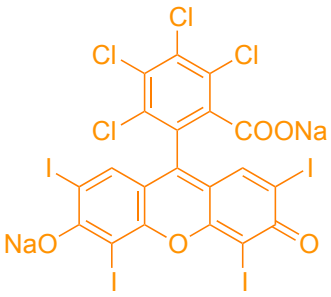

Rose bengal

11%

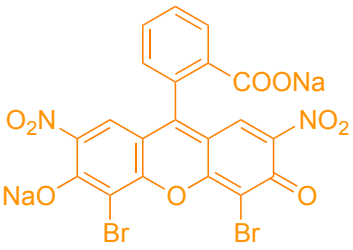

Eosin B

28%

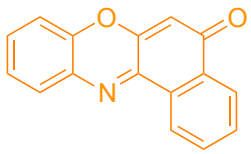

Nile red

26%

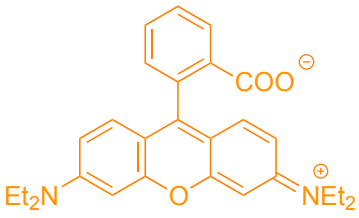

Rhodamine B

42%

$Ir(ppy)_2(dtbpy)PF_6$

31%

$Ru(bpy)_3Cl_2$

21%

Solvent screening with a Pd catalyst and Rhodamin B was conducted (Table 2-4). The reactivity changed drastically depending on solvents. Though the exact reason was not clear, I envisaged that a solubility of the Pd complex and Rhodamine B might influence the reactivity. Among different types of solvents, the highest yield was observed using dioxane as solvent (entry 9).

**Table 2-4.** Investigations of solvents with a Pd complex and Rhodamine B

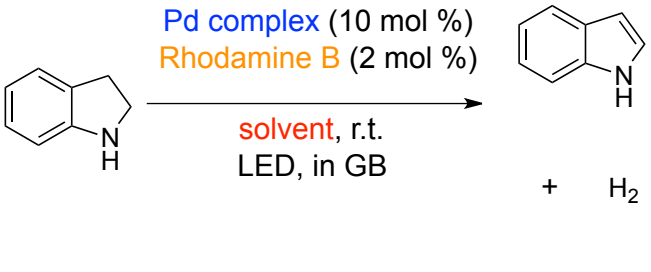


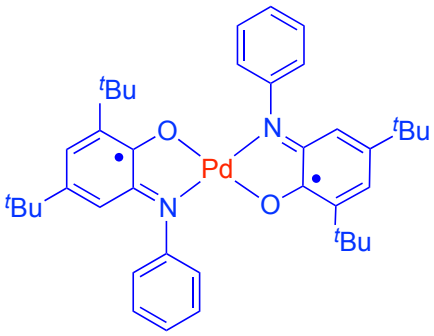


| entry | solvent | yield (%) |
|---|---|---|
| 1 | toluene | 32 |
| 2 | DCE | 20 |
| 3 | $Et_2O$ | 22 |
| 4 | EtOAc | 19 |
| 5 | MeOH | 43 |
| 6 | PhCN | 0 |
| 7 | MeCN | 56 |
| 8 | THF | 42 |
| 9 | **dioxane** | 58 |

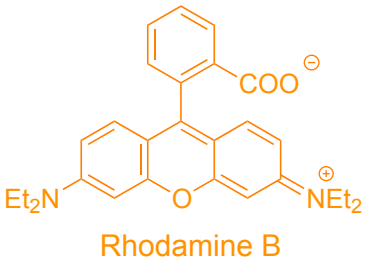


I also surveyed several redox non-innocent complexes bearing Pd metals (Table 2-5). Surprisingly, a Pd complex with SMe-type redox non-innocent ligand, which showed moderate reactivity in Cu complex, afforded no products at all. I surmised that a proper combination of a Pd complex and a photo-catalyst would be the key for high reactivity. Other tetra-dentate Pd complex[42] and penta-dentate Pd complex never improved the result.

**Table 2-5.** Investigations of Pd redox non-innocent complexes

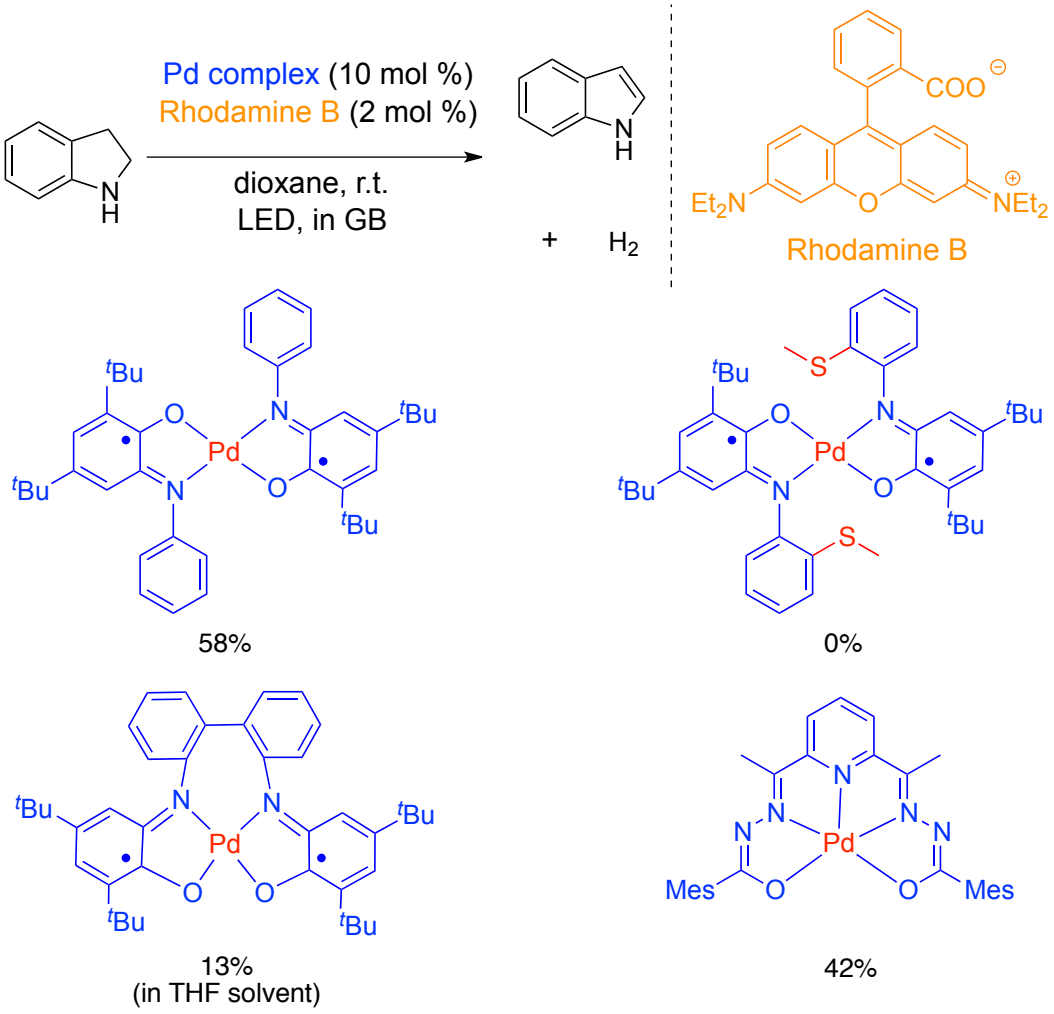


At this stage, I tried the dual reaction similar to Scheme 2-10. Trials for the dual reactions involving dehydrogenation and hydrogenation, however, were a little difficult because the reactivity got worse under larger scale conditions. After several studies, I found out that a longer reaction time (for 72 h) and the increase of the catalyst amount (20 mol %) were important to achieve higher reactivity under 2.0 mmol scale. Finally, in the presence of 20 mol % of the Pd complex and 2 mol % of Rhodamine B, the dehydrogenation reaction proceeded smoothly to afford the desired product in 79 % yield for 72 h (Scheme 2-10). In addition, the hydrogenation reaction of cyclohexene also occurred to give the saturated compound in 12 % yield. Although the yield of hydrogenation reaction was still unsatisfactory, I believe that hydrogen gas was released in my Pd catalyst system.

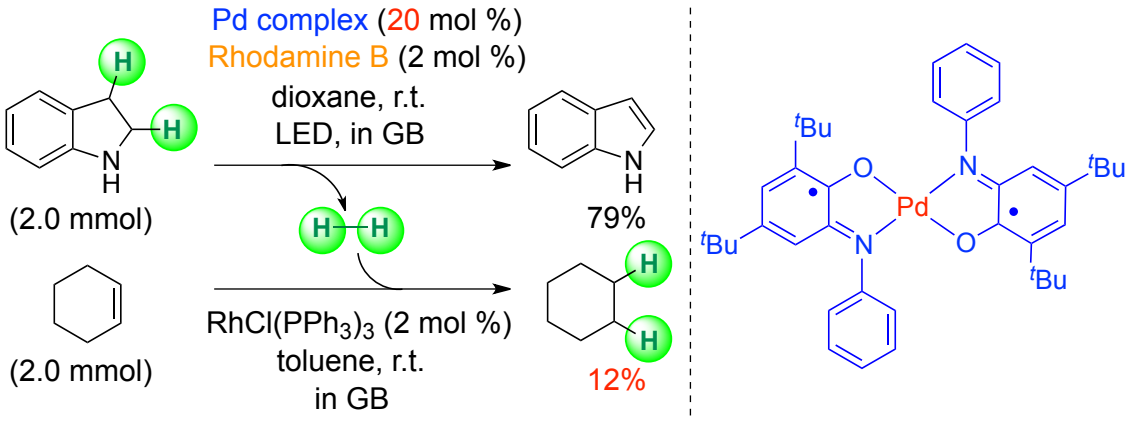


**Scheme 2-10.** Dual reaction using Pd catalyst system

## 2-3-3. Pd catalysts for dehydrogenation of a tetrahydroisoquinoline

Preliminary studies revealed hydrogen gas evolution using an indoline as a substrate under the Pd-catalyst system. Thus, I tried to expand the substrate scope of the cooperative RCRC system (Table 2-6). Although I examined various *N*-heterocycles bearing larger $H_2$ density than indoline, the desired products were rarely observed in almost all cases.

**Table 2-6.** Preliminary studies on substrate scope

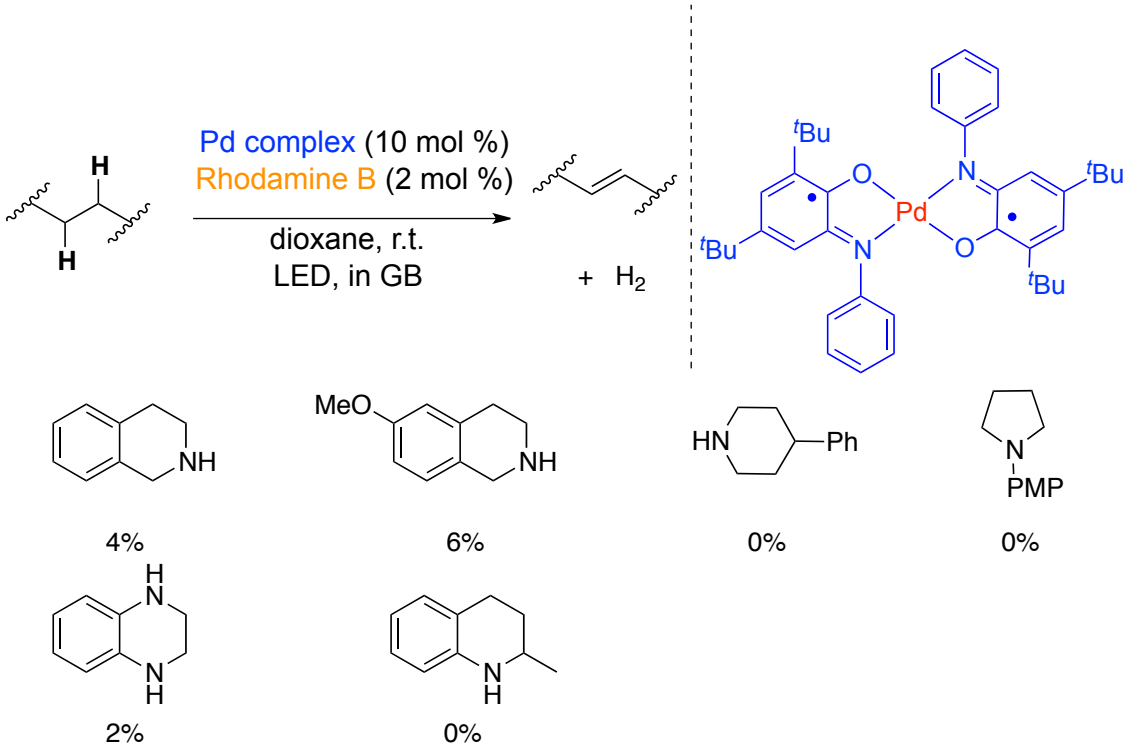


I expected that a photo-catalyst with stronger oxidation power might be necessary to realize the broad substrate scope because the first one electron oxidation step would be the essential step to generate a Pd-amide intermediate in the absence of any strong bases. To test the assumption, I conducted the reaction with tetrahydroisoquinoline as a substrate in the presence of acridinium type photo-catalyst, which was reported to exhibit stronger reduction potential than other photo-catalysts. The acridinium salt showed $E_{red}^{3*}$ = 1.88 V[38a]. In contrast, other photo-catalysts in general showed $E_{red}^{3*}$ = around 0.8 V[39] (for example, Eosin B showed $E_{red}^{3*}$ = 0.83 V). Actually, as shown in Table 2-7, the use of acridinium-type photocatalyst accelerated

the reaction to afford the product in 31% combined yield (compound A: 12% yield, and compound B: 19% yield), while the use of Rhodamine B gave almost no product.

The result prompted me to continue further studies using a photo-catalyst with stronger oxidation power to expand the substrate generality.

**Table 2-7.** Preliminary study on a tetrahydroisoquinoline as a substrate

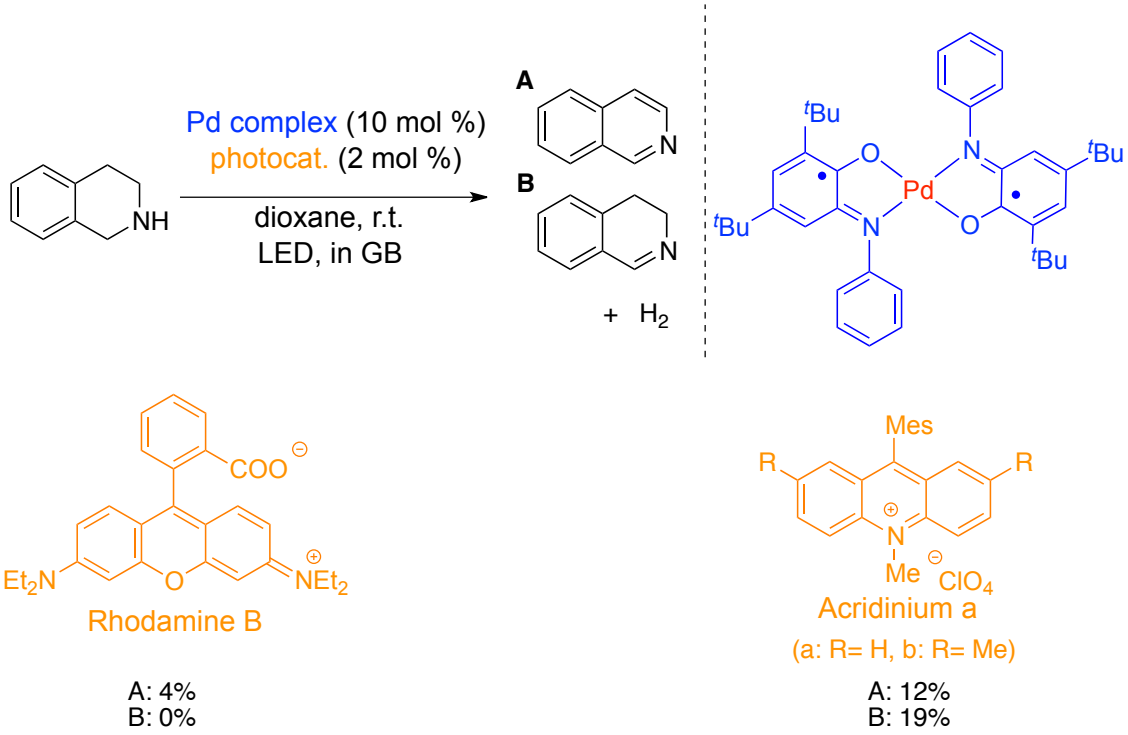


The reaction with tetrahydhdroisoquinoline was performed in the presence of 10 mol % of a Pd catalyst and 2 mol % of a photo-catalyst in DCE solvent under 400 nm LED irradiation. 400 nm LED was used because acridinium photo-catalyst was reported to possess absorption peak at around 430 nm. Acridinium salt, rivoflavin tetraacetate (RFTA)[40], and triphenyl pyririum tetrafluoroborate (TPT) [41] were utilized as photo-catalysts because these photo-catalysts have stronger oxidation power (TPT: $E_{red}^{3*}$ = 2.28 V[41b]). The results were summarized in Table 2-8.

With Pd complex **1**, acridinium a showed a little better reactivity than RFTA and TPT (entries 1-3). The screening of Pd complexes indicated that Pd complex **4**[42] exhibited similar reactivity to Pd complex **1** (entries 4-6). In the case of Pd complex **4**, the use of RFTA and TPT as photo-catalyst never improved the result (entry 7, 8). Because in entry 1 the reaction mixture became a little complicated, I selected the conditions in entry 6 as optimum conditions.

**Table 2-8.** Investigation of the combination of a Pd complex and a photo-catalyst

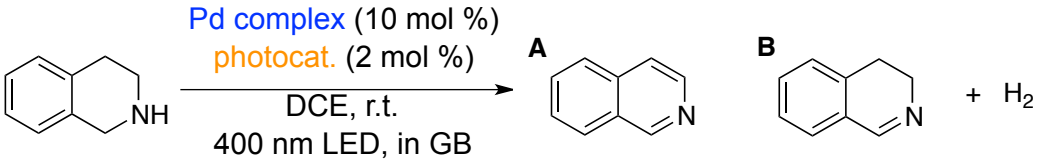


| entry | Pd complex | photocat. | yield of A (%) | yield of B (%) |
|---|---|---|---|---|
| 1 | Pd **1** | Acridinium a | 12 | 19 |
| 2 | Pd **1** | RFTA | 3 | 15 |
| 3 | Pd **1** | TPT | 4 | 16 |
| 4 | Pd **2** | Acridinium a | 9 | 20 |
| 5 | Pd **3** | Acridinium a | 8 | 9 |
| 6 | Pd **4** | Acridinium a | 12 | 18 |
| 7 | Pd **4** | RFTA | 3 | 17 |
| 8 | Pd **4** | TPT | 0 | 10 |

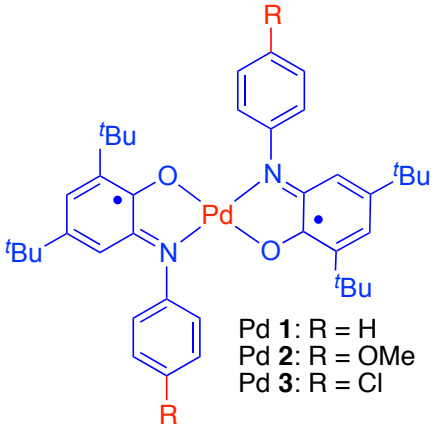


Pd **1**: R = H
Pd **2**: R = OMe
Pd **3**: R = Cl

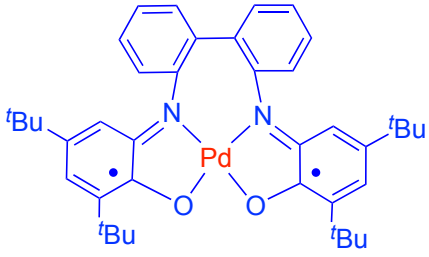


Pd **4**

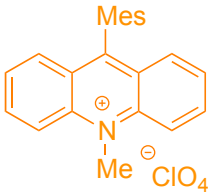


Acridinium a

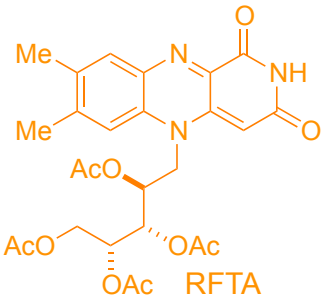


RFTA

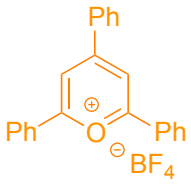


TPT

Solvent effects were also examined in Table 2-9. The obvious difference in reactivity was observed depending on solvents. DCM was proved to be beneficial to give the product in about 40% combined yield (entry 2).

**Table 2-9.** Investigation of solvents

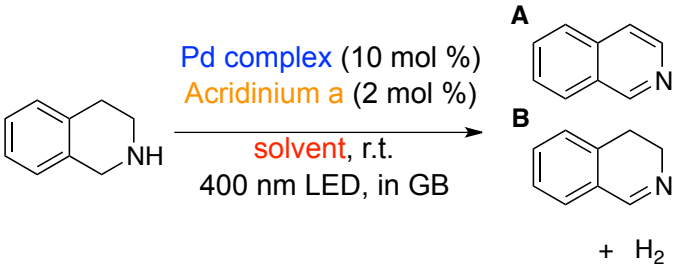


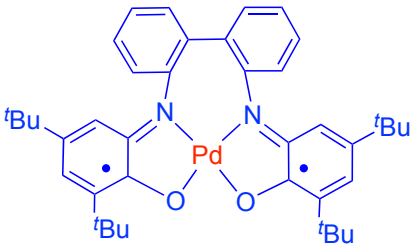


| entry | solvent | yield of A (%) | yield of B (%) |
|---|---|---|---|
| 1 | DCE | 12 | 18 |
| 2 | DCM | 14 | 27 |
| 3 | THF | 2 | 5 |
| 4 | IPA | 0 | 5 |
| 5 | MeCN | 6 | 11 |
| 6 | toluene | 1 | 9 |
| 7 | dioxane | 6 | 15 |

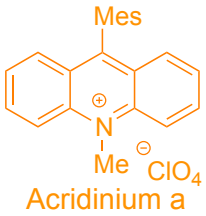


In order to enhance the reactivity, my next attention was paid to additive effects. First, I studied various Lewis basic additives because I envisioned that the addition of a Lewis base might accelerate β-hydride elimination step by increasing the electron density of the Pd complex by coordination to Pd metal center (Table 2-10). However, the addition of Lewis basic additives resulted in the similar yield or the decreased yield.


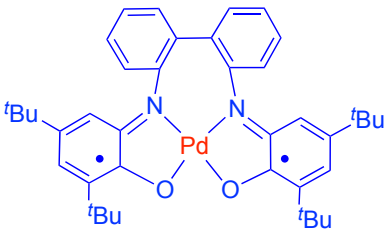


none: A 14%, B 27%

$PMe_3$, $PPh_3$=O, pyridine, 1,10-phenanthlorine, THF: no positive effects

**Table 2-10.** Effects of Lewis basic additives

In 2011, MacMillan group reported α-amino C-H arylation reaction using an Ir photo-catalyst and a Brønsted base[43]. In their report, Brønsted bases drastically affected the reactivities. They proposed that the choice of an adequate Brønsted base was essential for the generation of α-amino C radical species after one electron oxidation of the substrate (Table 2-11).

**Table 2-11.** Photo-catalytic C-H arylation reaction by MacMillan group

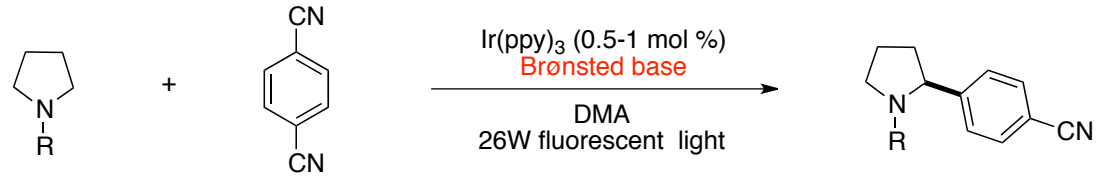


Base effects

| entry | base | yield (%) |
|---|---|---|
| 1 | NaOAc | 82 |
| 2 | NaOTFA | 30 |
| 3 | LiOTFA | 24 |
| 4 | NaOTFA | 66 |
| 5 | KOTFA | 29 |
| 6 | NaOBz | 7 |
| 7 | NaOPiv | 72 |

Formation of C-radical intermediates

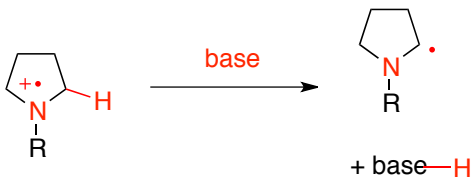


MacMillan, D. W. C. *et al. Science* **2011**, *334*, 1117

In my system using tetrahydroisoquinoline as a substrate, the second dehydrogenation from compound B would be difficult because I assume the generation of benzylic C-radical species might be required. Based on the MacMillan's report, I anticipated that an adequate selection of Brønsted bases might influence the reactivity on the PCET process (one electron oxidation and deprotonation) for benzylic C-radical generation also in my case (Table 2-12). Though I examined many kinds of inorganic bases and organic bases with a different range of basicity, no positive effects on the reactivity were observed.

**Table 2-12.** Brønsted base effects

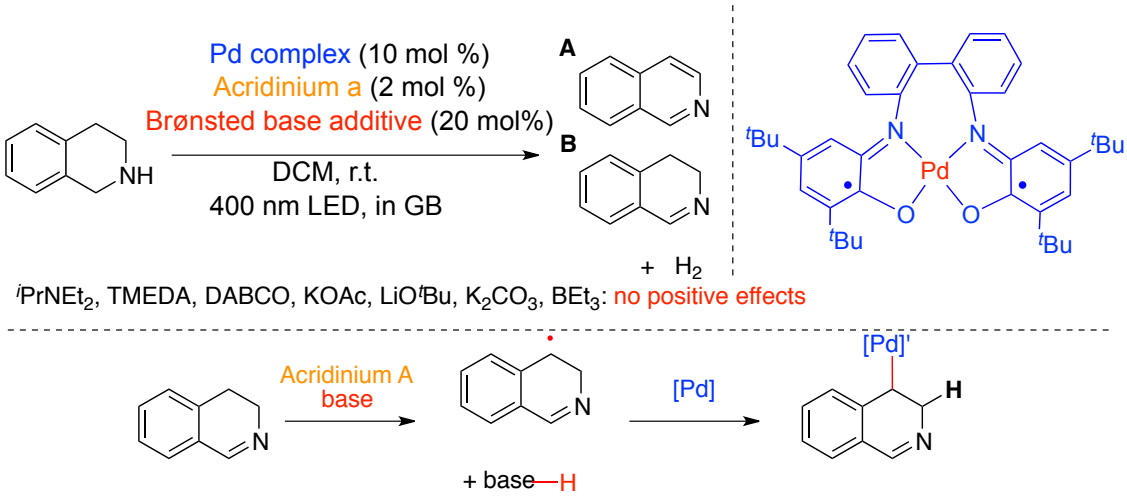


Then, I investigated the Brønsted acid effects (Table 2-13). During the course of the studies, a little improvements of yields were observed in the presence of increased amount of photo-catalyst (8 mol %). Whereas boronic acids, CSA, amino acids and carboxylic acids proved to have no effects on the reactivity, I found out that the addition of phosphoric acids derivatives or $HBF_4$ were beneficial to accelerate the reaction as shown in entries 2-3 *vs* entry 1. Additionally, a little modification of the acridinium salt improved the reactivity to afford the desired products in 66% combined yield (entry 4).

Although there are no supporting data, I guess two reasons for the improvement by the addition of phosphoric acid. 1) Phosphoric acids might inhibit the generation of byproducts, which were formed by the substitution reaction of DCM solvent by tetrahydroisoquinoline. In the presence of phosphoric acid derivatives or $HBF_4$, the byproduct formations were indeed suppressed. 2) Phosphoric acid may work as an external proton source to facilitate the hydrogen gas evolution step. In 2013, in the report for the Ir-catalyzed dehydrogenation reactions of *N*-heterocycles by Xiao group, they mentioned that the use of TFE as solvent was critical for the high reactivity because TFE would work as a strong proton donor for the resulting Ir hydride species thus accelerating the hydrogen gas evolution step[20] (Scheme 2-11).

.

**Table 2-13.** Effects of Bønsted acids

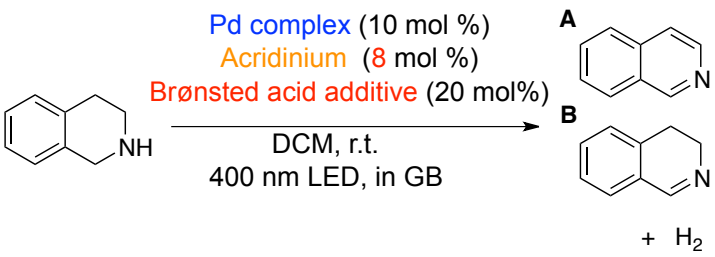


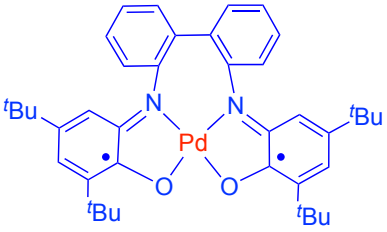


$K_2HPO_4$, $B(OH)_3$, CSA, oxalic acid, Val, Ts-Val, Ts-Gly, TfOH

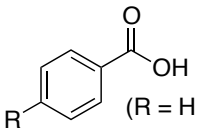


: no positive effects

phosphoric acid, $HBF_4$

: a little improvement

| entry | Acridinium | additive | yield of A (%) | yield of B (%) |
|---|---|---|---|---|
| 1 | a | none | 14 | 27 |
| 2 | a | $HBF_4$ | 26 | 25 |
| 3 | a | phosphoric acid | 11 | 38 |
| 4 | b | phosphoric acid | 20 | 46 |

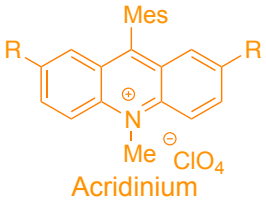


Acridinium
(a: R= H, b: R= Me)

phosphoric acid

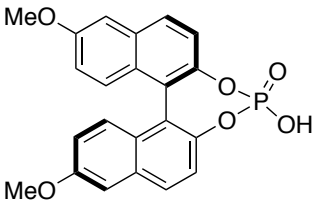


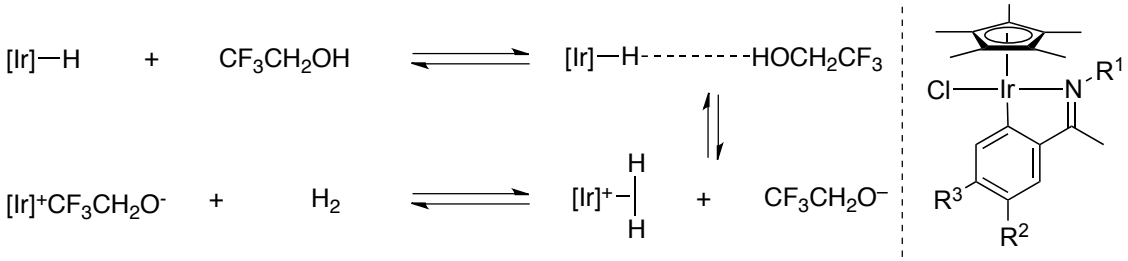


Xiao, J. *et al. Angew. Chem. Int. Ed.* **2013**, *52*, 6983

**Scheme 2-11.** Effects of Brønsted acids for the hydrogen gas release step

Finally, I reviewed other different kinds of redox non-innocent complexes bearing Pd or Ru metals under the similar conditions. The results were described in Table 2-14. Generally, the yields were quite unsatisfactory in the presence of Ru-based redox non-innocent complexes. Though I studied tridentate-type redox non-innocent complexes, no enhancements of the reactivity were gained. The optimum conditions using tetrahydroisoquinoline as a substrate so far were summarized in Scheme 2-12. In the presence of 10 mol % of Pd redox non-innocent complex, 8 mol % of acridinium salt b and 20 mol % of phosphoric acid, the reaction proceeded at room temperature to afford the desired products in 66% combined yield.

**Table 2-14.** Re-examination of redox non-innocent complexes

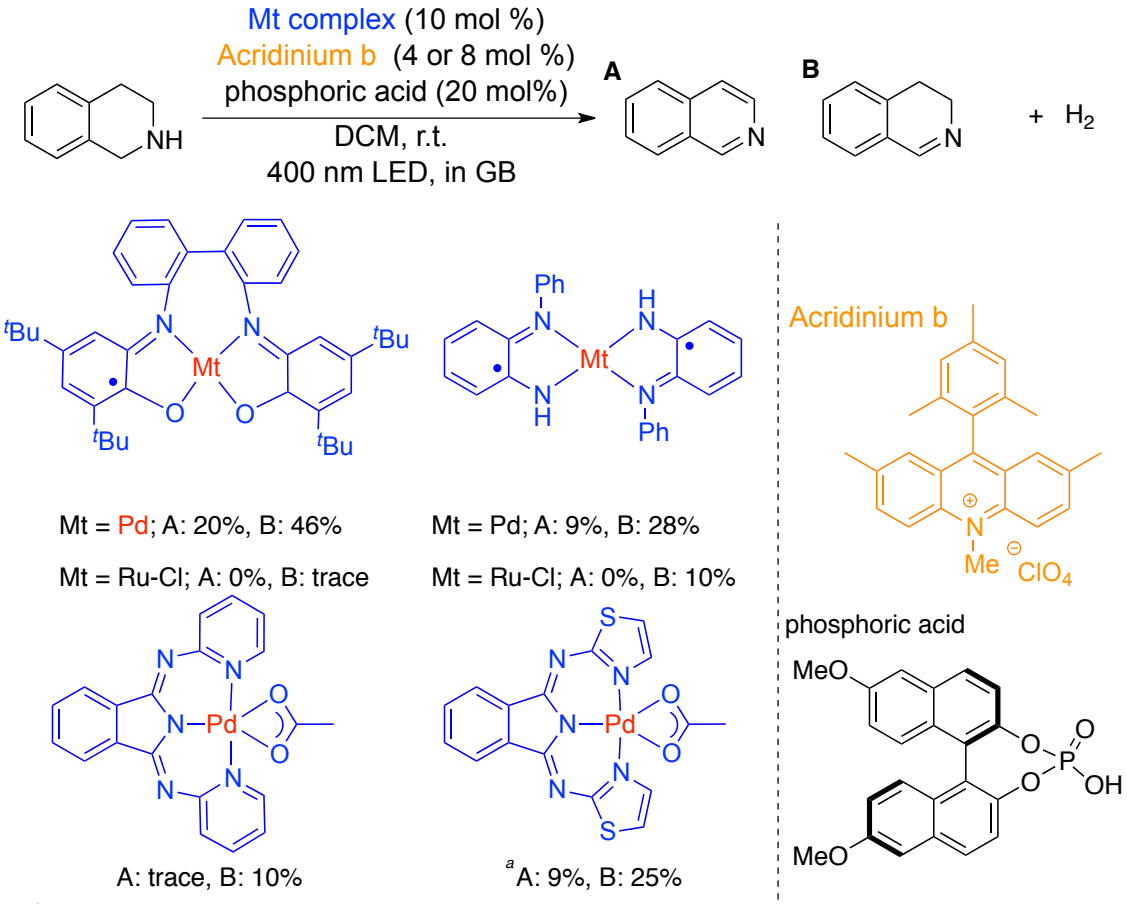


[a] The reaction was conducted in the absence of the phosphoric acid.

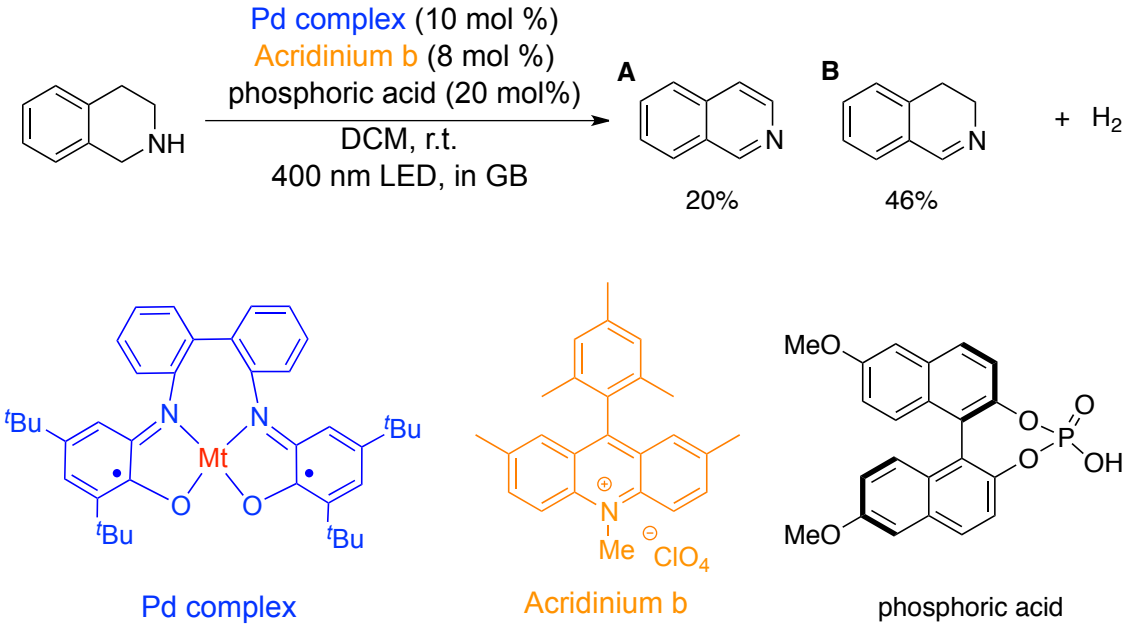


**Scheme 2-12.** Optimum conditions for the dehydrogenation of tetrahydroisoquinoline

## 2-3-4. Detection of hydrogen gas by GC analysis with TCD detector

Though hydrogen gas evolution in my system was strongly indicated from the dual reaction experiment involving dehydrogenation and hydrogenation (Scheme 2-11), I considered that more unambiguous evidence for the hydrogen gas release would be necessary. In order to gain the clear evidence of hydrogen gas release, I tried to detect hydrogen gas directly by using GC device with TCD detector. First of all, I struggled to establish the promising method to collect and analyze hydrogen gas in quantitative manner because in the preliminary investigations, I failed to detect hydrogen gas quantitatively by GC device even I injected hydrogen gas itself.

The studies in test tube were carried out as the following schemes. 1) 0.5 mmol of hydrogen gas and 0.5 mmol of helium gas as an internal standard were injected into the test tube. 2) The test tube was stirred for x hours with connected or not connected to an argon balloon. 3) Ar bubbling to put out gases in the solvent phase into an argon balloon was conducted for y minutes. 4) Gases collected in the balloon were directly injected to the GC device with TCD detector. The investigation results were summarized in Table 2-15. During the studies, several essential aspects were observed. 1) The time for Ar bubbling is important (entries 1-3). 2) During the stirring, hydrogen gas leaks were observed (entries 4-5). 3) With connected to the Ar balloon during the stirring time, significant hydrogen gas leaks were observed (entries 4-5).

**Table 2-15.** Studies to detect hydrogen gas in test tubes

test tube → ($H_2$ 11.2 ml (0.5 mmol), He 11.2 ml (0.5 mmol), dioxane, r.t., LED, 0.5 mmol scale, x h) → Ar bubbling (y min) → GC analysis

| entry | x | y | others | $H_2$ yield (%) |
|---|---|---|---|---|
| 1 | 0 | 1 | - | 33 |
| 2 | 0 | 5 | - | 71 |
| 3 | 0 | 15 | - | 70 |
| 4 | 26 | 5 | connected to baloon | 13 |
| 5 | 24 | 5 | not connented to baloon | 57 |

I also studied the similar examinations using snap vials as reaction vessels and 0.1 mmol of hydrogen gas (Table 2-16). For the experiments using snap vials, the size of needles used for Ar bubbling revealed to be important (entries 1-4). Hydrogen gas was collected in 91% yield using the 23 gauge needle (entry 2). After stirring for 24 hours, the yield of collected hydrogen gas was decreased to 69% yield (entry 5).

**Table 2-16.** Studies to detect hydrogen gas in snap vials

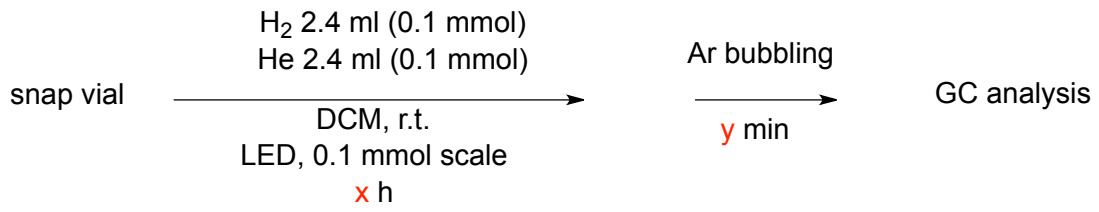


| entry | x | y | others | $H_2$ yield |
|---|---|---|---|---|
| 1 | 0 | 1 | Ar bubbling *via* 23 gauge syringe | 51 % |
| 2 | 0 | 5 | Ar bubbling *via* 18 gauge syringe | no |
| 3 | 0 | 5 | Ar bubbling *via* 23 gauge syringe | 91 % |
| 4 | 0 | 15 | Ar bubbling *via* 23 gauge syringe | 79 % |
| 5 | 24 | 5 | Ar bubbling *via* 23 gauge syringe | 69 % |

Though the yield of hydrogen gas was still moderate in around 60%, I applied the established method for my dehydrogenation catalytic system to confirm the hydrogen evolution. The reaction with tetrahydroisoquinoline as a substrate was conducted under the optimum conditions discussed in Chapter 2-3-3 (Table 2-17). I performed the extensive investigations for different reaction times under different scales, but in all cases hydrogen gases were not detected.

**Table 2-17.** Studies to confirm hydrogen gas evolution in my catalytic system with tetrahydroisoquinoline

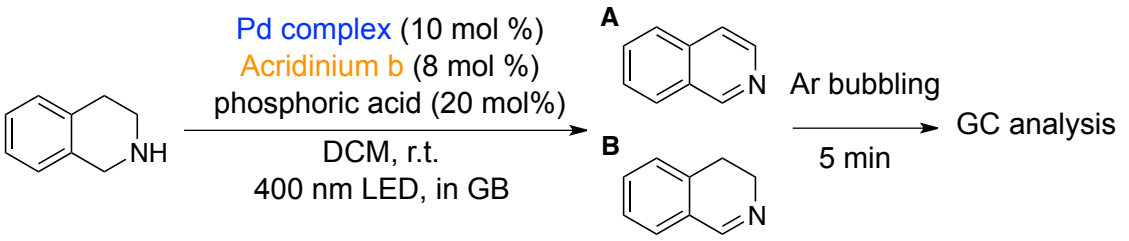


| entry | scale (mmol) | yield of A (%) | yield of B (%) | yield of $H_2$ (%) |
|---|---|---|---|---|
| 1 | 0.1 | 37 | 24 | 0 |
| 2 | 1 | 5 | 18 | 0 |

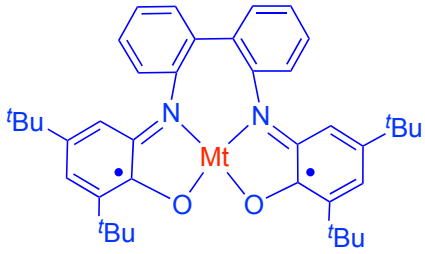


Pd complex

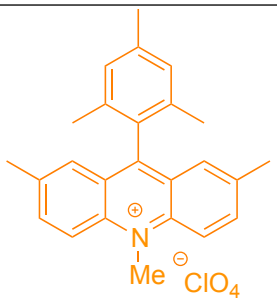


Acridinium b

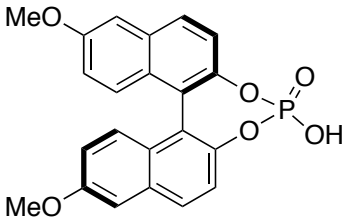


phosphoric acid

The reaction with indoline as a substrate was also tested under the optimized conditions in Chapter 2-3-2 (Table 2-18). On the contrary to the reaction with tetrahydroisoquinoline (Table 2-17), hydrogen gas was obviously detected although the yield was quite low (entries 1-2). Interestingly, no hydrogen gas was detected after stirring for 98 hours in control experiment (entry 3).

From these experimental observations altogether, several possible assumptions were considered. 1) While hydrogen gas release process occurred in the presence of the normal photo-catalysts with moderate oxidation power (like Rhodamine B), the oxidation process instead of the hydrogen gas release might be involved in the presence of the photo-catalysts with stronger oxidation power like acridinium salts. 2) Long reaction time may cause the critical hydrogen gas leaks from the reaction vessels.

**Table 2-18.** Studies to confirm hydrogen gas evolution in my catalytic system with indoline

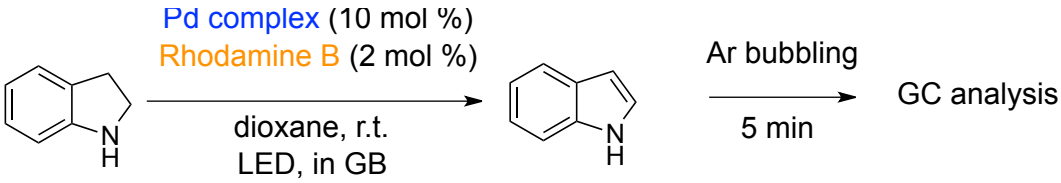


| entry | scale (mmol) | reaction time (h) | yield of indoline (%) | yield of $H_2$ (%) |
|---|---|---|---|---|
| 1 | 0.1 | 39 | 61 | 7 |
| 2 | 1 | 44 | 37 | 9 |
| 3[a] | 1 | 98 | - | 0 |

[a]The hydrogen gas was injected to the test tube as a control experiment.

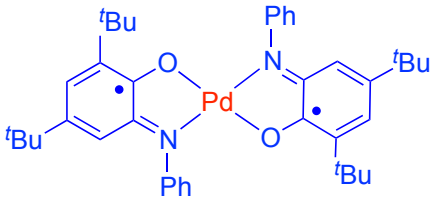


Pd complex

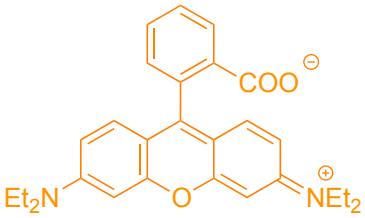


Rhodamine B

## 2-3-5. Investigations for the quantitative detection of hydrogen gas

Based on the considerations above, I re-examined the combinations of a Pd redox non-innocent complex and a normal photo-catalysts (except acridinium salts) for 20 hours. In order to facilitate the reactivity for short reaction time, I envisaged that tridentate complexes might be better than tetradentate complexes because tridentate complexes with less steric demand around the metal centers may accelerate both the coupling with substrates and β–hydride elimination (Scheme 2-13).

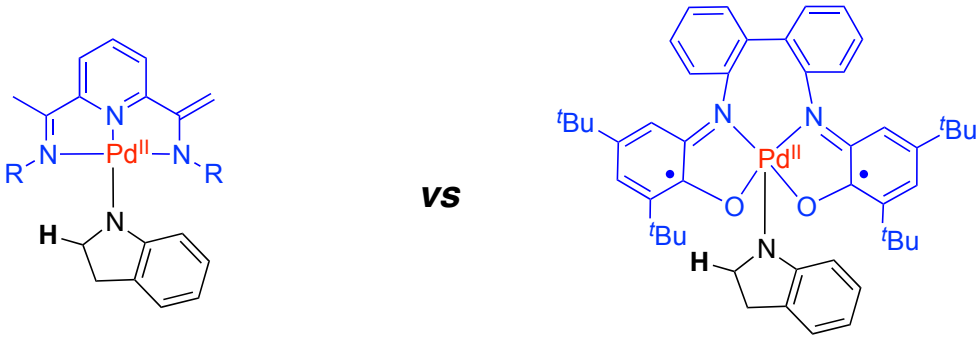


**Scheme 2-13.** Use of tridentate complexes *vs* use of tetradentate complexes

The summarized experimental results were shown in Table 2-19. After the extensive screening of each component, I gained several key features. 1) The combination of the tridentate pincer-type Pd complex and Eosin B in MeOH solvent gave the best result. 2) The addition of a proper metal salts proved to be critical for the improvement in yields for 5 hours reaction time. I speculated that a metal additive might function as a simple Lewis acid or as an accelerator of an anion exchange with the Pd complex to generate the naked Pd complex. The optimized conditions were as follows; in the presence of 5 mol % of the Pd complex[44], 2 mol % of Eosin B and 5 mol % of $LiPF_6$, the desired product was obtained in 50 % yield for only 5 hours at room temperature.

**Table 2-19.** Summarized optimization study

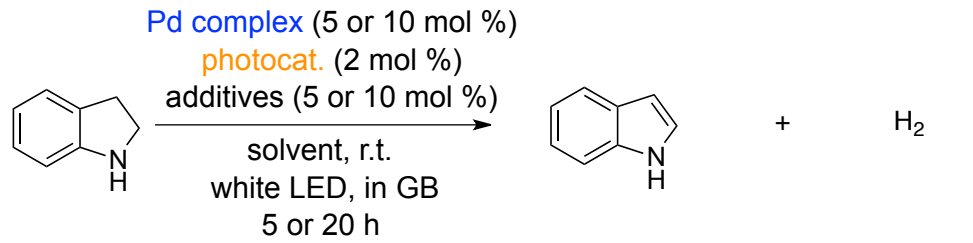


Metal complex

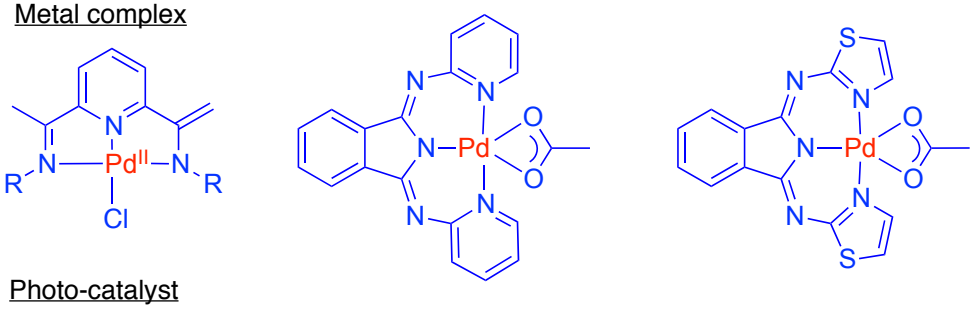

Photo-catalyst

Eosin Y, Fluoroscein, Rhodamine B, Eosin B, Nile red, Erythrosine B, Rose bengal

$Ru(bpy)_3Cl_2$, $Ir(ppy)_2(dtbpy)PF_6$

Solvent

DCM, THF, dioxane, toluene, $PhCF_3$, DMF, MeOH, $CF_3CH_2OH$

Additive

$LiBF_4$, $NaBF_4$, LiOTf, $Li_2SiF_6$, $LiPF_6$, $NaPF_6$, $KPF_6$, $NBu_4PF_6$, $NBu_4BF_4$, LiCl, NaBArF

---

Optimized conditions

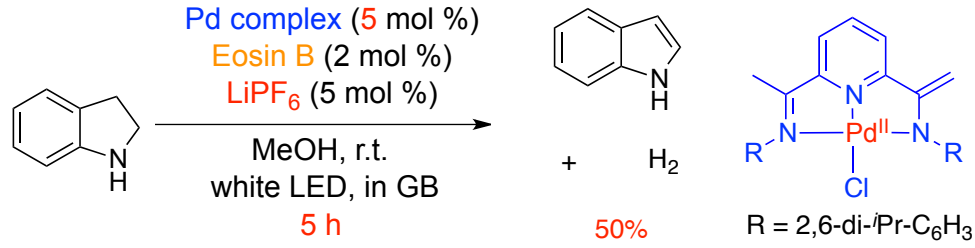


Although the reactivity was raised, I also had hard time to achieve the detection of hydrogen gas quantitatively. The tendencies based on the experiments were as below; 1) 5 hour reaction time was important to detect the hydrogen gas. If the reaction was conducted for over 5 hours, such as 8 hours and 24 hours, the yield of the collected hydrogen gas was drastically decreased. 2) 0.05 mmol scale was also essential. Under 0.1, 0.2, and 0.3 mmol reaction scales, I observed the deterioration of the yield of hydrogen gas. Though the yields were not satisfactory, I gained the obvious evidences of hydrogen gas release using indoline and 2-methyl indoline as

substrates in my catalyst system (Scheme 2-14). Around 30 % of hydrogen gas was detected by GC analysis in each case.

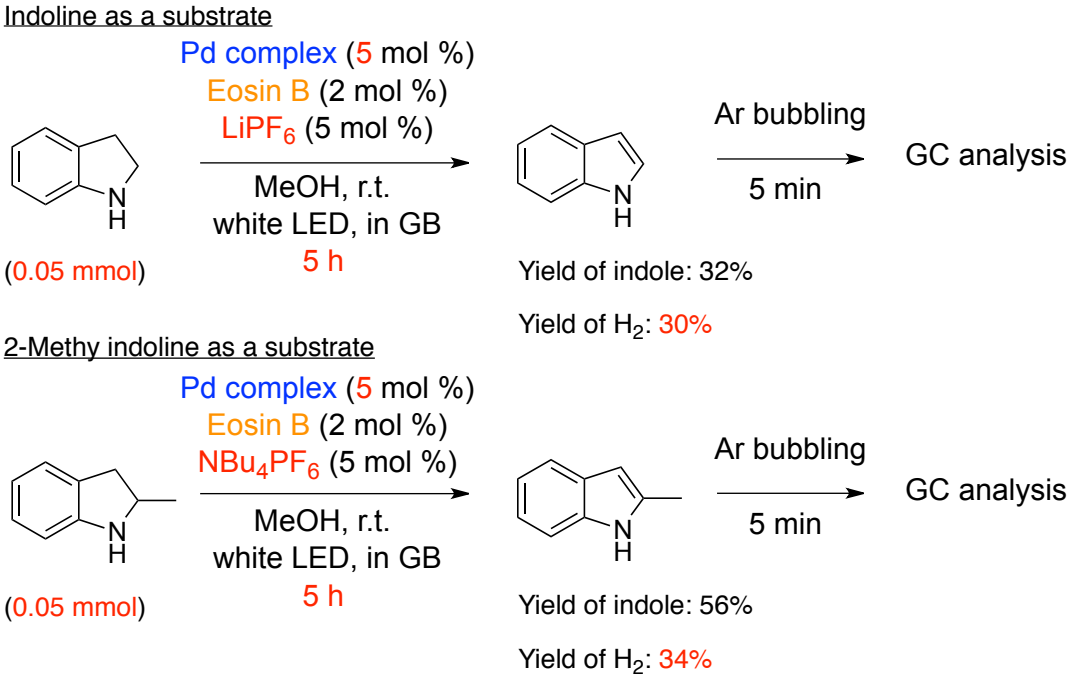


**Scheme 2-14.** Studies to confirm hydrogen gas evolution under the optimized conditions

Although I got the direct evidence of hydrogen gas release, the yield of hydrogen gas was not improved due to the experimental difficulties. Thus, I determined to re-investigate the dual reaction involving dehydrogenation and hydrogenation using *COware® apparatus*. As described in Scheme 2-15, in COware® apparatus, the reaction vessels were separated, but the gas phase was strictly joined. Dehydrogenation of 2-methyl indoline under my catalytic conditions proceeded smoothly to afford the product in 78% yield. At the same time, the hydrogenation reaction of cyclohexene also occurred giving the saturated product in 71% yield (Scheme 2-16). The result apparently indicates that the hydrogen gas released from 2-methyl indoline transferred to another vessel and was utilized for the hydrogenation of cyclohexene.

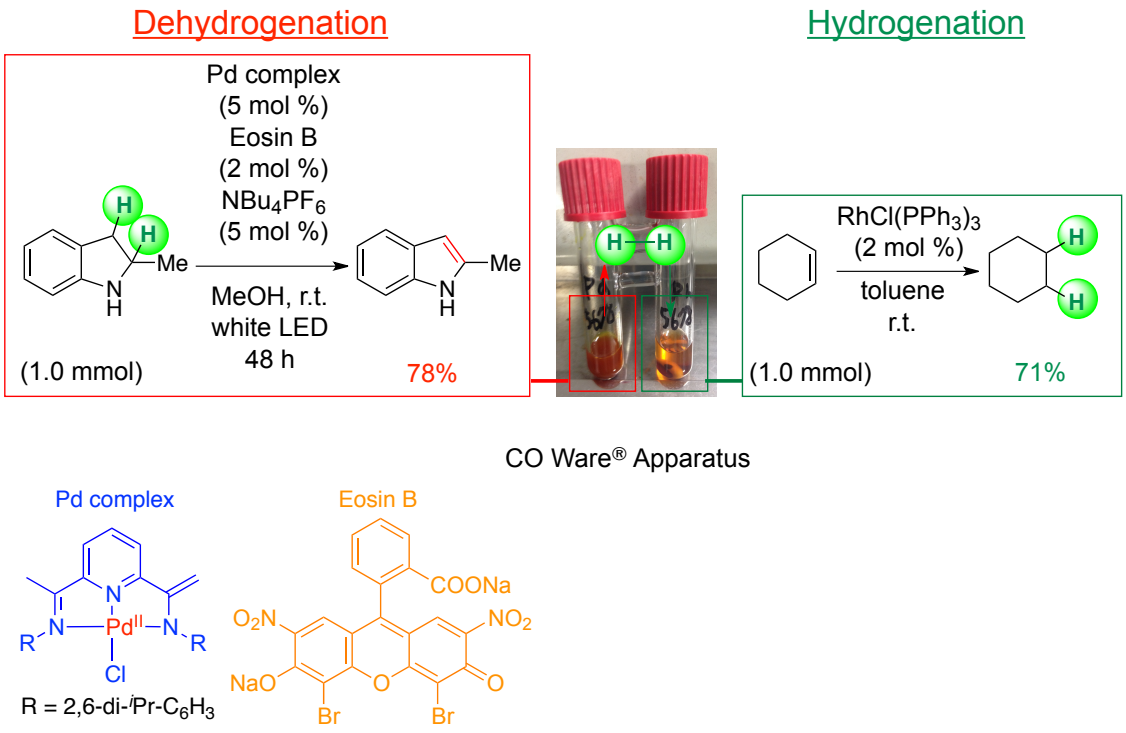


**Scheme 2-15.** Dual reaction using COware® apparatus

Additionally, I discovered that the dual reaction also succeeded in the presence of acridinium-type photo-catalyst (Scheme 2-16). Whereas I surmised that in the presence of the photo-catalyst with strong oxidation power, the hydrogen gas release would not occur, the result clearly indicated that the desired hydrogen release proceeded also in this system.

The encouraging result motivated me to further pursuit this system with the acridinium-type photo-catalyst because the system revealed to be the most reactive system and have the

possibility to expand the substrate generality.

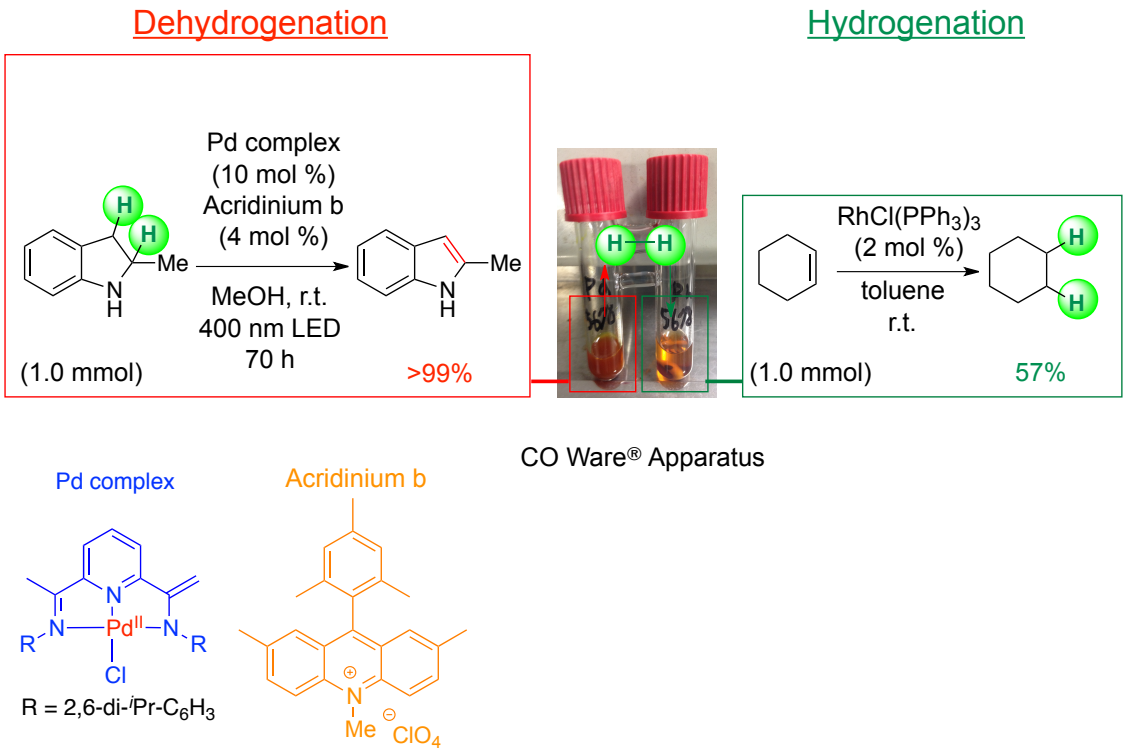


**Scheme 2-16.** Dual reaction using COware® apparatus in the presence of acridinium-type photo-catalyst

## 2-3-6. Final optimization studies

Final optimization studies were initiated with the investigations of additives using 2-methyl indoline as a substrate (Table 2-20). Similarly for the previous case, I surveyed several metal salts. Among them, $NBu_4BF_4$ was the best additive (entry 5). I expected that in the presence of the additive the anion exchange with Pd complex might occur to give the more active intermediate bearing more coordination site around the metal (Table 2-20).

**Table 2-20.** Investigation of additives

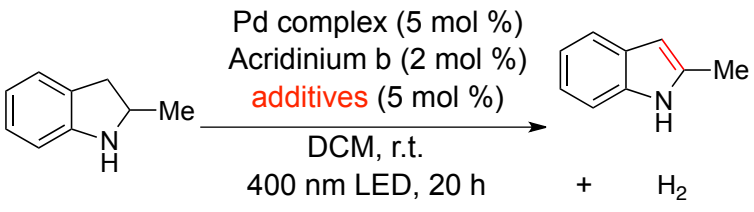


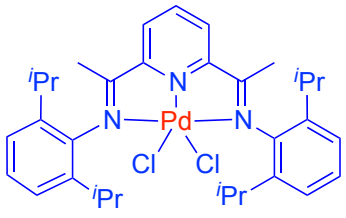


| Entry | Additives | Yield (%) |
|---|---|---|
| 1 | none | 80 |
| 2 | LiOTf | 75 |
| 3 | $LiBF_4$ | 64 |
| 4 | $NaBF_4$ | 78 |
| 5 | $NBu_4BF_4$ | 97 |

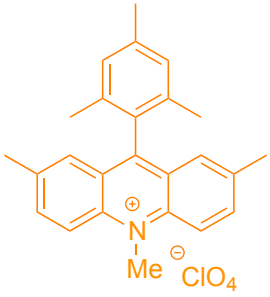


Acridinium b

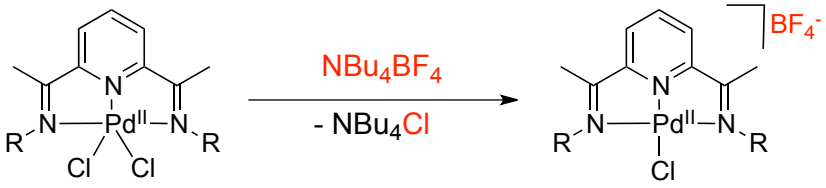


I re-surveyed the metal centers, but resulted in no improvements. The reactivity was remarkably dropped down in the presence of the redox non-innocent complexes with Ru, Mn, Ni and Cu metal centers (Table 2-21, entry 1 *vs* entries 2-5).

**Table 2-21.** Investigation of metals

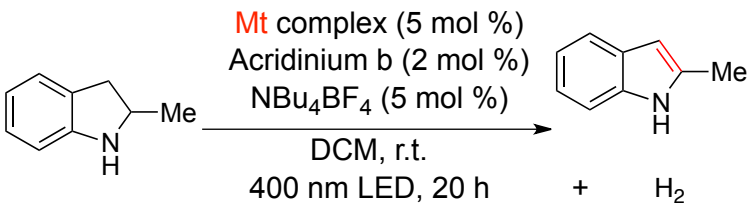


| Entry | Mt | Yield (%) |
|---|---|---|
| 1 | Pd | 97 |
| 2 | Ru | 6 |
| 3 | Mn | 0 |
| 4 | Ni | 0 |
| 5 | Cu | 13 |

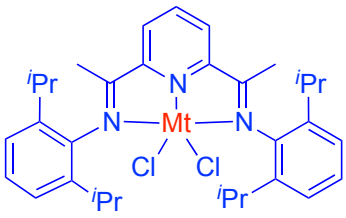


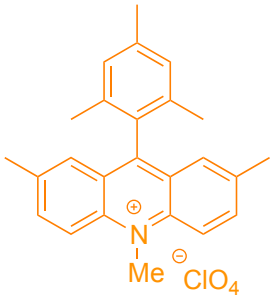


Acridinium b

Modifications of a tridentate pincer-type ligand for three key parts were implemented as shown in Table 2-22. For part **A**, I changed the aryl moiety to alkyl moiety or introduced the electron-donating and electron-withdrawing substituents on aryl moiety. However, no enhancements of the yield were observed. In contrast, it was surprising that the exchange of the methyl group to phenyl group for part **B** completely suppressed the reaction. One possible active intermediate of the Pd complex might be an enamide form by elimination of HCl because the resulting intermediate was expected to accelerate the radical coupling step or the β-hydride elimination step due to the two open coordination site[45] (Table 2-22). I anticipated that the exchange to phenyl group may refrain the complex from forming the active intermediate thus causing the low reactivity.

**Table 2-22.** Modification of redox non-innocent ligands

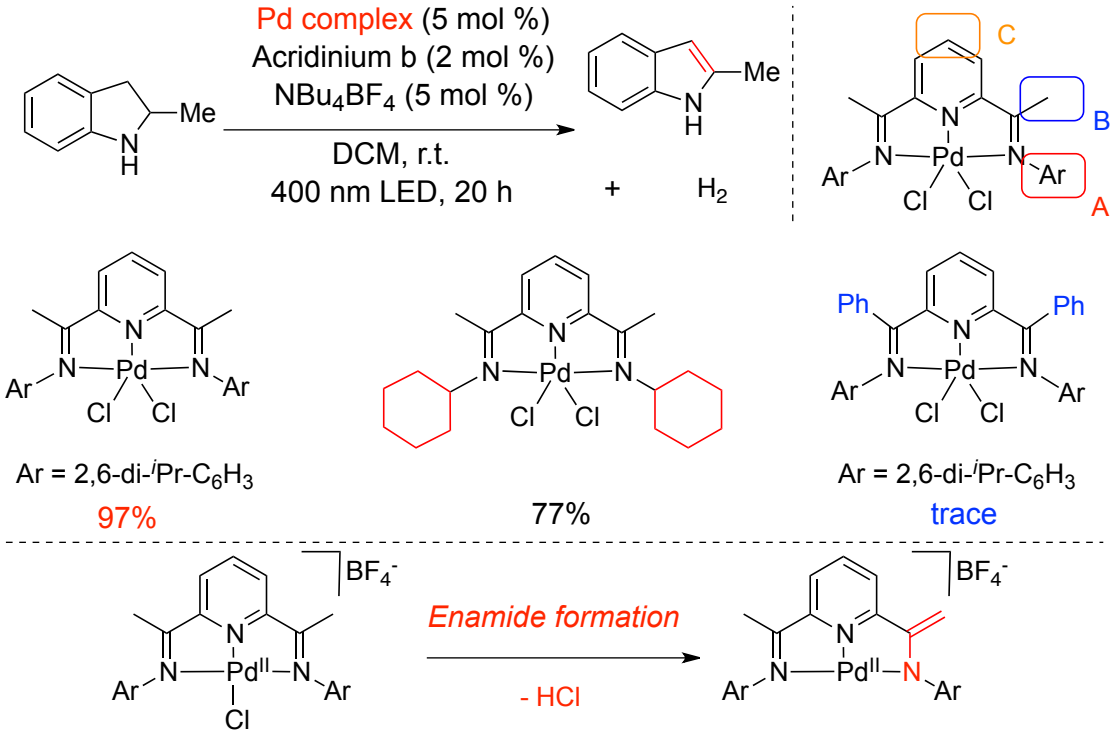


For Co complexes, see; Chirik, P. J. *et al. Inorg. Chem.* **2013**, *52*, 5403.

Investigations for the decrease of catalyst amounts were employed in Table 2-23. When I decreased the catalyst amount from 5 mol % to 1 mol %, a lower yield was observed (entry1). The use of hexane as solvent instead of DCM slightly improved the result (entry 2). After extensive studies for the high reactivity, I uncovered that the introduction of *tert*-butyl substituent on part **C** (C-4 position on the pyridine ring) markedly enhanced the reactivity to afford the product in 77% yield (entry 3). I envisaged that the β-hydride elimination step may be facilitated because the introduction of *tert*-butyl substituent increased the electron density of the Pd complex. It was probable that the *tert*-butyl moiety might protect the complex because in some reports the radical homo-coupling at C-4 position on the pyridine ring was thought to cause the decomposition of the complex. Finally, in the presence of 0.5 mol % of Pd redox non-innocent complex, 0.5 mol % of the acridinium salt and 0.5 mol % of $NBu_4BF_4$, the desired product was produced in quantitative yield in 40 hours (entry 5).

**Table 2-23.** Investigations for the decrease of the catalyst amount

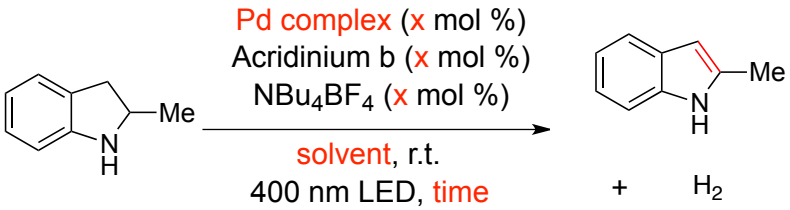


| Entry | cat. (x mol %) | R | Solvent | Time (h) | Yield (%) |
|---|---|---|---|---|---|
| 1 | 1 | H | DCM | 20 | 44 |
| 2 | 1 | H | hexane | 20 | 51 |
| 3 | 1 | $^{t}$Bu | hexane | 20 | 77 |
| 4 | 1 | $^{t}$Bu | hexane | 40 | >99 |
| 5 | 0.5 | $^{t}$Bu | hexane | 40 | >99 |

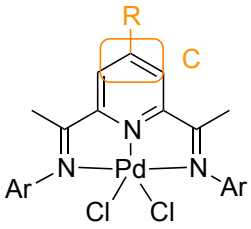


Ar = 2,6-di-$^{i}$Pr-$C_6H_3$

## 2-4. Discussion

### 2-4-1. Substrate generality

Having the optimum conditions in hand, I studied the substrate generality. The results are summarized in Table 2-24. For 1-phenyl tetrahydroisoquinoline as a substrate, the product was obtained in about 70 % combined yield. 2-methyl tetrahydroquinoline was converted to the unsaturated product in 24% yield. However, using other substrates like tetrahydronaphthalene, tetrahydroquinoxaline, dihydrobenzofuran, the reactivity was quite poor to provide the desired products in less than 10% yield. In order to realize the dehydrogenation of *N*-heterocycles with higher hydrogen density such as tetrahydroquinolines, perhydrocarbazole derivatives, the more sophisticated design of metal redox non-innocent complex is highly demanded.

**Table 2-24.** Substrate generality

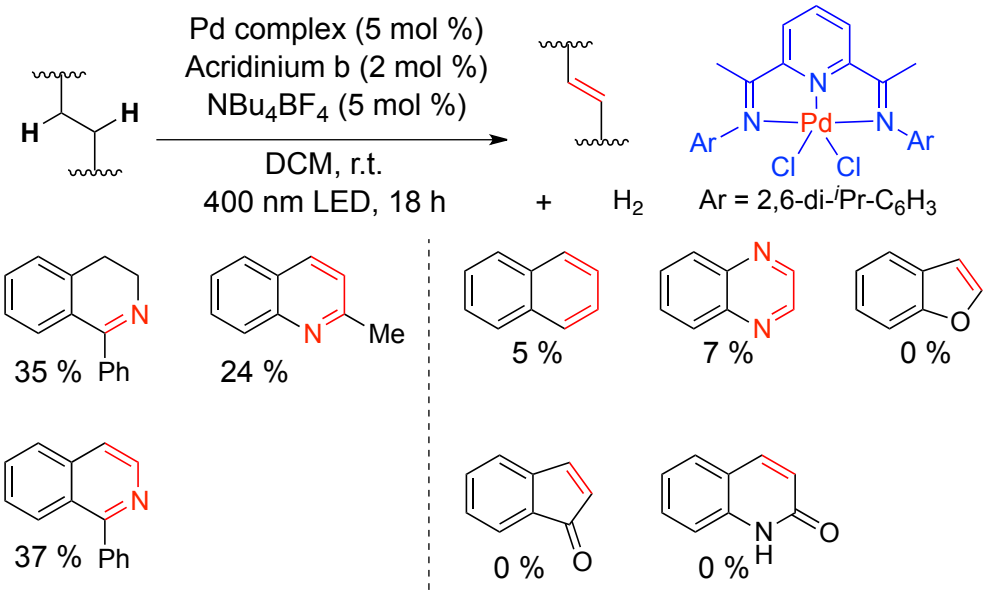

## 2-4-2. Metal amide intermediate *vs* metal alkyl intermediate

In the hypothetical catalytic cycle (shown in Figure 2-11), the radical coupling of between the metal complex and the radical cation from the substrate is one of the critical step for the following β-hydride elimination step. There are two possible intermediates after the radical coupling; metal amide and alkyl metal. In order to clarify the intermediate, I performed the reaction with an *N*-phenyl protected indoline as a substrate under optimized catalyst system (Table 2-25).

**Table 2-25.** The reaction with a *N*-phenyl protected indoline

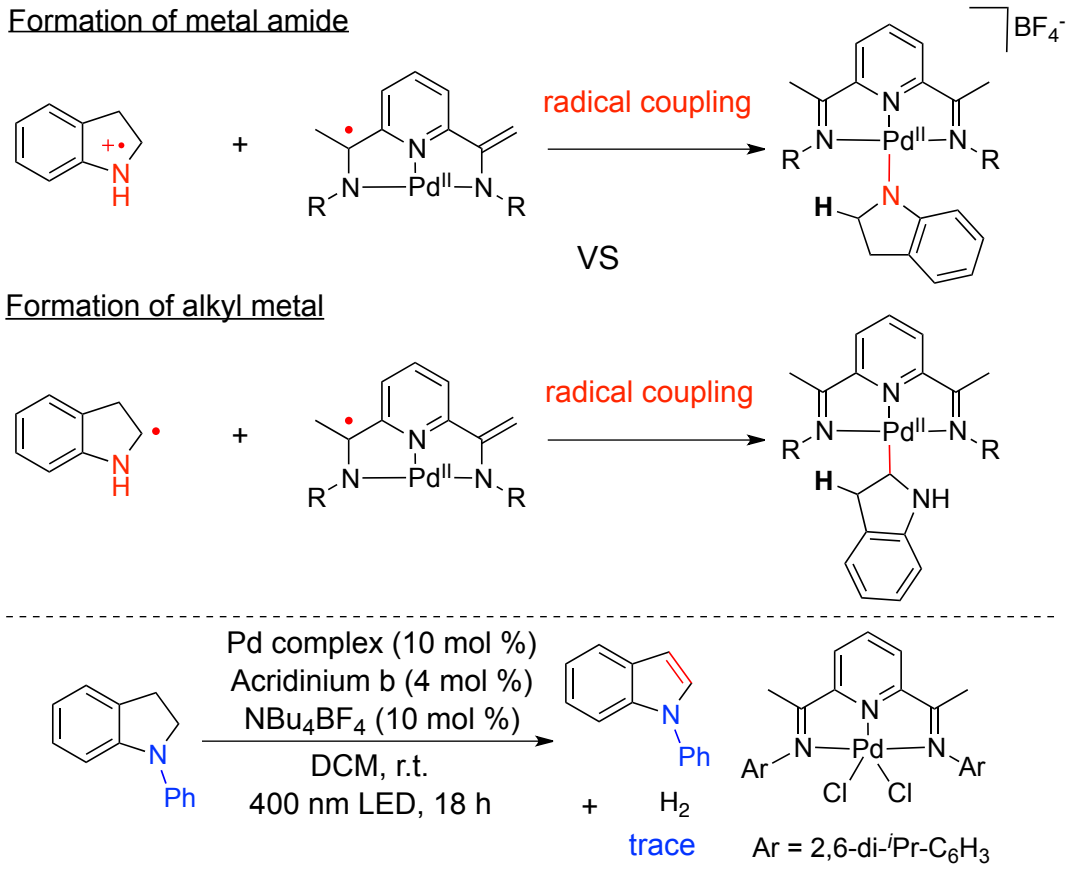


As shown in Table 2-25, almost no desired product was produced with an *N*-phenyl protected indoline as a substrate. From the result, it was probable that β-hydride elimination would occur from the metal amide intermediate, not from the alkyl metal intermediate.

## 2-4-3. A possible role of the photo-catalyst

During the course of the research, I found that the selection of photo-catalysts drastically influence the reactivity. Among them, acridinium-type photo-catalysts exhibited the better reactivity. Although I could not catch the clear tendency and the detailed mechanism study is required, explanation clue might be the remarkably strong oxidation power of the acridinium salts. The selected results for the screening of the photo-catalysts and their reduction potentials after the excitation were summarized in Table 2-26. While other photo-catalysts bear around 0.7-0.8 V for the reduction potential, the reduction potential of acridinium salt is much higher (1.88 V). Though no direct correlation between the value of the reduction potential and the yield was observed, the strong oxidation power of acridinium salt may be one of the possible reason for the high reactivity in the dehydrogenation reaction.

**Table 2-26.** Selected results for the screening of the photo-catalysts

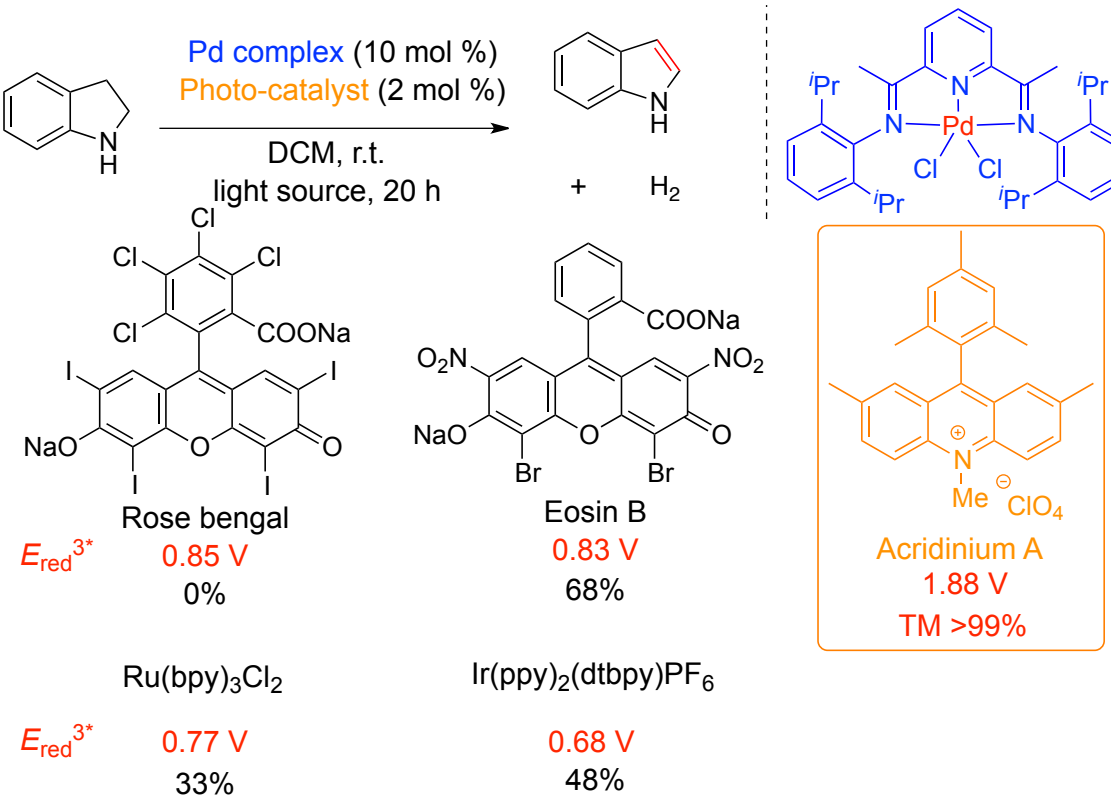


Eisenberg, R. *et al. Dalton. Trans.* 2012, *41*, 13004.

Two possible roles of the photo-catalyst were considerable. First role is in metal amide complex formation without any strong bases. In general, a strong base is necessary for deprotonation of NH of an indoline ($pK_a$ = 17) to form the metal amide intermediate. However, a strong base is reluctant to donate the proton at the hydrogen release step thus suppressing the catalyst turnover. The photo-catalyst may be able to generate the metal amide species without any strong bases under ambient conditions because the photo-catalyst might provide the two reactive radical intermediates by reversible oxidation and reduction.

Second role is for facilitation of the β-hydride elimination step. The assumption is depicted in Scheme 2-17. After the formation of the metal amide intermediate, the photo-catalyst might catalyze one electron transfer from indole to the Pd complex. As a result, C-H bond α to the nitrogen atom would be prone to radicalic cleavage. Also, the Pd complex, which accepted one electron, would possess higher electron density to cleave the β–C-H bond. In the reactive intermediate, H radical abstraction may proceed to give the desired Pd hydride species.

**Scheme 2-17.** Facilitation of β-hydride elimination step

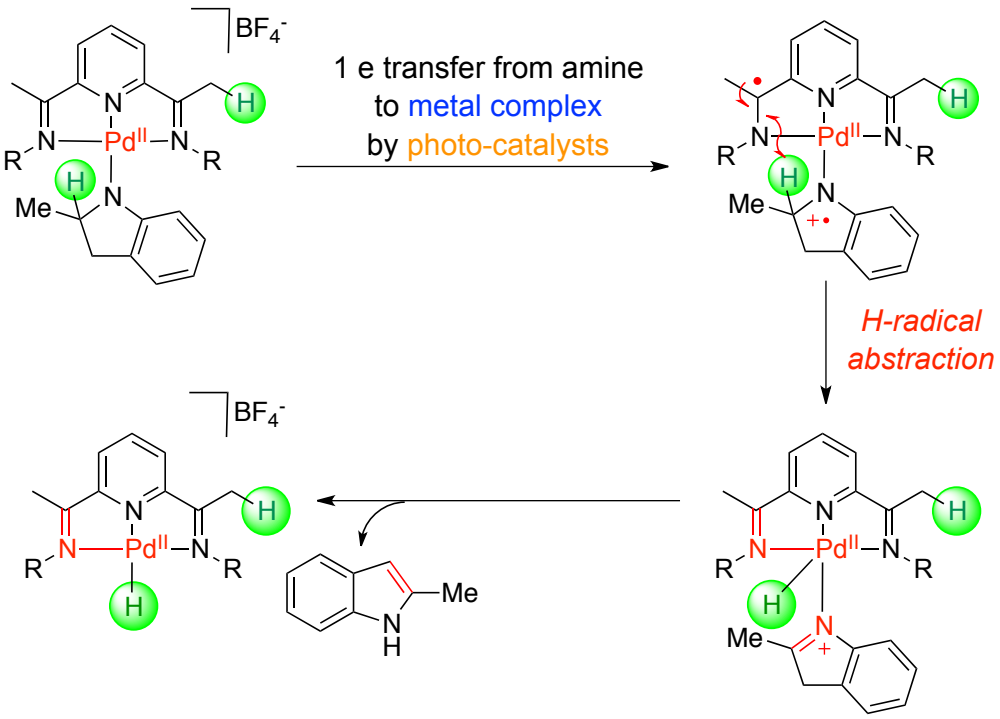

## 2-4-4. Hypothetical catalytic cycle

Based on the several considerations and the preliminary experiments, a hypothetical catalytic cycle is discussed in Figure 2-12. One of the possible active Pd complex might be generated by anion exchange followed by enamide formation. I surmised the oxidation of the substrate by the photo-catalyst, which was excited by 400 nm LED, would initiate the catalytic cycle giving the aminyl radical and the electron-rich photo-catalyst (Scheme I). The oxidation step of substrate indoline by the proper photo-catalyst with strong oxidation power might be the critical stage to initiate the desired conversion. If the resulting photo-catalyst has sufficient reducing power, the one-electron reduction of metal catalyst may proceed to give the radical intermediate (Scheme II). I expected that the use of a redox non-innocent complex favoring one electron mediation would facilitate the key radical coupling step between two reactive radical intermediates (Scheme III). β-Hydride elimination from the metal amide would afford the metal hydride and liberate the unsaturated product (Scheme IV). Subsequent intramolecular hydrogen gas release from the metal hydride is significant for regeneration of the metal catalyst and completion of the catalytic cycle (Scheme V).

**Figure 2-12.** Hypothetical catalytic cycle

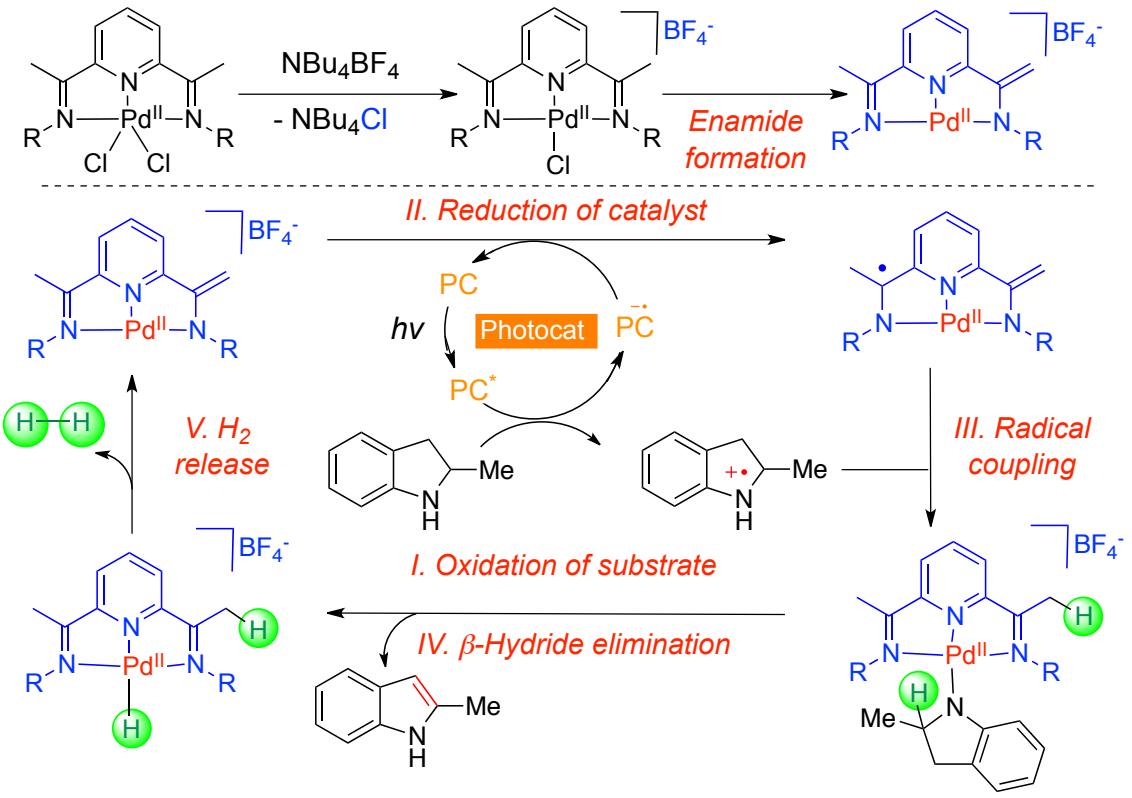

## 2-5. Conclusion and Perspective

In summary, I developed a new cooperative RCRC system using a Pd/redox non-innocent complex and the photo-catalyst. In the presence of only 0.5 mol % of the catalyst sets, the dehydrogenation reaction of 2-methylindoline proceeded to produce the desired product in quantitative yield at room temperature. Based on both the dual reaction experiments and the analysis by GC with TCD detector, it was apparent that the hydrogen gas release occurred in my catalyst system. I believe the following points are noteworthy. 1) The dehydrogenation reaction of *N*-heterocycles was achieved *at room temperature*. 2) *Merging RCRC system of redox non-innocent complex and photo-catalyst* might open up new avenues for other useful chemical conversions.

Despite these advantages, however, several formidable challenges have remained yet. 1) Expansion of substrate generality. 2) Strategic use of first-row-metals. 3) Elucidation and identification of the exact reaction mechanism.

For the first and second challenges, I will design and develop more sophisticated redox non-innocent complex on the basis of the optimum redox non-innocent ligand (Figure 2-13). Introduction of amine or ether moiety at C-4 position on the pyridine ring might influence the reactivity. I envisioned that the stronger σ-donating phosphine or NHC carbene moiety may accelerate β-hydride elimination step by increasing the electron density of the metal center. I believe the rational design, where redox non-innocent function and electric-tuning function would be adequately divided in the ligand, is possible.

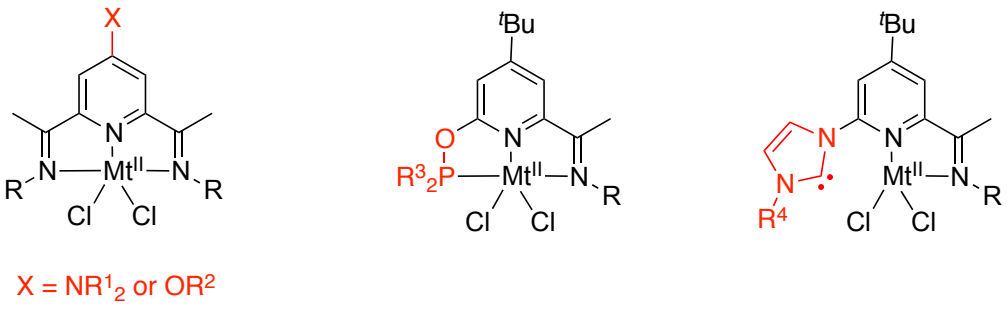


**Figure 2-13.** Possible modifications of metal complex

For the third challenge, I guess the each step and the each intermediate have to be monitored

by proper technical methods. X-ray analysis and CV analysis would provide the electronic information for redox non-innocent character of the metal complex. Though the hypothetical intermediates seemed to be unstable and short-lived, the transition absorption spectra and the EPR spectra might be of great help to ascertain the key radical intermediates.

Now my efforts are devoted to these three fundamental challenges.

## 2-6. References


1. Marban, G.; Valdes-Solis, T. *Int. J. Hydrogen Energy* **2007**, *32*, 1625.
2. Armaroli, N.; Balzani, V. *Energy for a Sustainable World. From the Oil Age to a Sun Powered Future*, Wiley-VCH, Weinhein, **2011**.
3. a) Rifkin, J. *The Hydrogen Economy: The Creation of the Worldwide Energy Web and the Redistribution of Power on Earth*, Penguin Putnan, NewYork, **2003**. b) Momirlan, M.; Veziroglu, T. N. *Int. J. Hydrogen Energy* **2005**, *30*, 795. c) Sartbaeva, A.; Kuznestrov, V. L.; Wells, S. A.; Edwards, P. P. *Energy Environ. Sci.* **2008**, *1*, 79. d) Armaroli, N.; Balzani, V. *ChemSusChem* **2011**, *4*, 21 and references cited therein.
4. a) Edwards, P. P.; Kuznetsov, V. L.; David, W. I. F. *in Energy Beyond Oil* ed. Armstrong, F.; Blundell, K. Oxford University Press, Oxford, **2007**. b) Sigfusson, T. I.; *Philos. Trans. R. Soc. London. Se. A* **2007**, *365*, 1025. c) Service, R. *Science* **2009**, *325*, 1644.
5. a) Luque, R.; Herrero-Davila, L.; Campelo, J. M.; Clark, J. H.; Hidalgo, J. M.; Luna, D.; Marinas, J. M.; Romero, A. A. *Energy Environ. Sci.* **2008**, *1*, 542. b) Gallezot, R. *ChemSusChem* **2008**, *1*, 734. c) Inderwildi, O. R.; King, D. A. *Energy Environ. Sci.* **2009**, *2*, 343.
6. Levene, J. I.; Mann, M. K.; Margolis, R. M.; Milbrandt, A. *Sol. Energy* **2007**, *81*, 773.
7. *Handbook of Fuel Cells Vol. 1-6* (Ed.: W. Vielstich), Wiley-VCH, Weinheim, **2009**.
8. a) *Handbook of Fuel Cells Vol. 3* (Ed.: W. Vielstich), Wiley-VCH, Weinheim, **2009**. b) Neyerlin, K. C.; Srivastava, R.; Yu, C. F.: Strasser, P. *J. Power Sources* **2009**, *186*, 261. c) Okamoto, M.; Fujigaya, T.; Nakashima, N. *Small* **2009**, *5*, 735.
9. a) Annemieke, W. C.; van den Berg.; Arean, C. Oetro. *Chem. Coummn.* **2008**, 668. b) 「水素エネルギーが分かる本」　市川勝著
10. a) Svec, F.; Germain, J.; Frechet, J. M. J. *Small* **2009**, *5*, 1098. b) Murray, L. J.; Dinca, M.; Long, J. R.; *Chem. Soc. Rev.* **2009**, *38*, 1294.
11. a) Graetz, J. *Chem. Soc. Rev.* **2009**, *38*, 73. b) Eberle, U.; Felderhoff, M.; Schuth, F. *Angew. Chem. Int. Ed.* **2009**, *48*, 6608. c) Yang, J.; Sudik, A.; Wolverton, C.; Siegel, D. J. *Chem. Soc. Rev.* **2010**, *39*, 656.
12. For recent reprentive reviews of organic hydride hydrogen storage systems, see: a) Teichmann, D.; Arlt, W.; Wasserscheid, P.; Freymann, R. *Energy Environ. Sci.* **2011**, *4*, 2767. b) Teichmann, D.; Stark, K.; Müller, K.; Zöttl, G.; Wasserscheid, P.; Arlt, W. *Energy Environ. Sci.* **2012**, *5*, 9044.c) Teichmann, D.; Arlt, W.; Wasserscheid, P.; *Int. J. Hydrogen*

*Energy* **2012**, *37*, 18118.

13. Pez, G. P.; Scott, A. R.; Cooper, A. C.; Cheng, H.; Wilhelm, F. C.; Abdourazak, A. H.; U. S. Patent 7351395 and 7429372, 2008, and prior patents cited.
14. a) Clot, E.; Eisenstein.; Crabtree, R. H. *Chem. Commun.* **2007**, *22*, 2231. b) Crabtree, R. H. *Energy Environ. Sci.* **2008**, *1*, 134.
15. For recent representative reports on heterogeneous catalysts for the dehydrogenation of *N*-heterocycles: a) Mikami, K.; Ebata, K.; Mitsudome, T.; Mizugaki, T.; Jitsukawa, K.; Kaneda, K. *Heterocycles* **2011**, *82*, 1371. b) Sotoodeha, F.; Huberb, B. J. M.; Smith, K. J. *Appl. Catal., A*, **2012**, *420*, 67.
16. a) Murahashi, S.-I.; Naota, T.; Taki, H. *J. Chem. Soc., Chem. Commun.* **1985**, 613. b) Yamaguchi, K.; Mizuno, N. *Angew. Chem. Int. Ed.* **2003**, *42*, 1480. c) Yamaguchi, K.; Mizuno, N. *Chem.-Eur. J.* **2003**, *9*, 4353. d) Choi, H.; Doyle, M. P. *Chem. Commun.* **2007**, 745. e) Murahashi, S.-I.; Okano, Y.; Sato, H.; Nakae, T.; Komiya, N. *Synlett* **2007**, 1675
17. a) Yamaguchi, R.; Ikeda, C.; Takahashi, Y.; Fujita, K. *J. Am. Chem. Soc.* **2009**, *131*, 8410. b) Fujita, K.; Tanaka, Y.; Kobayashi, M.; Yamaguchi, R. *J. Am. Chem. Soc.* **2014**, *136*, 4829.
18. a) Li, H.; Jiang, J.; Lu, G.; Huang, F.; Wang, Z.-X. *Organometallics* **2011**, *30*, 3131. b) Zhang, X.-B.; Xi, Z. *Phys. Chem. Chem. Phys.* **2011**, *13*, 3997.
19. a) Wang, Z.; Tonks, I.; Belli, J.; Jensen, C. M. *J. Organomet. Chem.* **2009**, *694*, 2854. b) Wang, Z.; Belli, J.; Jensen, C. M. *Faraday Discuss.* **2011**, *151*, 297.
20. Wu, J.; Talwar, D.; Johnston, S.; Yan, M.; Xiao, J. *Angew. Chem. Int. Ed.* **2013**, *52*, 6983.
21. a) Luca, O. R.; Huang, D. L.; Takase, M. K.; Crabtree, R. H. *New J. Chem.* **2013**, *37*, 3402. b) Chakraborty, S.; Brennessel, W. W.; Jones, W. D. *J. Am. Chem. Soc.* **2014**, *136*, 8564.
22. Selected recent reviews on visible-light photo-redox catalysis: a) Prier, C. K.; Rankic, D. A.; MacMillan, D. W. C. *Chem. Rev.* **2013**, *113*, 5322. b) Xi, Y.; Yi, H.; Lei, A. *Org. Biomol. Chem.* **2013**, *11*, 2387. c) Xuan, J.; Lu, L.-Q.; Chen, J.-R.; Xiao, W.-J. *Eur. J. Org. Chem.* **2013**, 6755. d) Schultz, D. M.; Yoon, T. P. *Science* **2014**, *343*, 985.
23. For a more detailed description of the photo-activation of $[Ru(bpy)_3]^{2+}$ and related catalysts, see: Tucker, J. W.; Stephenson, C. R. J. *J. Org. Chem.* **2012**, *77*, 1617.
24. A recent reviews on dual catalysts: Allen, A. E.; MacMillan, D. W. C. *Chem. Sci.* **2012**, *3*, 633.
25. A Review on dual catalysts merging photo-catalysts and other catalysts: Hopkinson, M. N.; Sahoo, B.; Li, J.-L.; Glorius, F. *Chem. Eur. J.* **2014**, *20*, 3874.

26. Nicewicz, D. A.; MacMillan, D. W. C. *Science* **2008**, 322, 77.

27. a) Nagib, D. A.; Scott, M. E.; MacMillan, D. W. C. *J. Am. Chem. Soc.* **2009**, *131*, 10875. b) Shih, H.-W.; Vander Wal, M. N.; Grange, R. L.; MacMillan, D. W. C. *J. Am. Chem. Soc.* **2010**. *132*, 13600. c) Pirnot, M. T.; Rankic, D. A.; Martin, D. B. C.; MacMillan, D. W. C. *Science* **2013**, *339*, 1593. d) Petronijevic, F. R.; Nappi, M.; MacMillan, D. W. C. *J. Am. Chem. Soc.* **2013**. *135*, 18323.

28. DiRocco, D. A.; Rovis, T. *J. Am. Chem. Soc.* **2012**. *134*, 8094.

29. Bergonzini, G.; Schindler, C. S.; Wallentin, C.-J.; Jacobsen, E. N.; Stephenson, C. R. J. *Chem. Sci.* **2014**, *5*, 112.

30. a) Tarantino, K. T.; Liu, P.; Knowles, R. R. *J. Am. Chem. Soc.* **2013**. *135*, 10022. b) Rono, L. J.; Yayla, H. G.; Wang, D. Y.; Armstrong, R. R.; Knowles, R. R. *J. Am. Chem. Soc.* **2013**. *135*, 17735. c) Kojima, M.; Oisaki, K.; Kanai, M. *Tetrahedron Lett.* **2014**, *in press*.

31. a) Kalyani, D.; McMurtrey, K. B.; Neufeldt, S. R.; Sanford, M. S. *J. Am. Chem. Soc.* **2011**. *132*, 18566. b) For the first report on a dual Pd/photo-redox catalyst system, see: Ozawa, M.; Nagai, H.; Akita, M. *Dalton Trans.* **2007**, 827. c) Ye, Y.; Sanford, M. S. *J. Am. Chem. Soc.* **2012**. *134*, 9034. d) Sahoo, B.; Hopkinson, M. N.; Glorius, F. *J. Am. Chem. Soc.* **2013**. *135*, 5505. e) For a similar dual Au/photo-catalyst system for arylative ring expansion reactions, see: Shu, X-Z.; Zhang, M.; He, Y.; Frei, H.; Toste, F. D. *J. Am. Chem. Soc.* **2014**. *136*, 5844. f) During the preparation of my Ph.D thesis, two papers on a dual Ni/photo-catalyst system were reported: Tellis, J. C.; Primer, D. N.; Molander, G. A. *Science* **2014**, *345*, 433, Zuo, Z.; Ahneman, D. T.; Chu, L.; Terrett, J. A.; Doyle, A. G.; MacMillan, D. W. C. *Science* **2014**, *345*, 437.

32. For recent reviews on redox non-innocnet ligands: a) Eisenberg, R.; Gray, H. B. *Inorg. Chem.* **2011**, *50*, 9741. b) Praneeth, V. K. K.; Ringenberg, M. R.; Ward, T. R. *Angew. Chem. Int. Ed.* **2012**, *51*, 10028. c) Lyaskovskyy, V.; de Bruin, B. *ACS Catal.* **2012**, *2*, 270. d) Luca, O. R.; Crabtree, R. H. *Chem. Soc. Rev.* **2013**, *42*, 1440. e) Annibale, V. T.; Song, D. *RSC Adv.* **2013**, *3*, 11432.

33. Thomas, F. *Eur. J. Inorg. Chem.* **2007**, 2379.

34. a) Bouwkamp, M. W.; Bowman, A. C.; Lobkovsky, E.; Chirik, P. J. *J. Am. Chem. Soc.* **2006**. *128*, 13340. b) Chirik, P. J.; Wieghardt, K. *Science* **2010**, *327*, 794. c) Sylvester, K. T.; Chirik, P. J. *J. Am. Chem. Soc.* **2009**. *131*, 8772. d) Russell, S. K.; Lobkovsky, E.; Chirik, P. J. *J. Am. Chem. Soc.* **2011**. *133*, 8858.

35. a) Blackmore, K. J.; Lal, N.; Ziller, J. W.; Heyduk, A. F. *J. Am. Chem. Soc.* **2008**. *130*, 2728.

b) Nguyen, A. I.; Zarkesh, R. A.; Lacy, D. C.; Thorson, M. K.; Heyduk, A. F. *Chem. Sci.* **2011**, *2*, 166. For their initial works using similar Zr redox non-innocent complexes, see: c) Blackmore, K. J.; Ziller, J. W.; Heyduk, A. F. *Inorg. Chem.* **2005**, *16*, 5559. d) Haneline, M. R.; Heyduk, A. F. *J. Am. Chem. Soc.* **2006**. *128*, 8410.

36. Ye, S.; Sarkar, B.; Lissner, F.; Schleid, T.; van Slageren, J.; Fiedler, J.; Kaim, W. *Angew. Chem. Int. Ed.* **2005**, *44*, 2103.
37. For a cross-coupling reaction using Co complex with the same ligand set, see: Smith, A. L.; Hardcastle, K. I.; Soper, J. D. *J. Am. Chem. Soc.* **2010**. *132*, 14358.
38. a) Fukuzumi, S.; Kotani, H.; Ohkubo, K.; Ogo, S.; Tkachenko, N. V.; Lemmetyinen, H. *J. Am. Chem. Soc.* **2004**. *126*, 1600. For recent reviews on the related photo-catalysts, see: b) Fukuzumi, S.; Ohkubo, K. *Chem. Sci.* **2013**, *4*, 561. c) Fukuzumi, S.; Ohkubo, K.; Suenobu, T. *Acc. Chem. Res.* **2014**, *47*, 1455. Nicewicz group has intensively reported anti-Markovnikov alkene functionalization reactions by the related photo-catalysts, see: Nicewicz, D. A.; Nguyen, T. M. *ACS Catal.* **2014**, *4*, 355 and references cited therein.
39. Eckenhoff, W. T.; Eisenberg, R. *Dalton Trans.* **2012**, *41*, 13004.
40. Reviews on molecular transformations with flavins: a) Imada, Y.; Naota, T. *Chem. Rec.* **2007**, *7*, 354. b) Gelacha, F. G. *Chem. Rev.* **2007**, *107*, 3338. c) de Gonzalo, G.; Fraaije, M. W. *ChemCatChem* **2013**, *5*, 403.
41. For recent examples on chemical conversions with TPT photo-catalyst, see: a) Riener, M.; Nicewicz, D. A. *Chem. Sci.* **2013**, *4*, 2625. b) Gesmundo, N. J.; Nicewicz, D. A. *Beilstein J. Org. Chem.* **2014**, *10*, 1272. For a review on TPT photo-catalysts, see: Miranda, M.; Garcia, H. *Chem. Rev.* **1994**, *94*, 1063.
42. Mukherjee, C.; Weyhermüller, T.; Bothe, E.; Chaudhuri, P. *Inorg. Chem.* **2008**, *47*, 11620.
43. McNally, A.; Prier, C. K.; MacMillan, D. W. C. *Science* **2011**, *334*, 1114.
44. a) Liu, P.; Zhou, L.; Li, X.; He, R. *J. Organomet. Chem.* **2009**, *694*, 2290. The bis(imino)pyridine family of ligands were pioneered by Brookhart group and Gibson group in base-metal olefin polymerization catalysis: b) Small, B. L.; Brookhart, M. *J. Am. Chem. Soc.* **1998**. *120*, 7143. c) Britovsek, G. J. P.; Gibson, V. C.; Kimberley, B. S.; Maddox, P. J.; McTavish, S. J.; Solan, G. A.; White, A. J. P.; Williams, D. J. *Chem. Commun.* **1998**, 849. For a review on the bis(imino)pyridine ligands, see: Gibson, V. C.; Redshaw, C.; Solan, G. A. *Chem. Rev.* **2007**, *107*, 1745.
45. For a Co complex, see: a) Carmen, C.; Atienza, H.; Milsmann, C.; Semproni, S. P. Turner, Z. R.; Chirik, P. J. *Inorg. Chem.* **2013**, *52*, 5403.

# 3. Experimental Section

**General:** Infrared (IR) spectra were recorded on a JASCO FT/IR 410 Fourier transform infrared spectrophotometer. NMR spectra were recorded on JEOL JNM-ECX500 spectrometers, operating at 500 MHz for $^{1}$H NMR and 125 MHz for $^{13}$C NMR or JNM-ECS400 spectrometers, operating at 400 MHz for $^{1}$H NMR and 100 MHz for $^{13}$C NMR. All spectra were obtained at ambient temperature. The chemical shifts (δ) were recorded in parts per million (ppm). The coupling constants (*J*) were shown in Hertz (Hz). Chemical shifts in $CDCl_3$ were reported in the scale relative to residual $CHCl_3$ (7.24 ppm for $^{1}$H NMR, 77.0 ppm for $^{13}$C NMR) as an internal reference. ESI mass spectra for HRMS were measured on a JEOL JMS-T100LC AccuTOF spectrometer. All manipulations of air and moisture sensitive compounds were performed under Ar in a glovebox. Toluene of deoxidized grade was purchased from Wako Pure Chemicals and stored in a glovebox with molecular sieves 4 Å. Pyridines (liquid) were purified by distillation prior to use. Styrene derivatives and aliphatic alkenes were dried over $CaH_2$ and purified by distillation prior to use. Purified aliphatic alkenes were further degassed by three freeze-pump-thaw cycles and stored in a glovebox.

**General Procedure for Direct Alkylation of Pyridines with Styrene Derivatives (Table 1-3):**

A screw-cap vial equipped with a stir bar was dried at 150 °C prior to use. To a suspension of $CoBr_2$ (2.0 mg, 9.0 μmol, 1.0 mol %) in toluene (3.0 mL) in the screw-cap vial at ambient temperature were successively added $Et_3B$ in THF (1.0 M, 180 μL, 0.18 mmol), pyridine derivative **1** (0.90 mmol), styrene derivative **2** (0.945 mmol, 1.05 equiv), and HMPA (0.27 mmol). Then, a solution of $LiBEt_3H$ in THF (1.0 M, 180 μL or 270 μL, 0.18 mmol or 0.27 mmol, as indicated in Table 2) was added. The reaction mixture was heated at 70 °C for 20 h in the glovebox. The resulting mixture was quenched by adding *sat. aq.* $NH_4Cl$ solution, and was extracted with ethyl acetate (× 4). Combined organic layers were washed with $H_2O$ and brine, dried over $Na_2SO_4$, and filtered. After evaporation of the solvent, the regioselectivity was determined at this stage by $^{1}$H NMR analysis of the crude mixture. The crude residue was purified by flash silica gel column chromatography (hexane/ethyl acetate as eluent) to afford product **3**.

**General Procedure for Direct Alkylation of Pyridine with Aliphatic Alkenes (Table 1-4):**

A screw-cap vial equipped with a stir bar was dried at 150 °C prior to use. To a suspension of $CoBr_2$ (11.8 mg, 54 μmol, 6.0 mol % for **2g**, **2h**; 17.7 mg, 81 μmol, 9.0 mol % for **2i**) in toluene (1.5 mL for **2g**, 0 mL for **2h**, **2i**) in the screw-cap vial at ambient temperature were added pyridine **1a** (0.90 mmol) and then aliphatic alkene (12.0 mmol for **2g**; 13.5 mmol for **2h**; 15.2 mmol for **2i**). Then, a solution of $Et_3B$ in THF (1.0 M, 180 μL, 0.18 mmol, 20 mol %) and a solution of $LiBEt_3H$ in THF (1.0 M, 1.8 mL, 1.8 mmol, 2.0 equiv for **2g**, **2h**; 2.7 mL, 2.7 mmol, 3.0 equiv for **2i**) were added to the vial. The reaction mixture was heated at 70℃ for 20-23 h under Ar in the glovebox, and then quenched by adding *sat. aq.* $NH_4Cl$ solution, and was extracted with ethyl acetate (× 4). Combined organic layers were washed with $H_2O$ and brine, dried over $Na_2SO_4$, and filtered. After evaporation of the solvent, the regioselectivity was determined at this stage by analysis of crude $^1H$ NMR. After evaporation of the solvent, the regioselectivity was determined at this stage by $^1H$ NMR analysis of the crude mixture. The crude residue was purified by flash silica gel column chromatography (hexane/ethyl acetate as eluent) to afford product **3**.

**4-(1-phenylethyl)pyridine (3aa):** (known compound)

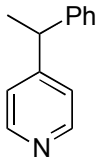


A orange oil; $^1H$ NMR ($CDCl_3$, 500 MHz) δ 1.62 (d, $J$ = 7.1 Hz, 3H), 4.10 (q, $J$ = 7.1 Hz, 1H), 7.09-7.12 (m, 2H), 7.15-7.23 (m, 3H), 7.26-7.31 (m, 2H), 8.47 (brd, $J$ = 4.6 Hz, 2H); $^{13}C$ NMR ($CDCl_3$, 125 MHz) δ 21.0, 44.2, 123.0, 126.6, 127.6, 128.6, 144.4, 149.8, 155.1; LRMS (ESI): *m/z* 184 $[M+H]^+$; Spectra data matched well with those reported in the literature, Lit. Nakao, Y.; Kashihara, N.; Kanyiva, K. S.; Hiyama, T. *J. Am Chem. Soc.* **2008**, *130*, 16170.

**4-(1-(4-(*tert*-butyl)phenyl)ethyl)pyridine (3ab):**

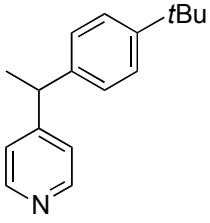


A green oil; IR (neat) ν 2964, 1595 $cm^{-1}$; $^1H$ NMR ($CDCl_3$, 500 MHz) δ 1.29 (s, 9H), 1.61 (d, $J$ = 7.4 Hz, 3H), 4.06 (q, $J$ =7.4 Hz, 1H), 7.08-7.13 (m, 4H), 7.29-7.33 (m, 2H), 8.46 (brd, $J$ = 4.3 Hz, 2H); $^{13}C$ NMR ($CDCl_3$, 125 MHz) δ 21.0, 31,2, 34.3, 43.7, 122.9, 125.4, 127.1, 141.1, 149.3, 149.5, 155.3; HRMS (ESI): *m/z* calculated for $C_{17}H_{21}NNa^+$ $[M+Na]^+$: 262.1567, found: 262.1576.

**4-(1-(*p*-tolyl)phenyl)ethyl)pyridine (3ac):**

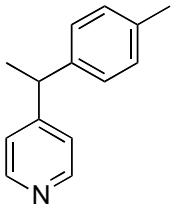

A orange oil; IR (neat) ν 2970, 1595 $cm^{-1}$; $^{1}H$ NMR ($CDCl_3$, 500 MHz) δ1.60 (d, *J* =7.3 Hz, 3H), 2.30 (s, 3H), 4.06 (q, *J* =7.3 Hz, 1H), 7.05-7.12 (m, 6H), 8.46 (brd, *J* = 4.6 Hz, 2H); $^{13}C$ NMR ($CDCl_3$, 125 MHz) δ 20.9, 21.0, 43.7, 122.8, 127.4, 129.2, 136.1, 141.3, 149.6, 155.3; HRMS (ESI): *m/z* calculated for $C_{14}H_{15}NNa^{+}$ $[M+Na]^{+}$: 220.1097, found: 220.1096.

**4-(1-(4-methoxylphenyl)ethyl)pyridine (3ad):** (known compound)

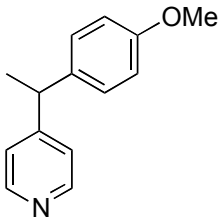

A yellow oil; $^{1}H$ NMR ($CDCl_3$, 500 MHz) δ 1.59 (d, *J* = 7.3 Hz, 3H), 3.77 (s, 3H), 4.05 (q, *J* =7.3 Hz, 1H), 6.80-6.84 (m, 2H), 7.06-7.11 (m, 4H), 8.48 (brs, 2H); $^{13}C$ NMR ($CDCl_3$, 125 MHz) δ 21.2, 43.4, 55.2, 114.0, 123.0, 128.5, 136.5, 149.7, 155.6, 158.2; LRMS (ESI): *m/z* 214 $[M+H]^{+}$; Spectra data matched well with those reported in the literature, Lit. Barluenga, J.; Tomás-Gamasa, M.; Aznar, F.; Valdés, C. *Nat. Chem.* **2009**, *1*, 494.

**4-(1-(naphthalen-2-yl)ethyl)pyridine (3ae):**

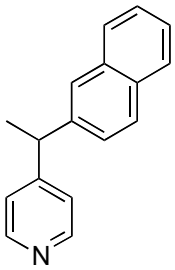

A orange oil; IR (neat) ν 2969, 1596 $cm^{-1}$; $^{1}H$ NMR ($CDCl_3$, 500 MHz) δ 1.72 (d, *J* = 7.3 Hz, 3H), 4.26 (q, *J* =7.3 Hz, 1H), 7.15 (d, *J* = 5.7 Hz, 2H), 7.22-7.25 (m, 1H), 7.41-7.48 (m, 2H), 7.66 (brs, 1H), 7.74-7.80 (m, 3H), 8.48 (brd, *J* = 5.7 Hz, 2H); $^{13}C$ NMR ($CDCl_3$, 500 MHz) δ 21.0, 44.3, 123.1, 125.7, 125.7, 126.2, 126.3, 127.6, 127.7, 128.3, 132.3, 133.4, 141.8, 149.8, 154.9; HRMS (ESI): *m/z* calculated for $C_{17}H_{15}NNa^{+}$ $[M+Na]^{+}$: 256.1097, found: 256.1097.

**4-hexylpyridine (4ag):**

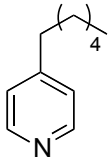

A yellow oil; IR (neat) ν 2928, 1602 $cm^{-1}$; $^{1}H$ NMR ($CDCl_3$, 500 MHz) δ 0.83 (t, *J* = 6.6 Hz, 3H), 1.21-1.31 (m, 6H), 1.54-1.60 (m, 2H), 2.54 (t, *J* = 7.7 Hz, 2H), 7.03-7.06 (m, 2H), 8.41-8.44 (m, 2H); $^{13}C$ NMR ($CDCl_3$, 125 MHz) δ 13.9, 22.4, 28.7, 30.2, 31.5, 35.2, 123.8, 149.5, 151.7; HRMS (ESI): *m/z* calculated for $C_{11}H_{17}NNa^{+}$ $[M+Na]^{+}$: 186.1254, found: 186.1254.

**4-dodecylpyridine (4ah):**

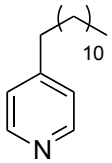

A yellow oil; IR (neat) ν 2925, 1602 $cm^{-1}$; $^{1}H$ NMR ($CDCl_3$, 500 MHz) δ 0.82 (t, *J*

= 6.9 Hz, 3H), 1.15-1.25 (m, 18H), 1.51-1.59 (m, 2H), 2.52 (t, *J* = 7.7 Hz, 2H), 7.03 (brd, *J* = 4.6 Hz, 2H), 8.41 (brd, *J* = 4.6 Hz, 2H); $^{13}$C NMR ($CDCl_3$, 125 MHz): δ 14.0, 22.6, 29.1, 29.2, 29.3, 29.4, 29.5, 29.5, 29.5, 30.2, 31.8, 35.1, 123.8, 149.4, 151.7; HRMS (ESI): *m*/*z* calculated for $C_{17}H_{29}NNa^+$ [M+Na] $^+$: 270.2193, found: 270.2183.

**4-(5-(benzyloxy)pentyl)pyridine (4ai):**

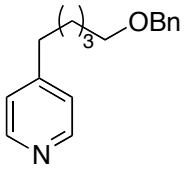


A yellow oil; IR (neat) ν 2935, 2857, 1601, 1102 cm$^{-1}$; $^1$H NMR ($CDCl_3$, 500 MHz) δ 1.36-1.44 (m, 2H), 1.58-1.66 (m, 4H), 2.57 (t, *J* = 7.7 Hz, 2H), 3.44 (t, *J* = 6.6 Hz, 2H), 4.47 (s, 2H), 7.09 (brs, 2H), 7.25-7.35 (m, 5H), 8.52 (brs, 2H); $^{13}$C NMR ($CDCl_3$, 125 MHz): δ 25.8, 29.5, 30.0, 35.1, 70.1, 72.9, 124.0, 127.5, 127.6, 128.3, 138.5, 149.5, 151.4; HRMS (ESI): *m*/*z* calculated for $C_{17}H_{21}NNaO^+$ [M+Na]$^+$: 278.1516, found: 278.1507.

**3-methyl-4-(1-phenylethyl)pyridine (3ba):**

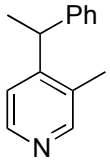


A yellow oil; R (neat) ν 1591, 1450 cm$^{-1}$; $^1$H NMR ($CDCl_3$, 400 MHz) δ 1.58 (d, *J* = 7.3 Hz, 3H), 2.16 (s, 3H), 4.24 (q, *J* = 7.3 Hz, 1H), 7.05-7.31 (m, 6H), 8.31 (brs, 1H), 8.40 (d, *J* = 5.0 Hz, 1H); $^{13}$C NMR ($CDCl_3$, 100 MHz) δ 16.3, 21.2, 40.7, 121.3, 126.3, 127.5, 128.5, 131.5, 144.1, 147.7, 150.8, 152.5; HRMS (ESI): *m*/*z* calculated for $C_{14}H_{15}NNa^+$ [M+Na] $^+$: 220.1097, found: 220.1090.

**4-(1-(4-(*tert*-butyl)phenyl)ethyl)-3-methylpyridine (3bb):**

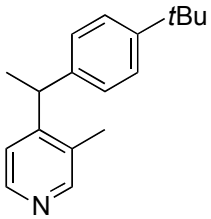


A yellow oil; IR (neat) ν 2964, 1592 cm$^{-1}$; $^1$H NMR ($CDCl_3$, 500 MHz) δ 1.27 (s, 9H), 1.57 (d, *J* = 7.3 Hz, 3H), 2.19 (s, 3H), 4.22 (q, *J* = 7.3 Hz, 1H), 7.01-7.05 (m, 2H), 7.14 (d, *J* = 5.2 Hz, 1H), 7.25-7.29 (m, 2H), 8.30 (s, 1H), 8.39 (d, *J* = 5.2 Hz, 1H); $^{13}$C NMR ($CDCl_3$, 125 MHz) δ 16.3, 21.1, 31.2, 34.2, 40.1, 121.3, 125.3, 127.1, 131.4, 140.8, 147.6, 149.0, 150.7, 152.8; HR MS (ESI): *m*/*z* calculated for $C_{18}H_{23}NNa^+$ [M+Na] $^+$: 276.1723, found: 276.1723.

**3-methyl-4-(1-(*p*-tolyl)phenyl)ethyl)pyridine (3bc):**

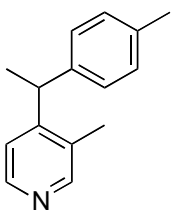


A clear yellow oil; IR (neat) ν 2969, 1592, 1512, 1451 cm$^{-1}$; $^1$H NMR ($CDCl_3$, 500 MHz) δ 1.56 (d, *J* = 7.2 Hz, 3H), 2.17 (s, 3H), 2.28 (s, 3H), 4.20 (q, *J* = 7.2 Hz, 1H), 6.96-7.02 (m, 2H), 7.04-7.09 (m, 2H), 7.14 (d, *J* = 5.2 Hz, 1H),

8.30 (s, 1H), 8.39 (d, $J$ = 5.2 Hz, 1H); $^{13}$C NMR ($CDCl_3$, 125 MHz) δ 16.3, 20.8, 21.2, 40.2, 121.2, 127.4, 129.1, 131.4, 135.8, 141.0, 147.7, 150.7, 152.7; HRMS (ESI): *m*/*z* calculated for $C_{15}H_{17}NNa^+$ [M+Na] $^+$: 234.1254, found: 234.1262.

**3-methyl-4-(1-(*o*-tolyl)ethyl)pyridine (3bf):**

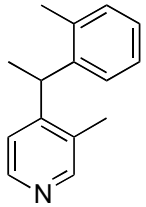

A yellow oil; IR (neat) ν 1591 cm$^{-1}$. $^1$H NMR ($CDCl_3$, 400 MHz) δ 1.52 (d, $J$ = 7.2 Hz, 3H), 2.18 (s, 3H), 2.21 (s, 3H), 4.32 (q, $J$ = 7.2 Hz, 1H), 6.97-7.01 (m, 1H), 7.01-7.06 (m, 1H), 7.11-7.17 (m, 3H), 8.29-8.37 (m, 2H); $^{13}$C NMR ($CDCl_3$, 100 MHz): δ 15.9, 19.1, 20.0, 37.1, 121.3, 126.1, 126.3, 130.4, 131.2, 135.6, 142.0, 147.7, 150.6, 152.9; HRMS (ESI): *m*/*z* calculated for $C_{15}H_{17}NNa^+$ [M+Na] $^+$: 234.1254, found: 234.1260.

**3-methoxy-4-(1-phenylethyl)pyridine (3ca):**

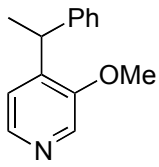

A yellow oil; IR (neat) ν 2968, 1590, 1291, 1255 cm$^{-1}$; $^1$H NMR ($CDCl_3$, 500 MHz) δ 1.55 (d, $J$ = 7.3 Hz, 3H), 3.83 (s, 3H), 4.51 (q, $J$ = 7.3 Hz, 1H), 7.03 (d, $J$ = 4.6 Hz, 1H), 7.14-7.21 (m, 3H), 7.23-7.27 (m, 2H), 8.15-8.19 (m, 2H); $^{13}$C NMR ($CDCl_3$, 125 MHz) δ 20.0, 37.0, 55.9, 121.9, 126.1, 127.5, 128.2, 133.0, 142.7, 143.1, 144.2, 153.0; HRMS (ESI): *m*/*z* calculated for $C_{14}H_{16}NO^+$ [M+H] $^+$: 214.1227, found: 214.1233.

**3-methoxy-4-(1-(4-(*tert*-butyl)phenyl)ethyl)pyridine (3cb):**

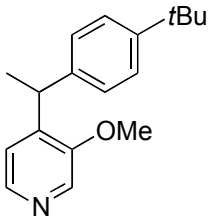

A yellow oil; IR (neat) ν 1590, 1291, 1255cm$^{-1}$; $^1$H NMR ($CDCl_3$, 500 MHz) δ 1.28 (s, 9H), 1.54 (d, $J$ = 7.2 Hz, 3H), 3.87 (s, 3H), 4.51 (q, $J$ =7.2 Hz, 1H), 7.04 (d, $J$ = 4.6 Hz, 1H), 7.11-7.16 (m, 2H), 7.27-7.30 (m, 2H), 8.14-8.24 (m, 2H); $^{13}$C NMR ($CDCl_3$, 125 MHz) δ 20.1, 31.3, 34.3, 36.4, 56.0, 122.2, 125.2, 125.2, 127.2, 133.0, 141.0, 142.7, 143.6, 149.0; HRMS (ESI): *m*/*z* calculated for $C_{18}H_{23}NNaO^+$ [M+Na]$^+$: 292.1672, found: 292.1683.

**3-methoxy-4-(1-(*p*-tolyl)phenyl)ethyl)pyridine (3cc):**

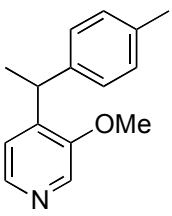

A yellow oil; IR (neat) ν 1632 cm$^{-1}$; $^1$H NMR ($CDCl_3$, 500 MHz) δ 1.54 (d, $J$ = 7.3 Hz, 3H), 2.29 (s, 3H), 3.84 (s, 3H), 4.50 (q, $J$ =7.3 Hz, 1H), 7.03 (d, $J$ = 5.5 Hz, 1H), 7.06-7.12 (m, 4H), 8.15-8.19 (m, 2H); $^{13}$C NMR ($CDCl_3$, 125 MHz): δ 20.0, 20.8, 36.5, 55.8, 121.9, 127.4, 128.9, 132.9, 135.6, 141.2, 142.6, 143.2, 153.0; HRMS (ESI): *m*/*z* calculated for $C_{15}H_{17}NNaO^+$ [M+Na]$^+$: 250.1203, found:

250.1194.

**3-methoxy-4-(1-(*o*-tolyl)ethyl)pyridine (3cf):**

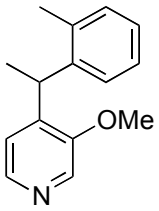


A colorless solid; mp 58 °C (decomp.); IR (KBr) ν 2965, 1586, 1290, 1255 $cm^{-1}$; $^1H$ NMR ($CDCl_3$, 500 MHz) δ 1.50 (d, *J* = 7.0 Hz, 3H), 2.17 (s, 3H), 3.88 (s, 3H), 4.63 (q, *J* =7.0 Hz, 1H), 6.88 (d, *J* = 4.9 Hz, 1H), 7.11-7.22 (m, 4H), 8.11 (d, *J* = 4.9 Hz, 1H), 8.18 (s, 1H); $^{13}C$ NMR ($CDCl_3$, 125 MHz) δ 19.3, 19.8, 33.5, 56.0, 122.0, 125.9, 126.3, 126.4, 130.3, 132.8, 136.2, 142.3, 142.8, 143.3, 153.1; HRMS (ESI): *m*/*z* calculated for $C_{15}H_{17}NNaO^+$ $[M+Na]^+$: 250.1203, found: 250.1210.

**2-methyl-2-(1-phenylethyl)pyridine (3da):**

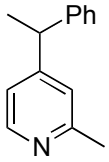


A yellow oil; IR (neat) ν 2969, 1599 $cm^{-1}$; $^1H$ NMR ($CDCl_3$, 500 MHz) δ 1.60 (d, *J* = 7.2 Hz, 3H), 2.48 (s, 3H), 4.05 (q, *J* = 7.2 Hz, 1H), 6.92 (d, *J* = 4.9 Hz, 1H), 6.97 (s, 1H), 7.16-7.23 (m, 3H), 7.26-7.32 (m, 2H), 8.35 (d, *J* = 4.9 Hz, 1H); $^{13}C$ NMR ($CDCl_3$, 125 MHz): δ 20.9, 24.3, 44.0, 119.9, 122.3, 126.4, 127.4, 128.4, 144.4, 148.9, 155.2, 158.2; HRMS (ESI): *m*/*z* calculated for $C_{14}H_{16}N^+$ $[M+H]^+$: 198.1278, found: 198.1278.

**6,6'-dimethyl-4,4'-bis(1-phenylethyl)-2,2'-bipyridine (3ea, a mixture of inseparable diastereomers):**

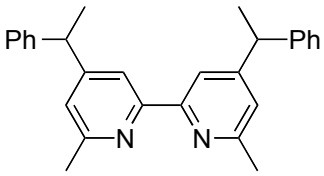


A colorless solid; mp 152 °C (decomp.); IR (KBr) ν 2965,1591 $cm^{-1}$; $^1H$ NMR ($CDCl_3$, 500 MHz) δ 1.67 (d, *J* = 7.3 Hz, 6H), 2.55 (s, 6H), 4.18 (q, *J* =7.3 Hz, 2H), 6.93 (s, 2H), 7.17-7.32 (m, 10H), 8.05 (s, 2H); $^{13}C$ NMR ($CDCl_3$, 100 MHz) δ 21.1, 24.6, 44.3, 117.9, 122.1, 126.3, 127.6, 128.4, 144.8, 155.9, 156.2, 157.8; HRMS (ESI): *m*/*z* calculated for $C_{28}H_{29}N_2^+$ $[M+H]^+$: 393.2326, found: 393.2328.

**4-methyl-2-(1-phenylethyl)pyridine (3fa):**

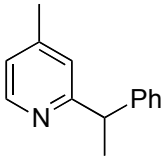


A yellow oil; IR (neat) ν 2968,1602 $cm^{-1}$; $^1H$ NMR ($CDCl_3$, 500 MHz) δ 1.67 (d, *J* = 7.0 Hz, 3H), 2.25 (s, 3H), 4.24 (q, *J* = 7.0 Hz, 1H), 6.88-6.92 (m, 2H), 7.15-7.21 (m, 1H), 7.25-7.30 (m, 4H), 8.40 (d, *J* = 5.2 Hz, 1H); $^{13}C$ NMR ($CDCl_3$, 100 MHz): δ 20.7, 21.0, 47.2, 122.2, 122.9, 126.2, 127.6, 128.4, 145.2, 147.4, 148.8, 164.7; HRMS (ESI): *m*/*z* calculated for $C_{14}H_{15}NNa^+$ $[M+Na]^+$: 220.1097, found:

220.1105.

**Procedures for Mechanistic Studies:**

***In Situ* Generation of Active Cobalt Species in the Absence of $LiBEt_3H$ and $Et_3B$ (Scheme 1-17):**

A screw-cap vial equipped with a stir bar was dried at 150 °C prior to use. To a solution of pyridine **1a** (15 μL, 0.18 mmol) in toluene (3.0 mL) at ambient temperature was added a solution of phenyllithium in cyclohexane-diethyl ether (1.07 M, 168 μL, 0.18 mmol). Then, $CoBr_2$ (2.0 mg, 9.0 μmol) was added to the vial and the mixture was stirred at ambient temperature for 1 min. Then, pyridine **1a** (72 μL, 0.90 mmol) and styrene **2a** (109 μL, 0.95 mmol) were added to the mixture. The reaction mixture was heated at 70 °C for 20 h. The resulting mixture was quenched by adding *sat. aq.* $NH_4Cl$, and was extracted with ethyl acetate (× 4). Combined organic layers were washed with $H_2O$ and brine, dried over $Na_2SO_4$ and filtered. After evaporation of the solvent, the regioselectivity was determined at this stage by $^1H$ NMR analysis of crude mixture. Yield was also determined by $^1H$ NMR analysis of with 1,2-dibromoethane as an internal standard.

**H/D Scrambling Experiment (Scheme 1-13):**

A screw-cap vial equipped with a stir bar was dried at 150 °C prior to use. To a suspension of $CoBr_2$ (2.0 mg, 9.0 μmol) in toluene (3.0 mL) at ambient temperature were successively added a solution of $Et_3B$ in THF (1.0 M, 180 μL, 0.18 mmol), $d_5$-pyridine (72 μL, 0.90 mmol), and styrene **2a** (109 μL, 0.95 mmol). Then, a solution of $LiBEt_3H$ in THF (1.0 M, 180 μL, 0.18 mmol) was added. The mixture was heated at 70 °C for 20 h. The resulting mixture was quenched by adding *sat. aq.* $NH_4Cl$ and was extracted by ethyl acetate. with ethyl acetate (× 4). Combined organic layers were washed with $H_2O$ and brine, dried over $Na_2SO_4$ and filtered. The crude residue was purified by PTLC (hexane/ ethyl acetate = 10/1 eluent) to afford the desired product. Assignment of H at C-3 position of the product was confirmed by DEPT, HMQC and HMBC techniques. NMR charts of **3aa** starting from pyridine **1a** and $d_5$-pyridine are shown in page S-8.

**General procedure for dehydrogenation of 2-methyl indoline under the optimum conditions (Table 2-22, entry 5):**

A screw-cap vial equipped with a stir bar was dried at 150 °C prior to use. To a suspension of Pd complex (0.7 mg, 1.0 μmol, 0.5 mol %), Acridinium b (0.4 mg, 1.0 μmol, 0.5 mol %) and $NBu_4BF_4$ (0.3 mg, 1.0 μmol, 0.5 mol %) in degassed hexane (200 μL) in the screw-cap vial at ambient temperature was added 2-methyl indoline (26μL, 0.20 mmol) in glove box. The reaction vial was placed about 3 cm from 400 nm LED device and stirred under argon atmosphere at room temperature. After 40 hours, the vial was put into the glove box. The reaction mixture was quenched with degassed alumina, washed with degassed MeOH, and concentrated *in vacuo*. The yield was determined by $^1$H NMR analysis of the crude mixture using 1,2-dibromoethane as an internal standard.

**General procedure for hydrogen gas by GC with TCD detector (Scheme 2-15):**

A screw-cap vial equipped with a stir bar was dried at 150 °C prior to use. To a suspension of Pd complex (1.7 mg, 2.5 μmol, 5.0 mol %), Eosin B (0.6 mg, 1.0 μmol, 2.0 mol %) and $NBu_4PF_6$ (2.0 mg, 2.5 μmol, 5.0 mol %) in degassed dichloromethane (50 μL) in the screw-cap vial at ambient temperature was added 2-methyl indoline (6.5μL, 0.05 mmol) in glove box. The reaction vial was placed about 3 cm from white LED device and stirred under argon atmosphere at room temperature. After 5 hours, helium gas (1.1 ml, 0.05 mmol) as an internal standard was added to the vial *via* syringe. An argon balloon was connected to the vial and argon bubbling was conducted for 5 minutes using Ar line to collect gases in the balloon. The gases in the balloon were directly injected to GC device wih TCD detector to determine the yield of hydrogen gas at this stage. Then, the vial was put into the glove box. The reaction mixture was quenched with degassed alumina, washed with degassed MeOH, and concentrated *in vacuo*. The yield of 2-methyl indole was determined by $^1$H NMR analysis of the crude mixture using 1,2-dibromoethane as an internal standard.

**General procedure for dual reaction involving hydrogenation and dehydrogenation (Scheme 2-17):**

A COware® apparatus equipped with a stir bar was dried at 150 °C prior to use. In one tube, to a suspension of Pd complex (31 mg, 50 μmol, 5.0 mol %), acridinium b (8.8 mg, 20 μmol, 2.0 mol %) and $NBu_4BF_4$ (16.5 mg, 50 μmol, 5.0 mol %) in degassed dichloromethane (1 mL) at

ambient temperature was added 2-methyl indoline (130μL, 1.0 mmol) in glove box. In another tube, to a suspension of Wilkinson catalyst (18 mg, 20 μmol, 2.0 mol %) in degassed toluene (1.5 mL), cyclohexene (101μL, 1.0 mmol) was added. The COware® apparatus was placed about 3 cm from 400 nm LED device and stirred under argon atmosphere at room temperature for 24 hours. The yield of cyclohexane was determined by GC analysis using dioxane as an internal standard. The yield of 2-methyl indoline was determined by $^1$H NMR analysis using 1,2-dibromoethane as an internal standard.

**Synthesis of the best Pd complex and ligand:**

**4-*tert*-Butyl-2,6-diacetylpyridine**

To a 200ml flask filled with 120ml $H_2O$ were successively added pyridine (2.0 g, 12.3 mmol), pivalic acid (6.3g, 61.0 mmol), $Na_2S_2O_8$ (10 g, 43.0 mmol) and chlorobenzene (20 mL). concentrated $H_2SO_4$ (1 mL, 18 mmol) was added to the mixture, and the resulting suspension was stirred at reflux for 8 h. The reaction mixture was quenched by the addition of *sat. aq*. NaOH until pH of the residue was 9. And the mixture was followed by celite filtration with $CH_2Cl_2$ and the filtrate was extracted with $CH_2Cl_2$ three times. Combined organic layers were washed with brine and dried over $Na_2SO_4$. After evaporation, the crude residue was purified by flash silica gel column chromatography with Hex/AcOEt (1:0 to 8:1 gradient, V:V) as eluent to afford 4-*tert*-Butyl-2,6-diacetylpyridine as colorless oil (2.5 g, 93% yield)

the characterization was referred to Burger. P., *Organometallics* **2001,** *20,* 4345.

**(*N*,*N*'*E*,*N*,*N*'*E*)-*N*,*N*'-((4-(*tert*-butyl)pyridine-2,6-diyl)bis(ethan-1-yl-1-ylidene))bis(2,6-diisopropylaniline) (4-*t*Bu-NNNpincer-type ligand)**

A 50ml flask charged with $Na_2SO_4$ (3.6 g, 25 mmol) was well dried under reduced pressure (around 1.0 kPa) using a heat gun. After cooling to room temperature, argon was re-filled, 2,6-Diisopropylaniline (2.8 ml, 15 mmol), 4-*tert*-Butyl-2,6-diacetylpyridine (1.1g, 5 mmol), MeOH (10 ml) and $HCO_2H$ (0.10 mL, 2.5 mmol) was added to the 50ml flask. The mixture was stirred at reflux for 19 h and followed by celite filtration with $CH_2Cl_2$. After evaporation of the filtrate, the mixture was recrystalized by AcOEt/MeOH to afford 4-*t*Bu-NNNpincer-type Ligand as yellow crystal (2.3g, 86% yield).

**$PdCl_2$-4-*t*Bu-NNNpincer-type complex**

A 30ml flask was well dried under reduced pressure (around 1.0 kPa) using a heat gun. After cooling to room temperature, argon was re-filled, 4-*t*Bu-NNNpincer-type Ligand (270 mg, 0.50 mmol), $PdCl_2$ (84 mg, 0.48mmol) was added to the 50ml flask. The 30ml flask was flashed with argon. Then, THF (7.0 mL) was added via syringe, and the resulting mixture was stirred at r.t. for 2 h and at 50 $^oC$ for 1 h. After cooled to ambient temperature, the mixture was followed by celite filtration with $Et_2O$. the residue was pumped up to afford $PdCl_2$-4-*t*Bu-NNNpincer-type complex as a black solid (326 mg, 91% yield)

# Acknowledgements

本研究の遂行にあたり、多大なる御指導、御鞭撻を賜りました、東京大学大学院薬学系研究科　金井求　教授に心より深謝申し上げます。

本研究を直接御指導頂き、常に有益なるご助言を賜りました東京大学大学院薬学系研究科　松永茂樹　准教授に心より感謝申し上げます。

学部、修士課程において、多大なる御指導御鞭撻を賜りました、公益財団法人·微生物化学研究会常務理事·微生物化学研究所所長　柴崎正勝　東京大学名誉教授に心より感謝致します。

折に触れ様々なご助言を賜りました、東京大学大学院薬学系研究科　生長幸之助　助教、清水洋平　助教に感謝申し上げます。

ご多忙の折時間を割いて頂き、副査として本博士論文の審査と有益な討論をして頂きました、東京大学大学院薬学系研究科　井上将行　教授、浦野泰照　教授、大和田智彦　教授、船津高志　教授に心より感謝申し上げます。

１章のコバルト触媒を用いたピリジン類の４位選択的なアルキル化反応開発研究の共同研究者である、東京大学大学院薬学系研究科　安藤高史博士、東京大学大学院薬学系研究科　山本昇平博士に感謝申し上げます。

研究を始めた当初より、実験操作から日々のご助言に至るまで、懇切なる指導を賜りました研究室の諸先輩方、特に元木理絵博士、冨田大介博士、半田晋也博士、山次健三博士（現 ERATO 金井触媒分子生命プロジェクト·グループリーダー)、田中雄太博士、木村康明博士に感謝申し上げます。

公私にわたりご協力、ご厚情を賜りました東京大学大学院薬学系研究科　有機合成化学教室及び ERATO 金井触媒分子生命プロジェクトの皆様に感謝申し上げます。その中でも特に、長きに渡り同じ実験室で切磋琢磨し合い日々の楽しい研究生活を提供して頂いた、同期である吉野達彦博士、後輩である三ツ沼治信氏、駒井宏友氏、加藤将太氏、鈴木雄大氏、金子敬一氏、池本英也氏に感謝致します。また、日々の研究生活を支えて頂いた金井研究室秘書、石神美和氏、内藤由紀子氏、師尾佐由利氏、太田杏奈氏に感謝致します。

最後に、私の研究生活を理解して頂き、いかなる時も私を支えて下さった、母と祖父に心より感謝申し上げます。